Impact of innate and adaptive immune cells

in tumor immune surveillance

Dissertation

zur Erlangung des Doktorgrades der Naturwissenschaften

(Dr. rer. nat.)

der Fakultät für Biologie und Vorklinische Medizin

der Universität Regensburg

vorgelegt von

Stephanie Blaimer

aus Kelheim

im Jahr 2020

Das Promotionsgesuch wurde eingereicht am: 21.02.2020

Die Arbeit wurde angeleitet von: Prof. Edward K. Geissler, PhD

Unterschrift Doktorandin:

Table of Contents

Acknowledgement

First of all, I am grateful to Prof. Dr. med. Hans J. Schlitt, the director of the Clinic and Polyclinic for Surgery, for providing a PhD position in the Department of Experimental Surgery.

I would like to express my very great appreciation to my supervisor Prof. Edward K. Geissler. He patiently guided me through my thesis and encouraged me day by day to never give up and do my best.

My sincere thanks go to Prof. Dr. Gunter Meister and Prof. Dr. med. Markus Guba for being my mentors and giving me good advice at my annual research report meetings.

I would like to offer my special thanks to Dr. med. Philipp Renner for enabling the PhD position at the Experimental Surgery and for guiding my PhD project.

Many thanks go to Dr. rer. nat. Elke Eggenhofer, who always had an open ear for me and always gave me good advice.

I am particularly grateful for the assistance given by Lydia Schneider. She taught me every experimental method and I could not have done my work without her experience and help.

I would like to thank my colleagues Tatjana Libeld and Manfred Haas for actively supporting me in the laboratory and helping me with my experiments.

I would like to thank all of my colleagues in the Department of Experimental Surgery for the friendly and supportive atmosphere, which made my work even more fun. My special thanks are extended to Christian Mulas and Regina Heindl, colleagues of my collaboration with the Department of Experimental Medicine, for helping me with one of my mouse projects and performing all transplantation work.

Finally, I wish to thank my family for their support and encouragement throughout my study.

1 Abstract

Cancer is one of the leading causes of death worldwide. In 2018, the International Agency for Research on Cancer (IARC) recorded 18.1 million new cancer cases and a mortality rate of 9.6 million cancer deaths with rising incidence. In 2040, an increase of 61.7% is expected compared to 2018. Treatment of cancer depends on type and stage, and treatment modalities range from surgery, radiotherapy, chemotherapy and hormone therapy to targeted therapy which can be used as single treatments or in combination. Most recently, immunotherapy has shown great promise to treat or cure cancer, immune cells can reach tissues where surgery is impossible and can even treat microscopic diseases or disseminated metastases. There are several types of immunotherapies including ones using tumor-specific immune cells ("cell therapy") to attack cancer cells, or those which enhance already existing tumor-specific immune responses in the body.

In my thesis, two different tumor mouse models mimicking natural tumor development were used to investigate the role of innate and adaptive immune cells, like NK cells and $CD8^+$ T cells, in natural tumor immune surveillance. We observed that tumor development in mice generally led to activation of the differentiation and activity of NK cells. However, sustained stimulation of NK cells by tumor cells resulted in the generation of terminally-differentiated $CD27^{low}$ NK cells with diminished anti-tumor capacities. While IL-15 treatment of mice promoted the development of these specific immune cell subsets, it led to the exhaustion of NK cells. In turn, tumor development did not alter the distribution of $CD8^+$ T cell subsets and naïve $CD8^+$ T cells were the predominant subpopulation over time. Only the treatment of mice with IL-15 led to accumulation of terminally-differentiated central memory T cells which were also characterized by low cytotoxicity and reduced cytokine production. Taken together, tumor cells that develop naturally in a spontaneous cancer model are able to evade immune destruction by promoting the generation of immune cells with low anti-tumor activities. Treatment of mice with IL-15 boosts the immune system, but accumulation of terminally-differentiated immune cells with an exhausted phenotype lead to the ultimate inefficiency of this cytokine treatment and to uncontrolled development of tumors and metastases.

2 Introduction

2.1 Cancer and metastasis

2.1.1 Development and characteristics

Noncommunicable diseases (NCDs) are the main cause of death worldwide. They are defined as persistent medical conditions resulting from genetic, environmental and physiological alterations. Besides cardiovascular and respiratory diseases, as well as diabetes, cancer is one of the main four types of NCDs[1]. In 2018, the International Agency for Research on Cancer (IARC) recorded 18.1 million new cancer cases and a mortality rate of 9.6 million cancer deaths worldwide. Lung, breast, colorectal, prostate and stomach cancer are the five most commonly diagnosed cancer types. Breast cancer represents the highest incidence in females (24.2%) in comparison to lung (14.5%) and prostate (13.5%) cancer in males[2]. Many factors can lead to cancer development. Genetic disorders, chemical and physical carcinogens, like ionizing radiation and UV light, but also bacteria, viruses or parasites can cause a malignant neoplasm[3].

Hanahan and Weinberg proposed six significant characteristics of cancer cells in “The Hallmarks of Cancer” in 2000[4]. They comprise sustained proliferative signaling, evasion from growth suppressors, resistance to cell death, replicative immortality, induction of angiogenesis and activation of invasion and metastasis[5]. Tumor metastases are actually the primary cause of cancer morbidity and mortality (90%) versus the primary tumor itself. In 2011, Hanahan and Weinberg extended these hallmarks with two additional characteristics: cancer cells are able to reprogram their energy metabolism and can evade destruction by the immune system (Fig.1)[5].

In a process, called angiogenesis, tumors can trigger the formation of new blood vessels. Detached cells can develop a mesenchymal-like phenotype (epithelial mesenchymal transition, EMT) and use the formed blood or lymphatic system to intravasate from tumor sites to surrounding tissues[6,7]. After evading the immune system and surviving in the circulation, these potentially “metastatic” cells adhere to vessel walls and extravasate in distant organs. Only <0.01% of circulating tumor cells overcome selection and are able to reactivate their proliferation and form new blood

vessels to provide the growing macroscopic tumor[8-11]. The most common sites of cancer spreading are lung, liver and bone. In 1889, Steven Paget already postulated that the spread of metastasis is not random into any organ. The “seed” (tumor cells) and the “soil” (organ) have to be compatible. The target organ or tissue where tumor cells with metastatic potential migrate must provide a proper microenvironment[5,12,13].

Since many years there is discussion as to how metastases form, resulting in two different models: the linear and the parallel progression models. In the linear model, disseminated tumor cells (DTCs) spread from late stage primary tumors, acquire genetic mutations and migrate into distant sites of the body. On the contrary, in the parallel progression model, DTCs detach early from first primary tumor lesions and develop as metastases in parallel with the primary tumor[14].

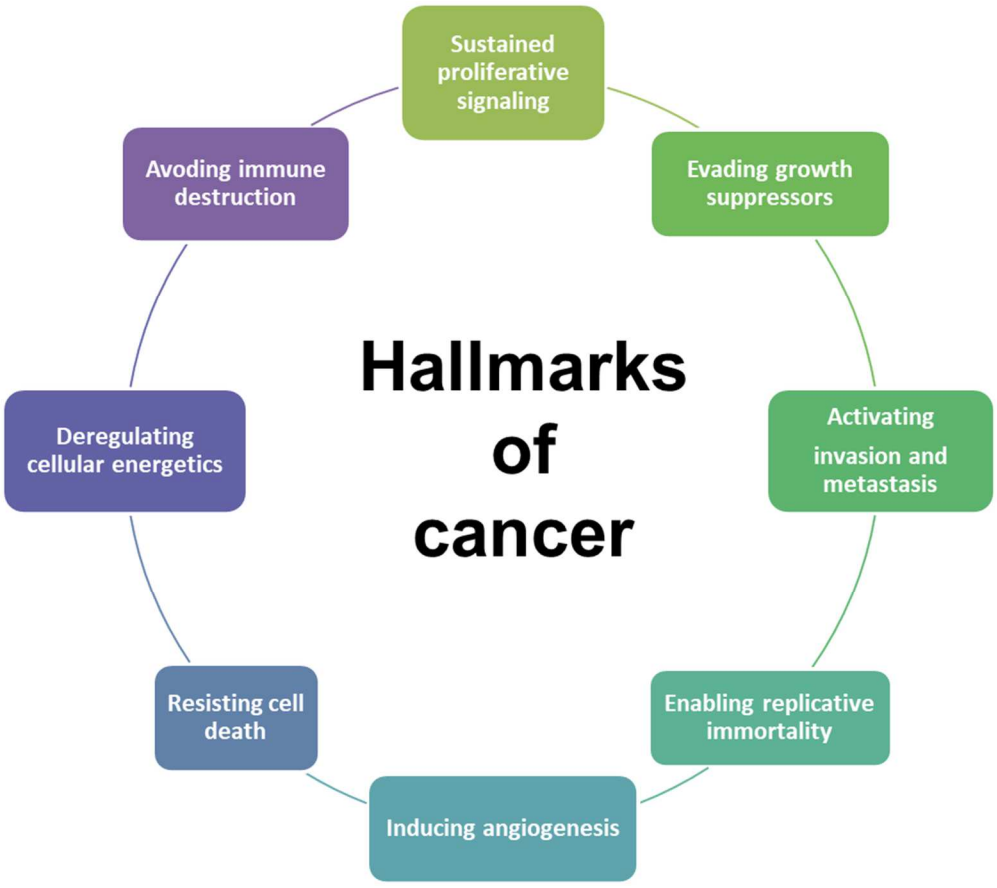

Figure 1: *Hallmarks of Cancer* postulated by Hanahan and Weinberg in 2000 and 2011*(modified from [4,5])*.

2.1.2 Treatment of cancer

Treatment of cancer is dependent of the type, location and stage of disease and has to be decided individually. There are many forms of treatment like surgery, radiotherapy, chemotherapy, hormone therapy or targeted therapy. The general problem of cancer treatment is that many patients remain asymptotic in early stages of the disease, and early signs and symptoms of cancer when they do occur are ignored. Thus, the tumor can spread undisturbed in different parts of the body, called "secondary or metastatic sites". Treatments of patients with metastatic cancer often fail while because primary tumors are indeed sensitive to radiotherapy or chemotherapy, metastases are more resistant to cytotoxic agents or cannot be precisely localized to be cut out[15]. Moreover, chemotherapy and radiotherapy have many severe side effects including non-specific effects on surrounding healthy tissues[16].

Immunotherapy became attractive and promising over the last few years. Endogenous immune cells can reach tissues where surgery is impossible and can even treat microscopic diseases and disseminated metastasis. Furthermore, immunotherapy offers long-term treatment in comparison to chemotherapy or radiotherapy that have effects only at the time they are being applied; the immune system has memory and often persists for a lifetime. The functions and activities of relevant immune cells is the main subject of this thesis work and will be concentrated on in the remaining part of this introductory section. There are several types of immunotherapies including ones using tumor-specific immune cells to attack cancer cells, or ones which generally enhance already existing tumor-specific immune responses in the body. Discussed below are some of the main immunotherapy approaches:

Monoclonal antibodies (mABs) made in laboratories are specific antibodies recognizing proteins, such as cancer cells. After binding tumor-associated proteins, immune cells are attracted and can bind the mABs via their Fc receptors. Afterwards, immune cells are capable of killing cancer cells in a process called antibody-dependent cell-mediated cytotoxicity (ADCC)[17]. Classically, natural killer (NK) cells are the main immune cell population which recognizes Fc domains of mABs. Secretion of perforin and granzymes by activated NK cells lyse tumor cells resulting in release of tumor antigens which are taken up by antigen-presenting cells (APCs).

Tumor antigens are presented on major histocompatibility complex (MHC) molecules to cytotoxic T cells (CTLs) which leads to activation of the CTLs and destruction of tumor cells[18]. Furthermore, B cells are stimulated by the presented tumor antigens, resulting potentially in the development of tumor-specific antibodies. mABs can also be used to therapeutically target cancer cells. For example, the mAB Trastuzumab recognizes the extracellular domain of the Her2/*neu* receptor, which belongs to the EGFR family and is overexpressed in 25% of breast cancers. Dimerization of the receptor leads to cell proliferation, cell survival and metastases[19]. By targeting these overexpressing tumors, a combination of Trastuzumab therapy with cytotoxic chemotherapy can promote survival in women with metastatic breast cancer compared to chemotherapy alone[20].

Another form of immunotherapy in use today involves **checkpoint inhibitors**. Cancer cells can evade immune destruction through expression of ligands that bind to checkpoint proteins on immune cells. Such proteins, like cytotoxic T-lymphocyte antigen 4 (CTLA-4), programmed death-1 (PD-1) and lymphocyte antigen gene 3 (LAG-3) regulate the immune system (generally inhibitory), and are important for self-tolerance. Attachment of tumor ligands to checkpoint proteins can potentially dampen the anti-tumor immune response. Therefore, antibodies against checkpoint proteins or against tumor ligands which bind to checkpoints (PD-L1) have been developed to achieve long-lasting immunity[21]. In more detail, T cell activation occurs via two signals, where the first signal involves the interaction between antigens that are presented on MHC molecules of APCs and the T cell receptor. T cells then require a second, co-stimulatory, signal that often involves the interaction of CD28 on T cells and CD80/CD86 on APCs. CTLA-4 is a CD28 homolog which rather transmits signals to inhibitory pathways in T cells after binding of CD80/CD86 [22]. Already in 1996, it was shown that blockade of CTLA-4 leads to the promotion of anti-tumor responses in mice[23]. In 2011, Ipilimumab was approved by the FDA as the first CTLA-4 checkpoint inhibitor that improved the overall survival of patients with metastatic melanoma[24,25]. PD-1 is also a CD28 homolog and binds to the ligands PD-L1 and PD-L2 that can be upregulated by IFN-γ[26,27]. Interaction between PD-1 and PD-L1/PD-L2 leads to immune suppression and is correlated with poor prognosis in some cancers like

melanoma and gastric cancer[28-30]. Pembrolizumab was the first antibody that was approved by FDA as a PD-1 inhibitor and is used for treatment in different cancer types[31]. Nivolumab is another PD-1 inhibitor that showed therapeutic responses of 44% and progression-free survival rates of 6.9 months in patients with melanoma. Combination therapy of nivolumab and the CTLA-4 inhibitor ipilimumab enhanced response rates to 58% and progression-free survival to 11.5 months[32,33]. In many cancer types, PD-L1 is constitutively expressed on tumor cells or the expression is induced by inflammatory signals[34,35]. Besides binding to PD-1, PD-L1 binds to CD80/CD89 which leads to dampening effects on T cell stimulation and anti-tumor activity[36]. The FDA has approved three different PD-L1 inhibitors at the moment: atezolizumab, durvalumab and avelumab[37-39].

Another promising cancer therapy uses **chimeric antigen receptor (CAR) T cells** (Fig.2). CARs are made by first harvesting T cells from patient blood. T cell receptors are genetically engineered in these cells *ex vivo* to improve the recognition of tumor-associated antigens (TAAs) without prior presentation of these antigens through MHC molecules[40-42]. Thus, it is no longer possible for tumor cells to escape immune destruction through downregulation of MHCs[43]. Moreover, since CAR T cells are not dependent of MHC class I or II, $CD8^+$ T cells as well as $CD4^+$ T cells can be modified[40]. T cell receptors are engineered in different ways to become CARs. Besides viral transduction and use of transposons, T cell receptors are altered by CRISPR/Cas9 vectors or through non-viral transfer methods. Currently, there is already the 4^{th} generation of CARs which are able to simultaneously recognize a broad range of tumor antigens with high specificity and activate themselves due to signaling and co-stimulatory domains in the intracellular part of the receptor[44]. After modification of T cell receptors, CAR T cells are expanded in culture with IL-2 and undergo extensive quality control before reinfusion into the cancer patient. During CAR T cell production in the laboratory, patients receive lympho-depleting chemotherapy to “make space” for the cells to be infused. Also, immune suppressive cells such as regulatory T cells (Tregs) and myeloid-derived suppressor cells (MDSCs) are depleted to improve the efficiency and persistence of CAR T cells[45,46].

Once the cells are back in the patient and after the recognition of TAAs, CAR T cells kill tumor cells via secretion of perforins and granzymes and/or via the expression of Fas ligands to activate the Fas death signaling in malignant cells. The repertoire of ligands that can be recognized by CAR T cells is huge and diverse. However, presently, the most promising results of CAR T cell therapy are observed against B cell malignancies by treatment with anti-CD19 CARs[47-49]. 65% of the current 113 registered CAR T cell trials are targeting hematological malignancies[50]. However, CAR T cell therapy of solid tumors is more challenging due to a lack of tumor-specific antigens. Additionally, in hematological diseases, modified T cells have easy access to cancer cells and their tumor antigens. In contrast, migration into solid tumors requires attraction by chemokines, overcoming of tumor stroma and specific recognition of TAAs.

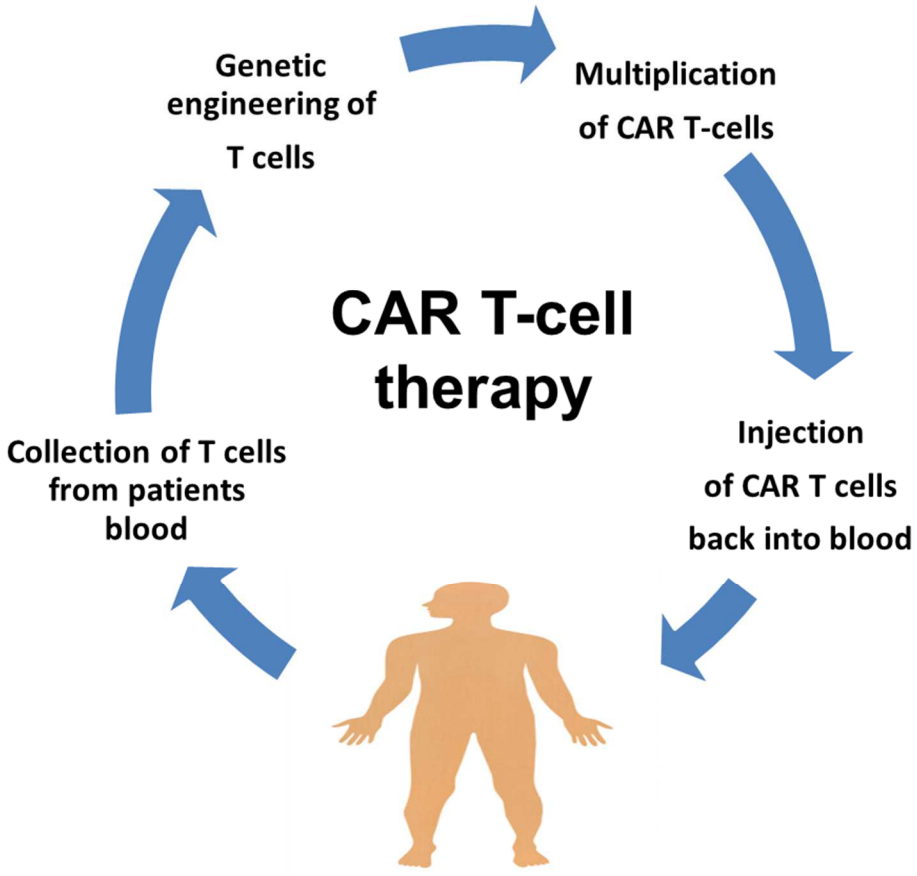

Figure 2: ***Principle of CAR T-cell therapy (modified from [41]).***

Cytokines regulate the development and maturation of innate and adaptive immune cells and their communication. In cancer therapy, cytokines are used to activate or maintain patients' immune responses against tumors. Mouse models first showed that interleukins (ILs) or interferons (IFNs) like IL-2, IL-12, IL-15, IL-21, GM-CSF (granulocyte-macrophage colony-stimulating factor) and IFN-α increase the number of effector immune cells and enhance their anti-tumor immunity[51,52]. Early on, IFN-α and high-dose IL-2 were approved for treatment of different human cancer types[53]. IFN-α is a type I IFN which upregulates the expression of MHC molecules on tumor cells[54-56]. Moreover, IFN-α activates different types of immune cells including dendritic cells (DCs), macrophages, $CD8^+$ T cells and NK cells[57,58]. Besides indirect effects of IFN-α on tumor cells through stimulation of anti-tumor immune cell activity, IFN-α directly interferes with proliferation and angiogenesis associated with malignant cells[59-61]. IL-2 is used to stimulate T cell activation and expansion[62]; furthermore, IL-2 leads to secretion of cytokines and enhanced anti-tumor activities of NK cells, as well as B cell expansion and differentiation. However, efficacy of cytokine therapy with IL-2 is overshadowed by severe side effects. Besides life-threatening toxicities, IL-2 not only activates effector immune cells but also immune suppressive cells like Tregs and MDSCs[63]. Moreover, the expression of inhibitory checkpoint proteins is enhanced by IL-2 and the secretion of immune suppressive factors like IL-10 and TGF-β is stimulated. IL-15 shares many features with IL-2 including the activation of development, differentiation and anti-tumor activity of $CD8^+$ T cells and NK cells[64]. However, it has some advantages in comparison to IL-2, since IL-15 is not as toxic and does not stimulate immune suppressive cells[65]. In Chapter 2.5 I will discuss IL-15 in more detail and the relevance for this thesis. Cytokines are not only used as *in vivo* adjuvants but also *in vitro* for stimulation and expansion of immune cells in adoptive cell therapy. Dendritic cells are stimulated with GM-CSF, IL-4, TNF-α, IL-6 and IL-1β, whereas IL-15 and IL-21 are the most prominent cytokines for activating and expanding T cells. Patients receive low-dose IL-2 after reinfusion of T cells to improve the survival of transferred cells leading to better clinical outcomes[66].

2.2 Tumor immune surveillance and immunoediting

The hypothesis that cancer development is monitored and controlled by immune cells was created decades ago. In the 20th century Frank MacFarlane Burnet and Lewis Thomas created the immune surveillance theory[67]. Different mouse models and also human studies confirmed this hypothesis and showed that the immune system, especially lymphocytes and their secreted cytokines, are able to recognize and eliminate primary tumors (reviewed in [68]). However, doubts gradually arose about this hypothesis because of the development of cancer in immunocompetent mice with an intact immune system. Different further experiments showed the formation of tumors with reduced immunogenicity or the acquirement of mechanisms to evade or suppress the immune system. Therefore, the term "cancer immunoediting" was created including the host-protecting and tumor-sculpting processes of the immune system[68]. Dunn *et al*. divided the cancer immunoediting in three phases (three Es) which will be described in the following chapters: **Elimination, Equilibrium and Escape** (Fig.3).

2.2.1 Elimination

The elimination phase is known as the conventional cancer immune surveillance raised by Burnet and Thomas. In this phase, the immune system recognizes and eliminates transformed tumor cells before they become clinically apparent. For example, APCs like dendritic cells are activated by tumor-secreted danger signals (DAMPs, danger-associated molecular patterns). In addition, T cells recognize tumor antigens with their T cell receptor provoking the induction of adaptive anti-tumor responses[69,70]. There are two different sorts of tumor antigens. A distinction is made between tumor-specific antigens (TSA) and tumor-associated antigens (TAA). TSAs are antigens that are only present on tumor cells but not on normal cells. In comparison, TAAs are expressed on tumor as well as on normal cells, however normally at lower levels on normal cells[71,72]. Besides APCs and T cells, NK cells and their receptors bind ligands (to be explained in a later chapter) expressed on tumor cell surfaces resulting in the release of immunomodulatory and pro-inflammatory cytokines which can kill tumor cells directly or again promote the development of tumor-specific adaptive immune responses[73-75].

At that time, researchers thought that the immune system is able to completely destroy tumor cells. However, there are rare tumor cell variants surviving the elimination phase and entering the next phase of the immunoediting process, the “equilibrium”.

2.2.2 Equilibrium

Some tumor cells which were not recognized and destroyed by immune cells in the aforementioned elimination phase go into dormancy[76]. These cells stop their proliferation, development and activity for periods of time up to decades in length. In this equilibrium phase tumor cells adapt to constant selection pressure of adaptive immune cells, especially by T cells or via genetic instability. T cells even sculpt the immunogenicity of the tumor, as was confirmed in different transplant models. For instance, tumors from mice with immunodeficiency were more immunogenic than tumors from immunocompetent mice, presumably because tumor cells with stimulatory antigens were not as likely to be eliminated. Transplantation of these tumors into wildtype mice showed a higher elimination rate of tumors raised in an immunodeficient background[76]. Only highly immunogenic cells were eliminated and non-immunogenic cells could grow[77]. Moreover, deficiencies in IL-12 and IFNγ signaling pathways lead to progressive tumor growth when transplanted into wildtype mice. This work served to demonstrate the role of adaptive immune components in changing (sculpting) tumor immunogenicity[78].

2.2.3 Escape

In the last phase of the immunoediting process, called the “escape” phase, edited tumor cells with low immunogenicity start growing again and appear as visible tumors. They are resistant to detection and elimination by the immune system. The entry into this phase can be caused by different events. Tumor cells are able to change the expression of tumor antigens and ligands (e.g. MHC components)[79]. Downregulation allows tumor cells to be invisible to immune cells and further tumor progression can occur[80,81]. Moreover, tumor cells producing immunosuppressive cytokines like tumor growth factor β (TGF-β), vascular endothelial growth factor (VEGF), indoleamine 2,3-dioxygenase (IDO) or IL-10 can favor the microenvironment towards tumor growth[82,83].

Recruitment of Tregs and MDSCs can also inhibit anti-tumor responses as another escape mechanism for tumor cells to evade immune surveillance.

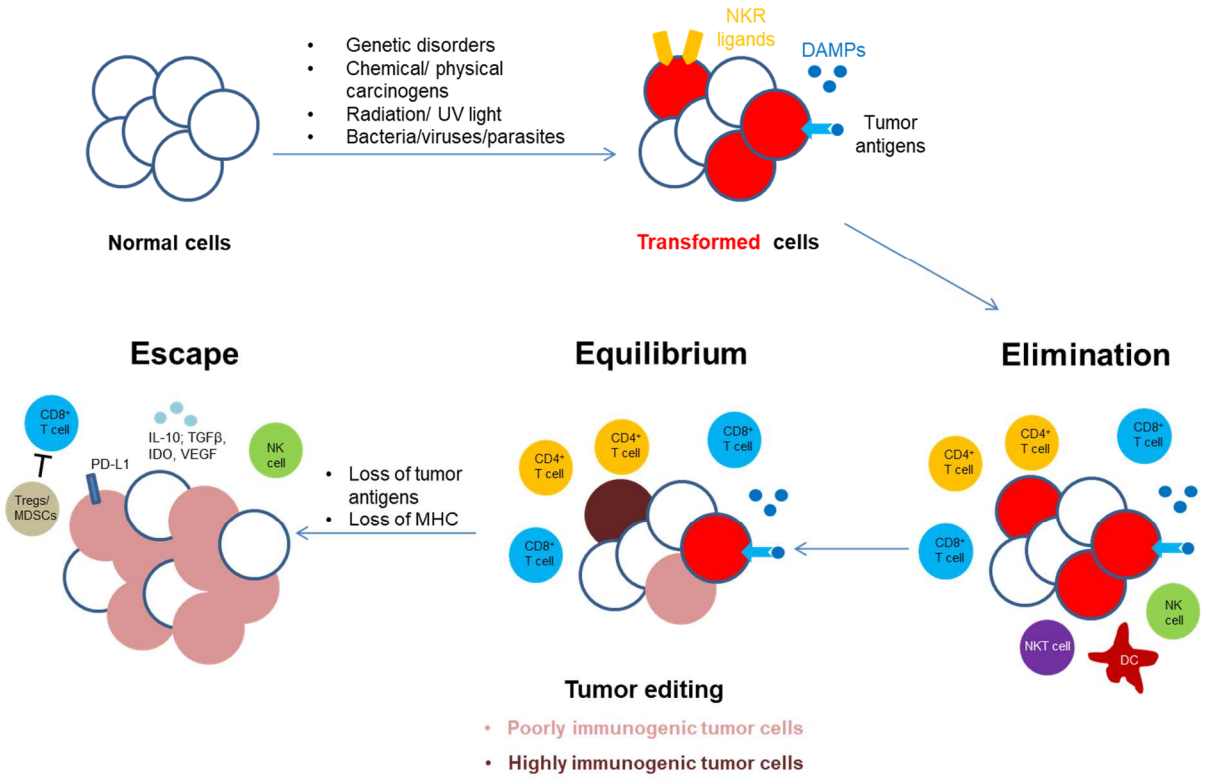

Figure 3: *Three E´s of cancer immunoediting*: Elimination, Equilibrium and Escape (modified from[68,84]). Abbreviations: NKR= natural killer cell receptor, DAMPs= danger-associated molecular patterns, NK cell= natural killer cell, DC= dendritic cell, NKT= natural killer T cell, MHC= major histocompatibility complex, IL= interleukin, TGF= transforming growth factor, IDO= Indolamin-2,3-Dioxygenase, VEGF= Vascular Endothelial Growth Factor, PD-L1= programmed cell death ligand 1, Tregs= regulatory T cells, MDSCs= myeloid-derived suppressor cells.

2.3 Natural Killer (NK) cells

2.3.1 General characteristics and functions

The innate immune system includes physical epithelial barriers, phagocytic leukocytes, dendritic cells and natural killer (NK) cells. The latter NK cells are large granulocytes which are widely distributed in minor fractions (2-10% in mouse, 2-18% in human) in lymphoid and non-lymphoid tissues. NK cells are capable to recognize and kill pathogen-infected or neoplastic cells without prior sensitization[85]. There are different ways how NK cells can act:

Firstly, NK cells secrete two main cytotoxic proteins. Effector NK cells release perforin resulting in disruption of cell membranes followed by secretion of granzymes. Granzymes are serine proteases that can pass cavernous cell membranes of target cells and induce apoptosis (Fig 4; 1)[86,87]. Different studies using perforin-deficient mice show the importance of this protein in NK cell cytotoxicity and tumor immune surveillance, whereas the role for granzymes is less well described[88,89].

Secondly, NK cells activate the Fas death receptor pathway by expressing FasL and tumor necrosis factor-related apoptosis-inducing ligand (TRAIL) on NK cell surfaces leading to programmed cell death[90,91] (Fig. 4; 2). Furthermore, secretion of IFN-γ by NK cells induces the expression of death receptors on target cells[92]. However, signaling through IFN-γ is slower than the perforin/granzyme pathway, occurring only after several hours.

Thirdly, for example, after treatment of patients with a monoclonal antibody therapy, NK cells recognize antibody-coated tumor cells with their Fc receptors (e.g. CD16). These receptors cross-link and activate NK cells and induce ADCC (Fig.4; 3).

After NK cell activation, secretion of cytokines like IFN-γ, TNF and GM-CSF leads to activation of further innate immune cells such as DCs, macrophages and neutrophils. Moreover, NK cells can activate the adaptive arm of the immune system, especially T cells[93] (Fig.4; 4). Different chemokines like IFN-γ, GM-CSF and TNF produced by NK cells attract the aforementioned effector cells to sites of inflammation. Especially IFN-γ can initiate the upregulation of MHC class I and II on other immune cells resulting in stimulation of antigen presentation and orchestration of immune cell interactions[85].

Tumor cell proliferation and growth can be dampened with the antiangiogenic interferon gamma-induced protein 10 (IP-10), also induced by IFN-γ[94].

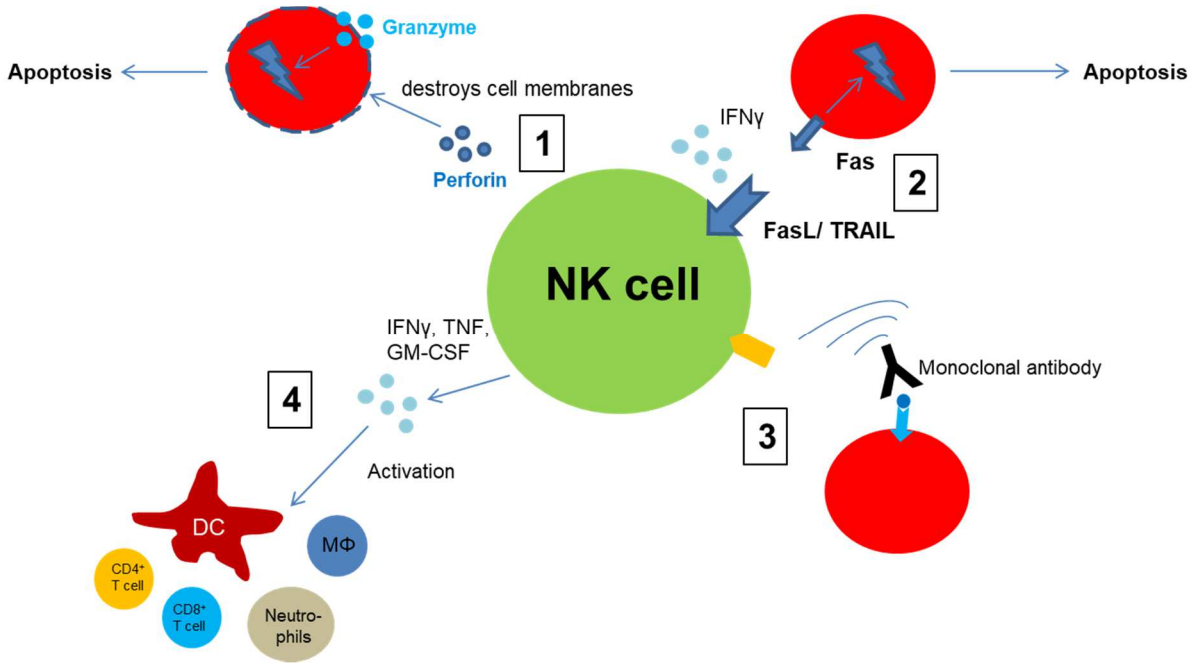

Figure 4: ***Different mechanisms of NK cell killing of tumor cells.*** **1. Secretion of perforin and granzymes; 2. Expression of FasL and TRAIL to initiate Fas death pathway; 3. Antibody-dependent cell cytotoxicity; 4. Cytokine secretion for activation of other innate and adaptive immune cells. Abbreviations: IFN= interferon, TRAIL= Tumor Necrosis Factor Related Apoptosis Inducing Ligand, TNF= tumor necrosis factor, GM-CSF= Granulocyte-macrophage colony-stimulating factor, DC= dendritic cell, MΦ= macrophages.**

2.3.2 Inhibitory and activating NK cell receptors

A wide range of inhibitory and activating cell surface receptors regulates NK cell activity. These receptors are genetically encoded in comparison to ones of B and T cells which are made by somatic recombination[85]. Expression of different combinations of receptors leads to heterogeneity within the NK cell population and offers the opportunity to respond to a diversity of stimuli.

Inhibitory receptors such as killer immunoglobulin-like receptors (KIRs, human) and C-type lectin-like receptors (Ly49, mouse) mainly bind to MHC class I molecules, which are human leukocyte antigen (HLA) class I molecules in humans[95,96]. Another group of inhibitory receptors such as CD94/NKG2A receptors recognize non-classical MHC class I molecules (HLA-E in human; Qa-1 in mouse)[97,98]. The receptors have cytoplasmic immune receptor tyrosine-based inhibitory motifs (ITIMs), which are phosphorylated after binding of these ligands. The phosphorylation results in recruitment and activation of tyrosine phosphatases SHP-1 and SHP-2, leading to downstream signaling and inhibition of NK cells[99,100]. Absence of MHC class I molecules on target cells ("missing-self") and/or stimulation of activating receptors activates NK cell cytotoxicity. Therefore, healthy cells that express high levels of MHC class I molecules are spared from NK cell activity. Killer cell lectin-like receptor G1 (KLRG1) binds cadherins and acts through an ITIM, like the receptors mentioned above[101,102]. In Table 1, inhibitory receptors of human and mouse NK cells with their corresponding ligands are listed.

Additionally to inhibitory receptors, NK cells also express a wide range of **activating receptors**. The signaling occurs through immune-receptor tyrosine-based activating motifs (ITAMs). Tyrosine residues are phosphorylated after binding of a ligand followed by recruitment of the kinases. Afterwards, downstream signaling leads to degranulation of cytokines and chemokines. However, stimulation of more than one activating receptors is required to activate NK cells[103], and strong stimuli are needed to overcome inhibitory signals. Besides signaling through activating KIRs and Ly49 receptors, stimulation of NKG2D leads to proliferation, cytotoxicity and cytokine production by NK cells[104].

Natural cytotoxicity receptors (NCRs), e.g. NKp30, NKp44 or NKp46 bind a wide range of bacterial-, virus- and parasite-originating ligands and are also involved in NK cell cytotoxicity against tumor cells[105-107]. CD16 recognizes specific antigens on tumor cells and induce tumor cell death by ADCC[108]. In Table 2, activating receptors of human and mouse NK cells with their corresponding ligands are listed.

Table 1: ***Inhibitory receptors of human and mouse NK cells***

Inhibitory receptors	Receptor	Ligand
Human	KIR	HLA-A/B/C
	CD94/NKG2A	HLA-E
	KLRG1	Cadherin E/N/R
Mouse	Ly49A/C/I/P	MHC class I
	CD94/NKG2A	Qa-1
	KLRG1	Cadherin E/N/R

Table 2: ***Activating receptors of human and mouse NK cells***

Activating receptors	Receptor	Ligand
Human	KIR	HLA-A/B/C/G
	NKG2C/E	HLA-E
	NKG2D	MICA/MICB/ULBP
	NKp30, NKp40, NKp46 (NCRs)	Viral-, bacterial, parasite-, cellular- ligands
	CD16	-
Mouse	Ly49D/H	MHC class I
	NKG2C/E	Qa-1
	NKG2D	H-60/Rae-1/Mult1

2.3.3 Human NK cell subpopulations

Human lymphocytes consist of 2-18% NK cells that are distinguishable from T cells due to the absence of CD3 expression. They can be divided into two subpopulations identified by the cell surface marker CD16 and CD56 [109]. On the one hand, there are $CD16^{bright}CD56^{dim}$ NK cells that are highly cytotoxic immune cells with poor cytokine production[110,111]. They constitute 90-95% of NK cells and are present in blood and at sites of inflammation[112]. The high expression of CD16 binding to immunoglobulins leads to killing of target cells through ADCC. On the other hand, $CD16^{dim/negative}CD56^{bright}$ NK cells predominantly located in lymph nodes are less cytotoxic but are potent producers of cytokines like IFN-γ, TNFβ, IL-10, IL-13 and GM-CSF after obtaining different activation signals[109]. NK cells respond to cytokines like IL-1, IL-2, IL-12, IL-15 or IL-18 released by other immune cells such as APCs or through signals recognized by their activating receptors CD16 and NKG2D[109,113].

2.3.4 Mouse NK cell subpopulations

Mouse NK cells do not express CD56, and are rather divided by their expression of surface markers CD11b and CD27 representing their differentiation status[114]. They develop from $CD11b^{neg}CD27^{high}$ immature (iNK), over $CD11b^{pos}CD27^{high}$ mature NK cells to $CD11b^{pos}CD27^{low}$ terminally-differentiated NK cells[115]. $CD27^{high}$ are comparable to $CD56^{bright}$ human NK cells also present in lymph nodes with a high capacity to produce cytokines like IFN-γ. They have the ability to kill tumor cells which express MHC I, which is consistent with the lower levels of inhibitory receptors for MHC I on $CD27^{high}$ NK cells[110]. Terminally-differentiated $CD27^{low}$ NK cells show low cytotoxicity and reduced production of cytokines. Concerning proliferation there are also differences between subsets. Immature and $CD27^{high}$ NK cells have high proliferation capacity in comparison to $CD27^{low}$ cells with a limited ability to divide. Mature NK cells also express KLRG1 which is an inhibitory receptor and marker of terminal differentiation[116]. NK cell development is dependent of different cytokines recognized by receptors containing a common gamma (γ_c) chain. Signaling through γ_c is required for their differentiation, homeostasis and function. This subunit is part of the recognition complex for cytokines such as IL-2, IL-4, IL7, IL-9, IL-15 and IL-21[117]. IL-12 and Type I IFNs activate NK cells leading to antitumor activity[118].

2.3.5 NK cells in cancer and metastasis

As described in chapters above and shown in many *in vitro* and *in vivo* studies, NK cells play an important role in tumor immune surveillance by spontaneous killing of tumors without prior sensitization[119,120]. In the course of immune evasion, malignant cells downregulate their expression of MHC class I to escape recognition by receptors of $CD8^+$ T cells. Consequently, NK cells are able to detect these tumor cells ("missing self") which results in NK cell proliferation and cytotoxicity including cytokine production and release of lytic granules[121,122]. Furthermore, expression of stress-induced molecules (MICA, MICB and UL-16) on tumor cells leads to stimulation of activating NKG2D receptor[122,123]. Studies showed that patients with high levels of peripheral blood NK cells have a longer metastasis-free survival[85]. However, mice with deficiencies in NK cell cytotoxicity components like perforin and IFN-γ show an increased incidence of tumors[75,124]. Moreover, perforin is important in controlling the formation of metastasis[125,126].

2.3.6 NK cells in immunotherapies

NK cells have been used in different therapy options against cancer. Autologous NK cell therapy includes extraction of NK cells from patients, followed by *in vitro* manipulation to expand them and increase their cytotoxicity before reinfusing into patients where they are then better able to seek out and destroy tumor cells[127,128]. However, this therapy has limitations, such as through inhibition of NK cells by tumor cell expression of self-HLA molecules[129]. Hence, allogeneic NK cell therapy is performed with transplantation of allogeneic hematopoietic stem cells or infusion of mature allogeneic NK cells. Administration of monoclonal antibodies is another method to induce ADCC by NK cells. These antibodies bind to tumor cells that are then recognized by the activating receptor CD16 on NK cells[130,131]. Besides use of different cytokines to expand and activate immune cells, modified NK cells called chimeric antigen receptor (CAR) NK cells have been utilized. These CAR NK cells are genetically engineered for more efficient and specific binding to tumor antigensf[132-134].

2.4 CD8$^+$ T lymphocytes

2.4.1 General characteristics and functions

CD8$^+$ T cells are cytotoxic T lymphocytes (CTLs) that are generated in the thymus and belong to the adaptive arm of the immune system. Their major role is the clearance of intracellular pathogens and tumors. After recognition of foreign MHC class I antigens presented by APCs, CD8$^+$ T cells perform effector functions comparable with those of NK cells. CD8$^+$ T cells release perforin and granzymes to kill malignant cells. Secretion of IFN-γ and TNF-α strengthens their immune response and activates other cells of the innate and adaptive immune system[135]. Like NK cells, CD8$^+$ T cells express FasL on the cell surface binding to the Fas receptor on target cells. After activation of the caspase cascade, targets cells to go into apoptosis.

2.4.2 Activation of CD8$^+$ T cells

Naïve CD8$^+$ T cells migrate from the thymus to secondary lymphoid organs, like lymph nodes and spleen, where they are activated to mediate immune responses[136]. The activation of CD8$^+$ T cells requires two different signals: Signal 1 is the binding of a MHC protein by specific T cell receptors (TCRs) which is provided by APCs like dendritic cells[137]. Importantly, CD8$^+$ T cells recognize the main structure of MHC class I molecules, rather than the specific peptide in the MHC molecule cleft which is recognized by CD4 helper T cells. Signal 2 is mediated via stimulation through a co-receptor interaction with e.g. CD28 receptor on the T cell surface and B7 proteins (CD80/CD86) on APCs. Signaling through CD28 enhances signal 1 and is necessary for proliferation and activation of effector functions. Absence of signal 2 leads to apoptosis of T cells and represents one mechanism of self-tolerance. After binding of MHC and CD80/CD86 by T cells, downstream signaling leads to IL-2 production and stimulation of CD8$^+$ cell proliferation in an autocrine and paracrine feedback loop. Effector cells produce cytokines like IFN-γ and TNF-α as well as perforin and granzymes. After performing their effector functions, 95% of the CD8$^+$ T cells die and only a small fraction of memory CD8$^+$ T cells persist. With the presence of specific cytokines like IL-15 these memory cells can survive in the host[138].

2.4.3 Human CD8$^+$ T cell subsets

Human CD8$^+$ T cell development occurs in the following order with increasing cell differentiation and effector functions and decreasing memory function and proliferation: naïve T cells (T_N), stem cell memory cells (T_{SCM}), T central memory cells (T_{CM}), T effector memory cells (T_{EM}) and T effector cells (T_{eff})[42]. Human CD8$^+$ T memory and effector cells can be divided by the markers CD27 and CD45RA. Naïve CD8$^+$ T cells express both markers in comparison to memory cells only expressing CD27 and effector cells only expressing CD45RA[139]. CCR7 is another marker distinguishing CD8$^+$ T subsets. Memory cells express this gene in contrast to effector cells which do not show CCR7 expression[140]. CCR7 is a chemokine receptor which is responsible for T cell trafficking and homing within secondary lymphoid organs[141].

2.4.4 Mouse CD8$^+$ T cell subsets

Mouse CD8$^+$ T cells differentiation is similar to that of human CD8$^+$ T cells. Naïve T cells differentiate to effector, T_{EM} and finally to T_{CM} cells[142]. CD8$^+$ T cell subsets in mice can be identified by the expression markers CD44 and CD62L. They differentiate from naïve CD44^{low} CD62L^{pos} T cells (TN) to CD44^{high} cells that can be further distinguish into CD62L^{neg} effector T cells (Teff) and CD62L^{pos} central memory T cells (TCM). These two effector cell subsets differ in location and effector functions (Fig. 5). Teff cells are found in inflamed peripheral tissue with high effector functions like production of high amounts of perforin, IL-4, IL-5 and IFN-γ after antigen stimulation[143]. On the contrary, TCM cells are in secondary lymphoid organs displaying less or no effector functions. However, TCM cells secrete IL-2 quickly after stimulation resulting in a feedback loop leading to their proliferation and differentiation into Teff cells with IFN-γ secretion[140]. TCM cells can be activated by antigen stimulation as well as by response to different cytokines. For example, *in vivo* mouse studies show proliferation of T cells after stimulation with IL-7 and IL-15 [144,145].

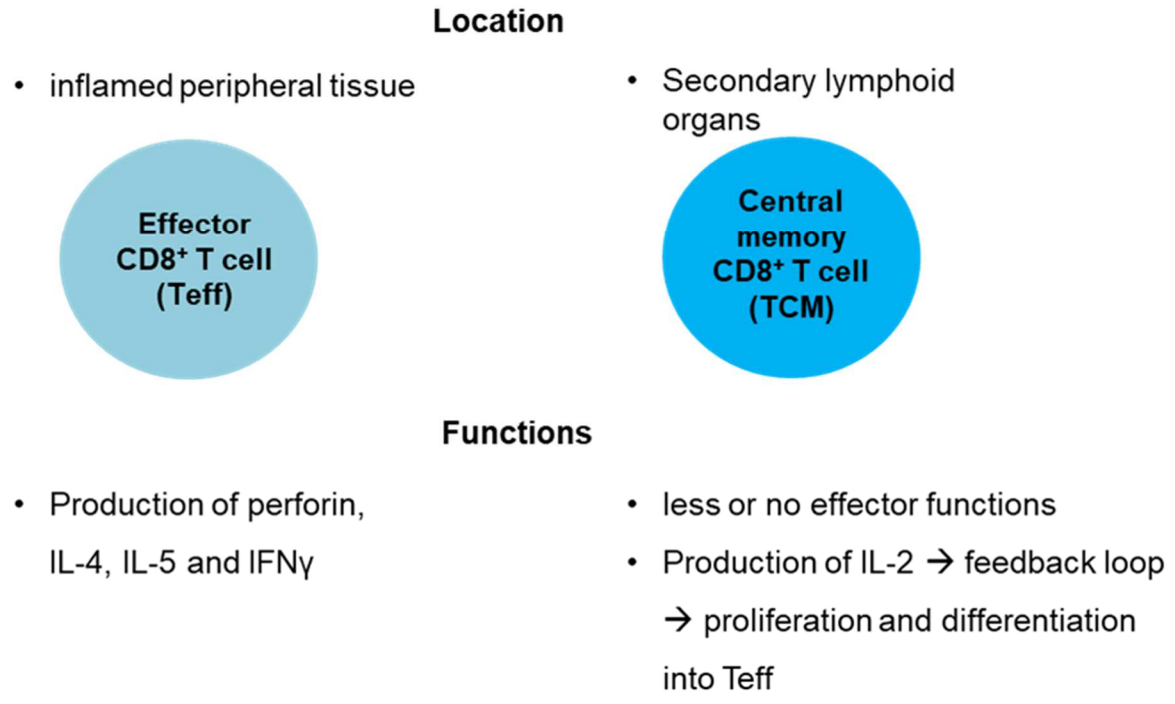

Figure 5: ***Mouse CD8⁺ T cell subsets with different locations and effector functions*****: effector CD8⁺ T cells (Teff); central memory CD8⁺ T cells (TCM)**

2.4.5 CD8⁺ T cells in cancer and metastasis

T cells entering tumors are called tumor-infiltrating lymphocytes (TILs) and are considered as a positive prognostic marker in many different solid tumors[146-148]. CD8⁺ T cells kill target cells in different ways comparable to the capabilities of NK cells. *In vivo* studies show earlier tumor onset in mice lacking lymphocytes or the IFN-γ receptor after injection of methylcholanthrene (MCA)-induced sarcoma in comparison to wildtype mice. Similar results are observed in mice developing spontaneous epithelial tumors[124]. However, during tumor progression CD8⁺ T cells can become exhausted and tumor cells evade tumor immune surveillance through different mechanisms[149]. CD8⁺ T cell-secreted IFN-γ enhances expression of PD-L1 on cancer cells which binds to PD-1 on T cells leading to suppression of their activity. Moreover, Tregs in the tumor microenvironment induce CTLA-4 expression on T cells by releasing adenosines, also resulting in immunosuppression after binding of the ligand CD80/CD86 on tumor cells[150]. Cancer cells stimulate MDSCs to produce TGF-β enhancing the activity of immunosuppressive Tregs[151].

Besides adenosines, many other immunosuppressive compounds are released by cancer cells to escape killing by $CD8^+$ T cells. Therefore, $CD8^+$ T cells can either destroy or spare cancer cells, depending on the exact circumstances in the tumor microenvironment.

2.4.6 $CD8^+$ T cells in cancer immunotherapy

To avoid peripheral tolerance of tumor cells by immune cells, immune-based therapy has become a standard or experimental procedure for treatment of many cancers[152,153]. The aim of such therapies is the reactivation and expansion of tumor-specific cytotoxic T cells resulting in more targeted killing of tumor cells.

A very promising therapy is the use of monoclonal antibodies against checkpoint proteins on T cells. Many solid and hematopoietic tumors are treated with antibodies against CTLA-4 and/or PD-1/PD-L1 which prevent T cell inhibition by tumor cells and boost the activation of effector T cells to kill these malignant cells[154]. Earlier in this review, the need for co-stimulation (signal 2) of T cells to activate or inhibit their activity was covered. Tumor cells can evade T cells by expressing inhibitory molecules, so the antibodies mentioned above serve to block these inhibitory ligands/receptors. Currently, there are different clinical studies evaluating the efficiency of checkpoint inhibitors. However, only a small portion of patients show benefits from these therapies because of the development of resistances against the inhibitors[155]. Combination therapies with e.g. chemotherapy or CAR T cell therapy show higher response rates than monotherapies[156].

Another approach is by CAR T cell therapy. In CAR T cell therapy, T cells from patients are isolated from blood and genetically engineered in a biotechnology laboratory to express a chimeric antigen receptor that specifically recognizes tumor antigens. The receptor consists of an extracellular domain binding to tumor cells and intracellular co-stimulatory and signaling domains responsible for proliferation and activation of effector functions of CAR T cells after binding of tumor antigens[157]. By changing the combinations of co-stimulatory and signaling domains the anti-tumor activity of these CAR T cells is improved significantly over time[158].

Presently, only CD19-specific CAR T cell therapies are approved by the FDA. However, the advantages of this therapy in comparison to the aforementioned use of monoclonal antibodies are a high response rate and small numbers or lack of minimal residual cancer. CAR T cells also express checkpoint proteins after contact with tumor cells, giving them long term activity. Therefore, combination therapies with checkpoint inhibitors are performed to improve the cytotoxicity of CAR T cells and their secretion of IFN-γ[159]. Moreover, CAR T cell efficiency is enhanced by use of interleukins like IL-2, IL-4, IL-7, IL-12, IL-15 and IL-21.

2.5 Interleukin 15 (IL-15)

Immunotherapy takes advantage of the immune system to kill malignant cells without affecting healthy tissue. However, tumor cells can evade immune surveillance by interfering with the development and function of anti-tumor responses. Cytokine therapy was one of the earliest approaches to stimulate immune responses and develop long-lived tumor immunity. In early studies decades ago, treatment with IL-2 sometimes caused impressive tumor regression responses. However, only few patients responded to this therapy and there were very severe side effects[160,161]. Interleukin 15 (IL-15), has more recently been used in cancer immunotherapy by the US National Cancer Institute and deserves further introduction especially with regard to this thesis[162].

2.5.1 Characteristics and signaling pathways

IL-15 is a four-α-helix protein belonging to the same family as IL-2. IL-15 can be produced by APCs. For example, dendritic cells produce IL-15 in the endoplasmic reticulum after their activation. Bound to an IL-15 receptor alpha subunit (IL-15Rα), IL-15 is transferred through the cytoplasm to the cell surface of APCs to be presented to effector immune cells[163]. A receptor complex on responding effector cells consisting of an IL-2/IL-15 receptor β (IL-15Rβ; CD122) subunit and a common gamma chain (γc; CD132) receptor subunit bind to IL-15 with high affinity (Fig. 6). This binding results in the activation of Janus kinases followed by initiation of the STAT5 pathway[164]. Moreover, IL-15 additionally stimulates the RAS-MAPK and PI3K-AKT pathway in effector immune cells[165]. Downstream signaling leads to proliferation, activation,

migration and decreased apoptosis of immune cells carrying the IL15 receptor complex like CD8+ T and NK cells[64,144,166,167]. IL-15 in complex with the α subunit is also found in soluble form after cleavage from cell surfaces upon inflammatory signals[168]. The binding of IL-15 to IL-15Rα is transient and short-lived but it prolongs the half-life of IL-15 and enhances the affinity to the other subunits[169].

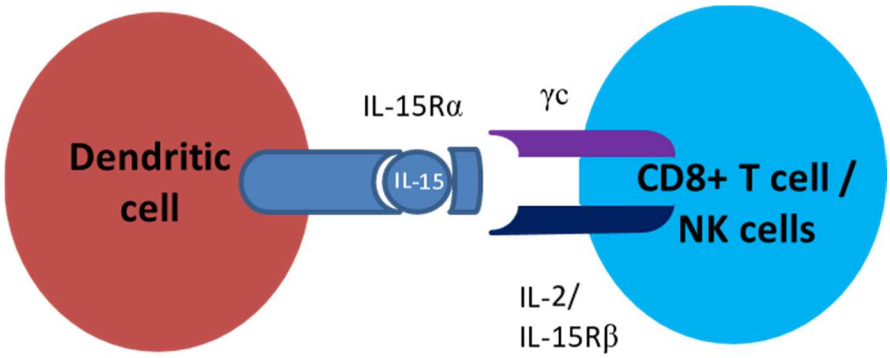

Figure 6*: IL-15 receptor complex*. IL-15 in complex with the IL-15α subunit is presented by APCs to the IL-2/IL-15β and IL-15γ subunit expressed on effector immune cells (modified from [170]).

2.5.2 Pro and contra of IL-15 immunotherapy

IL-15 was first tested in mice and non-human primates with enhancing effects on proliferation, differentiation and survival of CD8+ T cells and NK cells[64,166]. Additionally, in comparison to IL-2, treatment with IL-15 does not stimulate immunosuppressive Tregs. Systemic treatment with this cytokine shows tumor regression and lower numbers of metastases in murine tumor models[171-173]. Moreover, mice treated with IL-15 show more long-lasting anti-tumor effects of immune cells than mice treated with IL-2. Besides transient toxicities, animals respond well to treatment with IL-15 and therefore the cytokine was first given intravenously in adults with metastatic melanoma and renal cell cancer in an in-human phase I clinical trial. In this trial, Conlon *et al.* first observed a significant decrease in peripheral blood NK cells and memory CD8+ T cells shortly after IL-15 administration. After 4 hours, levels of NK cells were normalized again for 2-3 days, followed by a 10-fold increase in NK cell numbers which declined again over the following 6 weeks[174]. CD8+, but not CD4+, T cells showed a similar expansion due to enhanced proliferation after IL-15 administration. Reduction of lung metastases in melanoma patients was observed, however, treatment with higher

doses of IL-15 led to toxicities and elevated levels of pro-inflammatory cytokines. It must also be taken into consideration that IL-15 has a short half-life, resulting in the need for long-term administration to patients thereby enhancing the clinical side effects.

2.5.3 Improvements of IL-15 agents

Improvements in quality and efficiency of IL-15 have been made. Like mentioned before, IL-15 in complex with the IL-15α subunit is more stable and enhances the affinity to the other receptor subunits. One strategy has been the generation of a complex consisting of the recombinant protein IL-15 (rIL-15), murine IL-15Rα and the Fc portion of a human IgG1 antibody (IL-15/IL-15Rα-Fc). This complex prolongs the half-life of IL-15 from 1 hour to 20 hours[175]. Moreover, the complex shows more potent effects on immune cells with resulting improvement in anti-tumor immunity *in vivo* compared to IL-15 alone[169,176,177]. Different versions of such complexes have been created by different companies in the last years and are being tested.

2.5.4 IL-15 combination therapies

In addition to treatment with single IL-15 agents, the cytokine/cytokine complexes are used in combination with other therapies. For example, IL-15 is combined with chemotherapy to enhance anti-tumor responses where, for example, a reduction in tumor burden and longer survival of mice was observed[178,179]. The simultaneous administration of IL-15 complexes and checkpoint blocking antibodies against PD-1 and CTLA-4 enhances the activity of T cells in different tumor mouse models. Besides longer survival of the animals, tumor growth was reduced after treatment with the combination therapy[180,181]. The use of CD40 antibodies combined with IL-15 in mice results in activation of dendritic cells with following IL-15Rα expression[182]. Then, the effect of IL-15 is amplified and the anti-tumor activity of tumor-specific $CD8^+$ T cells and NK cells is enhanced[183]. After successful treatment of animals with IL-15 combination therapies, the agents are currently being tested in clinical trials to test the safety of IL-15[184]. Additionally, the most effective dose of IL-15 needs to be found to get optimal anti-cancer therapeutic treatments.

2.6 Spontaneous melanoma mouse model – Grm1

We have used a spontaneous melanoma mouse model generated by Pollock and colleagues in 2003 to study the role of NK and $CD8^+$ T cells[185]. This research group utilized a mouse mutant, TG3, carrying multiple tandem insertions of the transgene into intron 3 of the metabotropic glutamate receptor 1 (Grm1). These insertions resulted in deletion of 70kb of the intronic sequence leading to overexpression of Grm1. To only induce transgenic expression in melanocytes they created a further mouse strain in which the expression of Grm1 is driven by the *dopachrome tautomerase* (*Dct*) promotor. Dopachrome is an intermediate product in the biosynthesis of melanin. These mice, called Tg(Grm1)EPv, spontaneously develop melanomas at hairless skin regions (e.g. tail, ears) with 100% penetrance[185]. Metabotropic glutamate receptor 1 is a G-protein-coupled receptor binding *L*-glutamate followed by activation of phospholipase C. Subsequent formation of second messengers (IP3 and DAG) results in downstream signaling of pathways involving MAPK and PI3K/AKT, already known to participate in melanomagenesis[186,187]. In MAPK signaling, the G protein RAS activates RAF followed by activation of MEK and ERK leading to direct activation of transcription factors in the nucleus that regulate survival and proliferation of cells. Moreover, activation of ERK can stimulate the NF-κB pathway to also regulate survival, invasiveness and angiogenesis. The PI3K/AKT pathway activates on the one hand the mammalian target of rapamycin (mTOR) and on the other hand the NF-κB pathway resulting in cell proliferation and survival as well as cancer progression and angiogenesis[186]. Thus, overexpression of Grm1 leads to increased levels of the ligand glutamate in the extracellular space. This results in aberrant activation of the receptor in a paracrine feedback loop and constitutively activated downstream signaling[188]. Besides participation of the metabotropic glutamate receptor 1 in melanomagenesis, mutations in different other human cancer types have been observed, such as breast cancer[189-191], prostate cancer[192] and renal cell carcinoma[193].

2.7 BalbNeuT breast cancer model

In the spontaneous melanoma model (Grm1) we are able to study immune cell changes at specific time points during tumor progression and metastasis formation. To further analyze the role of immunoediting processes in metastatic progression we use another mouse model, called the BalbNeuT breast cancer model[194]. BalbNeuT mice have a gene, called *neu* (Erbb2), which is regulated by the mammary gland-specific MMTV promotor[195]. During puberty the *neu* gene is activated by this promotor resulting in development of independent carcinomas evolving to invasive tumors of the breast tissues. By transplantation of mammary glands of BalbNeuT mice into wt Balb/c mice we can change hosts and consequently the immune system (Fig.7) between primary and metastasis development. Thus, we can analyze the role of immunoediting processes after primary tumor establishment. By transplantation of mammary glands of BalbNeuT mice into immunodeficient mice lacking either NK (Balb/c IL2R$\gamma^{-/-}$) or B and T cells (Balb/c Rag2$^{-/-}$) specific roles of each immune cell population in tumor immune surveillance could be investigated closer. Besides the monitoring of tumor growth and metastasis formation *per se,* we could check immune cell subsets in the presence or absence of primary tumors/metastasis.

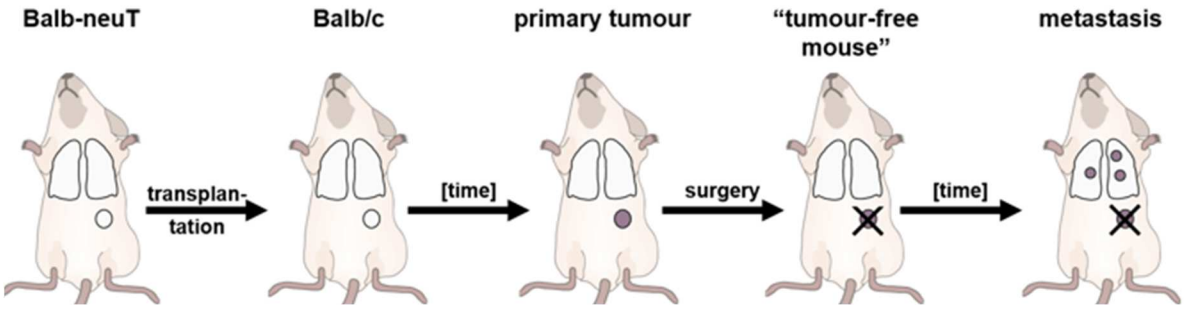

Figure 7: Schematic illustration of the BalbNeuT model

2.8 Glutamate – ligand of the Grm1 receptor

Glutamate (Glu) is known as a non-essential amino acid serving as the major excitatory neurotransmitter in the central and peripheral nervous system (CNS). Extracellular glutamate levels at physiological concentrations (1-10µM) are normally associated with processes like learning, memory and behavior[196]. Glutamate can modulate proliferation, differentiation, migration and survival of progenitor cells and immature neurons. However, aberrant Glu signaling can activate respective receptors leading to excitotoxicity, a process describing the excessive Glu release or persistence of Glu in the synaptic cleft. Massive calcium influx via ionotropic glutamate receptor channels can lead to apoptosis of neuronal cells followed by neurodegenerative diseases like Alzheimer's disease, amyotrophic lateral sclerosis, Parkinson's disease and multiple sclerosis[197-200].

Glutamate acts via different glutamate receptors. Besides the already described Grm1 receptor there are other metabotropic receptors (mGluRs) consisting of eight subtypes, mGluR1-mGluR8. These G-protein-coupled receptors are partitioned into three groups based on their sequence homology and intracellular signal transduction mechanisms. mGluR1 and mGluR5 belong to group I and are coupled to phospholipase C. Group II consists of mGluR2 and mGluR3, Group III of mGluR4, mGluR6, mGluR7 and mGluR8 whereas all are negatively coupled to adenylate cyclase[201]. Moreover, there are ionotropic receptors (iGluR) subdivided into N-methyl-D-aspartate receptors (NMDAR), 2-amino-3-hydroxy-5-methyl-oxazole-4-propionic acid (AMPA) receptors and kainic ammonia acid (KA) receptors[202]. These are ligand-gated ion channels activated after binding of the ligand.

Glutamate signaling is not only observed in the CNS, but also in peripheral tissues. *In vivo* studies with radiolabeled glutamate receptor binding agents have shown the expression of particular components of the glutamatergic system outside the CNS like in heart, kidney, intestine, lungs, muscles, liver, ovary, testis, bone and pancreas[203-205]. Glutamate is also present in blood and there is some evidence that glutamate can have different effects on immune cells, especially on T cells depending on the concentration[206].

Moreover, calcium influx can be promoted by low physiological concentrations[207]. However, at higher concentrations above 10^{-4}M Glu can have inhibitory effects on T cells[206,208,209].

During the experiments with the Grm1 model we also analyzed immune cells subsets of Grm1 Tbet$^{-/-}$ (*Tbx*$^{-/-}$) mice. Tbet is a key transcription factor involved in maturation and differentiation of naïve T cells in effector and memory T cells. We observed that Grm1 Tbet$^{-/-}$ mice showed a reduction in effector T cells and especially in central memory T cells in comparison to B6 wt mice or B6 Tbet$^{-/-}$ mice (Fig.8).

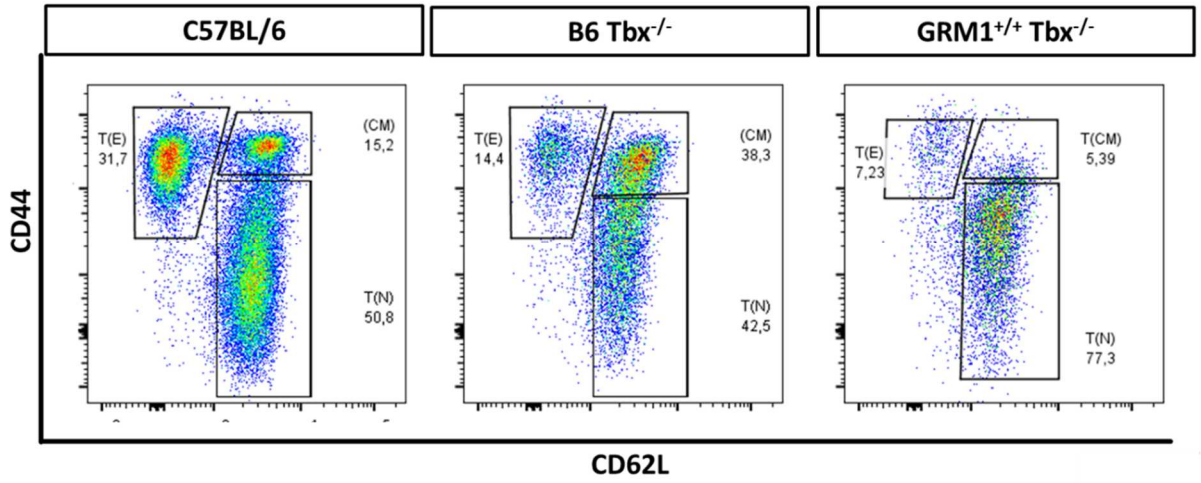

Figure 8: ***Comparison of CD8 T cell subsets in B6 wt, B6 Tbet$^{-/-}$ and Grm1 Tbet$^{-/-}$ mice.*** **Grm1 Tbet$^{-/-}$ mice show reduction of the central memory T cell subpopulation**

Moreover, recently, Shah *et al.* demonstrated elevated glutamate concentrations in mice with aberrant Grm1 expression (~50mM)[210]. Namkoong and colleagues also showed increased glutamate release by melanoma cells with constitutively activated Grm1 receptors *in vitro*[188].

On the basis of our observation and the finding of Shah *et al*., we became interested in studying the role of glutamate on different immune cells subsets in the context of spontaneous melanoma development in mice. We therefore investigated possible effects of glutamate on activation of T cells and their influence on anti-tumor activity.

2.9 Background and aim of this project

In 2014, Malaisé and other of our colleagues investigated the role of NK cells in the anti-tumor response to metastatic colorectal carcinoma (CRC) [211]. They used Balb/c Tbet$^{-/-}$ mice to evaluate the role of different subsets of NK cells. The transcription factor Tbet is important for maturation and development of NK cells. Interestingly, in Tbet$^{-/-}$ mice, terminally differentiated NK cells (CD27^{low} mature NK) do not develop. Therefore, Malaisé and co-workers hypothesized that the lack of this important subset can lead to pulmonary CRC metastases after adoptive transfer of CT26 CRC cells in Tbet$^{-/-}$ mice. They could show that intravenous injection (i.v.) of luciferase-labeled CT26 CRC cells (CT26-luc) leads to lung metastases within 8-11 days. After adoptive transfer of CT26 CRC cells in combination with sorted wt CD27$^{low/high}$ NK cells, reduced pulmonary metastasis formation was observed.

Since IL-15 is known to expand NK cells with high cytotoxic effector functions *in vivo*[212], Malaisé *et al*. treated Tbet$^{-/-}$ mice with IL-15 and injected CT26-luc cells 2 days later. They observed no metastasis formation in lungs after single dose treatment with this cytokine. Further analysis of NK cells revealed that IL-15 activated the transcription factor Eomes compensating for the lack of Tbet and enabled the formation of effector NK cells. With this study, it could be shown that distinct NK cell subsets are responsible for preventing pulmonary CRC metastases in mice. However, it must be noted that this mouse model does not reflect real metastasis formation, as intravenous injection of tumor cells is actually a “seeding” model. After intravenous infusion, tumor cells first become trapped in lungs, where they can form tumors. Therefore, in this PhD thesis work I preferentially used the spontaneous melanoma mouse model, described in section 2.6, to study the more natural role of innate and adaptive immune cell development of lung and liver metastasis during spontaneous (natural) melanoma progression. I also have used IL-15 as a treatment to boost immune cell activation and activity. The goal was to confirm the findings of Malaisé *et al*. and gain deeper insight into tumor immune surveillance. Furthermore, due to the potential activity of glutamate on T cells critical for melanoma metastasis formation in the melanoma transgenic Grm1 mouse model, I have studied the *in vitro* effects of glutamate on T cell populations, and have correlated these results with *in vivo* immune monitoring in Grm1 mice.

2.10 Hypotheses

We hypothesize that NK cells and $CD8^+$ T cells play a role in tumor immune surveillance in mice during the natural evolution process of neoplasm development, and their maturation and effector functions are inhibited over time as the cancer becomes increasingly malignant and metastatic.

2.10.1 Spontaneous melanoma mouse model – Grm1

We used the Grm1 melanoma mouse model to study the role of immune cells in tumor immune surveillance in the context of spontaneous tumor development. In previous work with a tumor-seeding model, we could observe that IL-15 activates effector immune cells *in vivo* that are able to kill tumor cells and prevent metastasis formation. We wanted to confirm these findings by treating Grm1 mice with IL-15. We hypothesized that repetitive IL-15 injections boost the immune system, which subsequently leads to slower tumor growth and smaller numbers of lung and liver metastases.

2.10.2 BalbNeuT breast cancer model

The BalbNeuT breast cancer model was used to study the role of immunoediting processes. After transplantation of mammary glands of BalbNeuT mice into Balb/c wt mice, we first expect tumor formation within several weeks. We think that malignant cells can adapt to the new microenvironment and form breast tumors. With development of tumors, we predict a change in the distribution of NK cell and $CD8^+$ T cell subsets more towards effector immune cells. Moreover, the activity of these cells should also be changed in the presence of tumor cells. After removal of the primary tumor we expect that immune cell subsets normalize again and are reactivated during metastasis formation a few weeks after curative surgery of the primary tumor. Again, we hypothesize that the activity of NK cell and $CD8^+$ T cell subsets is dependent on the absence or presence of primary or secondary tumor cells.

2.10.3 Glutamate

In pre-testing we have observed changes in the distribution of $CD8^+$ T cell subpopulations in Grm1 mice compared to wt mice. In the literature, it is described that melanocytes with aberrant Grm1 expression release high levels of glutamate *in vivo* and *in vitro*. Therefore, we hypothesize that elevated glutamate concentrations in Grm1 mice will lead to alterations in $CD8^+$ T cell subsets and effector activity.

3 Materials and methods

3.1 Materials

3.1.1 Mice

The following mice strains were either purchased from specific breeding companies or were provided by different cooperation partners:

- Grm1 wt: **Tg(Grm1)EPv** mice were provided by Anja Bosserhoff (Erlangen, Germany) and further bred in-house in our specific pathogen-free facilities. Only male mice were used for our experiments.
- Grm1 Tbet$^{-/-}$: **Tg(Grm1)EPv** mice (provided by Anja Bosserhoff, Erlangen, Germany) were crossbred with **B6.129S6-Tbx21tm1 Glm/J** mice (#004648, Jackson Laboratory) in-house in our specific pathogen-free facilities. Only male mice were used for our experiments.
- Four-week-old male wt **C57BL/6J** mice (B6) were obtained from Charles River Laboratory (Sulzfeld, Germany). They were applied as control or reference mice in the Grm1 project. Furthermore, they were used in the glutamate project.
- Four-week-old female **BalbNeuT** mice were provided by Christoph Klein (Regensburg, Germany) and served as donors for mammary gland transplantation.
- Four-week-old female wt **Balb/cJ** mice were purchased from Charles River Laboratory (Sulzfeld, Germany) and served as recipient mice in experiments for the BalbNeuT model. Furthermore, they were used in the glutamate project.

Before starting the experiments, all animals purchased by breeding companies were housed for at least one week in our specific pathogen-free facility with access to food and water *ad libitum.* Animal experiments were performed according to regulations of Upper Palatinate, Germany.

3.1.2 Reagents, cytokines and kits

- *InVivo*Mab anti-mouse NK1.1 clone PK136 (BE0036, BioXCell)
- MultiScreen-IP, 0,45µm, transparent, steril, Elispot Assay (MAIPS4510, Merck)
- Mouse IFN-γ ELISpot^{BASIC} (ALP) (3321-2A, Mabtech)
- NK Cell Isolation Kit II, mouse (130-096-892, Miltenyi)
- 1-Step™ NBT/BCIP Substrate Solution (34042, Thermo Scientific)
- Recombinant Human IL-15 Protein (247-ILB-025, R&D systems)
- Recombinant Mouse IL-15R alpha Fc Chimera Protein, CF (551-MR-100, R&D systems)
- mGluR1 (extracellular) polyclonal antibody (BML-SA610-0050, Enzo Lifesciences)
- Histofine simple stain max goat anti-rabbit polymer-HRP (414141F, Nichirei Biosciences)
- AEC+substrate-chromogen solution (K346111-2, Agilent DAKO)
- Mayers Haemalaum (109249; Merck Millipore)
- Buffer EL (79217, Qiagen)
- Foxp3 / Transcription Factor Staining Buffer Set (00-5523-00, eBioscience)
- Fixable Viability Dye eFluor506 (65-0866-14, eBioscience)
- NK Cell Isolation Kit, mouse (130-115-818, Miltenyi)
- Cell Proliferation Dye eFluor™ 450 (65-0842-85, eBioscience)
- Annexin V Apoptosis Detection Kit APC (88-8007-74, eBioscience)
- CellTrace Far Red Cell proliferation dye (C34564, ThermoFisher Scientific)
- YOYO-1 Iodide (Y3601, ThermoFisher Scientific)
- mTRAP^{TM} Lysis Buffer (29011, Active Motif)
- Rat anti-Mouse CD107a (1D4B, RUO), PE (558661, BD Pharmingen)
- GolgiPlug: Protein Transport Inhibitor (Containing Brefeldin A) (555029, BD Bioscience)
- GolgiStop: Protein Transport Inhibitor (Containing Monensin) (554724, BD Bioscience)

- Naive CD8a$^+$ T Cell Isolation Kit, mouse (130-096-543, Miltenyi)
- Cell Proliferation Dye eFluor™ 670 (65-0840-85, eBioscience)
- Anti-mouse CD3e Monoclonal Antibody (145-2C11) (14-0031-86, eBioscience)
- Anti-mouse CD28 Monoclonal Antibody (37.51), Functional Grade (16-0281-82, eBioscience)
- Mouse IL-2 (130-094-055, Miltenyi)
- Purified NA/LE Hamster Anti-Mouse CD178 (MFL3) (555290, BD Bioscience)
- L-glutamic acid monosodium salt hydrate (G5889, Sigma Aldrich)
- CD8a$^+$ T Cell Isolation Kit, mouse (130-104-075, Miltenyi)
- Fura-2, AM, cell permeant (F1201, ThermoFisher Scientific)
- Pluronic^{TM} F-127 (Thermo Fisher Scientific)
- Naive CD4$^+$ T Cell Isolation Kit, mouse (130-104-453, Miltenyi)
- RT^2 qPCR Primer Assay Plate (24 plates) (CLAM35809, Qiagen)
- RT² SYBR Green qPCR Mastermix (24) (330503, Qiagen)

3.1.3 Buffers, Media

- DPBS, no calcium, no magnesium (14190-094, Gibco/ThermoFisher Scientific)
- 10x MACS: 27,5g BSA, 22ml EDTA, 500ml DPBS
- 1% PFA in PBS pH 7,4
- RPMI 1640 (31870-074, Gibco)
- Fetal Bovine Serum (26140079, Gibco)
- L-Glutamine solution (G7513, Sigma Aldrich)
- Penicillin-Streptomycin (P0781, Sigma Aldrich)
- 2-Mercaptoethanol (50 mM) (31350010, Gibco)
- Ringer solution: 140mM NaCl, 5mM KCl, 2mM $CaCL_2$, 100µM Glycine, 10mM HEPES, pH 7.35

3.1.4 Cell lines

- Yac-1 (86022801; Sigma-Aldrich): suspension cells, mouse lymphoma, induced by inoculation of Moloney leukaemia virus into a new-born A/Sn mouse

- A20 (ATCC TIB-208, ATCC): suspension cells, reticulum cell sarcoma, Balb/cAnN

3.1.5 Flow cytometry antibodies

	Antibody (Clone)	Species Reactivity	Company	Cat.nr.
FITC	NK1.1	M	eBioscience	11-5941-85
	CD8a (53-6.7)	M	eBioscience	11-0081-85
	CD11c (N418)	M	eBioscience	11-0114-85
	CD127 (A7R34)	M	eBioscience	11-1271-85
	CD4 (GK1.5)	M	eBioscience	11-0041-86
	CD28 (CD28.2)	M	eBioscience	11-0289-41
	CD69 (H1.2F3)	M	eBioscience	11-0691-81
PE	CD335 (NKp46) (29A1.4)	M	eBioscience	12-3351-82
	TCR gamma/delta (eBioGL3 (GL-3, GL3))	M	eBioscience	12-5711-82
	FOXP3 (NRRF-30)	M	eBioscience	12-4771-82
	CD4 (RM4-5)	M	eBioscience	12-0042-83
	CD8a (53-6.7)	M	eBioscience	12-0081-83
	EOMES (Dan11mag)	M	eBioscience	12-4875-82

	Rat IgG2a kappa Isotype Control (eBR2a)	M	eBioscience	12-4321-80
	CD25 (PC61.5)	M	eBioscience	12-0251-81
	NK1.1 (PK136)	M	eBioscience	12-5941-83
PE-Cyanine7	CD27 (LG.7F9)	M	eBioscience	25-0271-82
	CD44 (IM7)	M	eBioscience	(25-0441-82
	Ly6G/Ly-6C (Gr-1) (RB6-8C5)	M	eBioscience	25-5931-82
	CD4 (RM4-5)	M	eBioscience	25-0042-82
	CD8a (53-6.7)	M	eBioscience	25-0081-82
	T-bet (eBio4B10 (4B10))	M	eBioscience	25-5825-82
	Mouse IgG1 kappa Isotype Control (P3.6.2.8.1)	M	eBioscience	25-4714-80
	CD134 (OX40) (OX-86)	M	eBioscience	25-1341-80
APC	KLRG1 (2F1)	M	eBioscience	17-5893-82
	CD4 (GK1.5)	M	eBioscience	17-0041-83
	CD8a (53-6.7)	M	eBioscience	17-0081-83
	CD25 (PC61.5)	M	eBioscience	17-0251-82
	CD335 (NKp46) (29A1.4)	M	eBioscience	17-3351-82

	CD152 (CTLA-4) (UC10-4B9)	M	eBioscience	17-1522-82
	Armenian Hamster IgG Isotype Control (eBio299Arm)	M	eBioscience	17-4888-82
APC-eFluor780 (APCCy7)	CD3e (145-2C11)	M	eBioscience	47-0031-82
	CD4 (GK1.5)	M	eBioscience	47-0041-82
eFluor 450 (PB)	CD11b (M1/70)	M	eBioscience	48-0112-82
	CD62L (L-Selectin) (MEL-14)	M	eBioscience	48-0621-82
	CD4 (RM4-5)	M	eBioscience	48-0042-82
	CD8a (53-6.7)	M	eBioscience	48-0081-82
	CD279 (PD-1) (RMP1-30)	M	eBioscience	48-9981-80
	Rat IgG2b kappa Isotype Control (eB149/10H5)	M	eBioscience	48-4031-82
	CD25 (PC61.5)	M	eBioscience	48-0251-82

3.2 Methods

3.2.1 Evaluation of tumor formation and – progression in Grm1 mice

Grm1 mice spontaneously develop melanomas in hairless skin regions at a certain time point in their development. Bosserhoff and colleagues established a specific 6-point grading system allowing the categorization of melanomas at different stages[213]. For evaluation ears, tail and anus are considered (Fig. 9). At grade 1, the first melanomas are palpable, but not visible. Grade 2 describes small, clearly visible melanomas on the ears. This stage declares the "tumor onset" for experiments which will be described later. Grade 3 – 5 includes melanomas on the ears, as well as thickenings and tumor knots at the tail and perianal regions. Strong tumor formation with risk of ulcerations is specified as tumor grade 6. At this stage mice are killed to avoid any serious effects of tumor burden.

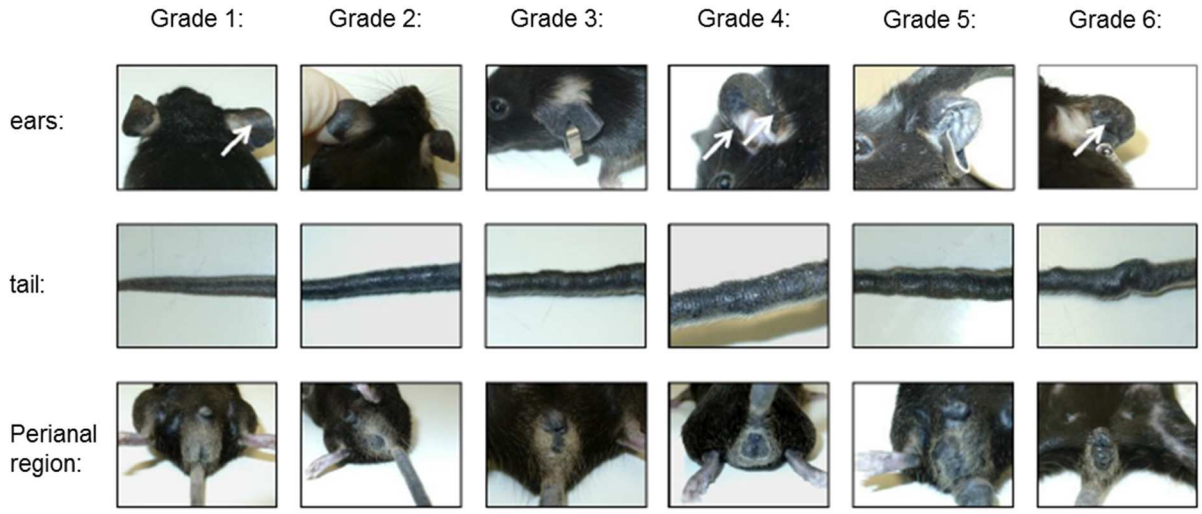

Figure 9: ***Grading system for evaluation of tumor formation and –progression in Grm1 mice*** [213]**. Grade 1: palpable, but invisible melanomas on the ears; grade 2: "tumor onset" – small, clearly visible melanomas on the ears; grade 3-5: melanomas on the ears and thickenings at the tail and perianal regions; grade 6: tumor formation with risk of ulcerations.**

3.2.2 IFNγ- Elispot of NK cells

On day 1, a MB Multiscreen PVDF plate (MAIPS4510, Millipore) was pre-coated with 15µg/ml IFNγ antibody (3321-2A, vial 1, green top, AN18, Mabtech) and incubated overnight (o/n) at 4°C. The next day (day 2), the plate was washed with PBS followed by blocking with full medium for 2 hours (h) at room temperature (RT). NK cells were isolated from spleens by using the NK cell isolation Kit II (130-096-892, Miltenyi). Effector and target cells were set up at different E:T ratios with a target cell number of 50,000 cells per well; the ratios were set at 1:1, 2:1 and 3:1. Cells were incubated together in the plates o/n at 37°C. On day 3, the plate was washed with PBS followed by incubation with 1 µg/ml detection antibody (3321-2A, vial 2, yellow top, R4-6A2, Mabtech) for 2h at RT. The antibody was diluted in PBS containing 0.5% FCS. Before and after addition of 100µl streptavidin-alkaline phosphatase conjugate (3321-2A, vial 3, white top, Mabtech) to each well, for 1h at RT in the dark, the plate was washed again with PBS. 100µl 1-Step NBT/BCIP (nitro-blue tetrazolium chloride/5-bromo-4-chloro-3'-indolyphosphate p-toluidine salt) substrate solution (34042, ThermoFisher Scientific) was added to each well and incubated for 7 minutes at RT in the dark. The reaction was stopped with tap water followed by three further washing steps with water. The plate was left to dry o/n at RT. On day 4, spots were counted with a specific Elispot reader (EliSpot Robotic System ELROB05i, AID Advanced Imaging Devices GmbH Straßberg).

3.2.3 Treatment of Grm1 mice with NK cell-depleting antibody PK136

To deplete NK cells in Grm1 mice, 5 week-old animals received an intraperitoneal (i.p.) injection of 200µg PK136 antibody, which is considered day 0 (BE0036, BioXCell). At this time, Grm1 mice did not yet show tumor formation. The antibody had a stock concentration of 9.3mg/ml and was kept in PBS. At day 2, mice received a second application of the same NK-depleting antibody, followed by weekly injection until reaching tumor grade 2. After tumor detection, treatment with the NK-depleting antibody was stopped and tumor grade monitoring was continued for further 8 weeks.

3.2.4 Preparation of soluble IL-15 pre-complexed to IL-15Rα

A cytokine–receptor complex containing a human recombinant IL-15 protein and a recombinant fusion protein consisting of the ectodomain of the mouse IL-15Rα-chain and human IgG1-Fc (IL-15Rα/Fc) were purchased from R&D Systems (Minneapolis, USA). IL-15 and IL-15Ra/Fc were resuspended in PBS solution and freshly mixed together at a ratio of 1:6 (IL-15:IL-15Ra/Fc). Before using the mixture for *in vivo* injections or *in vitro* experiments, it was incubated at 37°C for 30 min.

3.2.5 Treatment of Grm1 mice with pre-complexed IL-15

Grm1 mice were checked weekly for tumor formation. Melanomas were classified by the previously mentioned 6-point grading system (chapter 3.2.1). On the day of tumor onset, i.e. when Grm1 mice reached tumor grade 2, they received an i.p. injection of the IL-15/IL-15Rα/Fc complex for stimulating immune cells. One set of mice was used for extensive analysis of immune cell phenotypes on day 4 after the first IL-15 injection (chapter 3.2.7 and 3.2.8.2). Another set of mice received a second IL-15 injection on day 30. Tumor progression was monitored in these mice until day 60 followed by immune cell analysis (see chapter 3.2.7). Untreated Grm1 mice were monitored for the same time periods and analyzed at indicated time points. These mice served as a reference group.

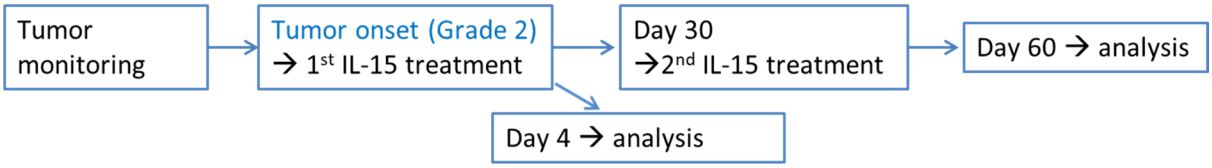

Figure 10: ***Experimental setup of IL-15 treatment in Grm1 mice***

3.2.6 Counting of metastases in lung and liver sections of Grm1 mice

Small lung and liver pieces were harvested 60 days after tumor onset of Grm1 mice. The organs were fixed in paraformaldehyde and embedded in paraffin. Immunostaining was performed on 3 µm serial sections. Slides were stained with a purified polyclonal rabbit mGluR1 antibody (BML-SA610, Enzo Lifesciences) followed by a secondary Histofine simple stain max goat anti-rabbit polymer-HRP (414141F,

Nichirei Biosciences) for detection. Sections were exposed to an AEC+substrate-chromogen solution (K346111-2, Agilent DAKO) complemented by visualization with Mayers Haemalaum (109249; Merck Millipore). Slides were analyzed and images were acquired with a Zeiss Axio Observer Z1 microscope (Carl Zeiss, Munich, Germany).

3.2.7 Phenotypical analysis of different immune cell subpopulations in Grm1 mice on day 4 and day 60

Spleen cells were isolated as a single cell suspension on day 4 and day 60 and used for further immune cell analysis. One million cells per flow cytometry tube were stained with the Fixable Viability Dye eFluor506 (65-0866-14, eBioscience) diluted 1:1000 in PBS followed by further washing with MACS (PBS +BSA+EDTA) and PBS. Afterwards, cells were stained with antibodies listed in the following table:

Table 3: Immune cell panels for flow cytometry analysis - surface and intracellular staining

Fluorophore	NK cells	$CD8^+$ T cells	MDSCs	CD4 T_{regs} (IC)
FITC	NK1.1	CD8	CD11c	CD127
PE	NKp46	gdTCR	-	Foxp3 (IC)
PeCy7	CD27	CD44	GR-1	-
APC	KLRG1	CD4	CD8	CD25
APCCy7	CD3	CD3	CD3	CD3
PacificBlue	CD11b	CD62L	CD11b	CD4

Flow cytometry was performed on a FACSCanto II (BD Biosciences). Data were analyzed using FlowJo software (Tree Star, Ashland, OR, USA).

3.2.8 Cytotoxicity assay of NK cells from Grm1 mice

3.2.8.1 *In vitro* stimulation

For *in vitro* assays, NK cells were isolated from splenic single- cell suspensions by a NK cell isolation kit (130-115-818, Miltenyi) with the autoMACS Pro Separator (130-092-545, Miltenyi). Sorted NK cells were then cultured in full medium containing pre-complexed IL-15 (8µl/ml) for 24 hours. Untreated NK cells were also cultured and used as control cells. The next day, Yac-1 lymphoma cells were stained with the cell proliferation dye eFluor450 (65-0842-85, eBioscience) allowing the later distinction between NK cells and Yac-1 cells. Finally, NK cells were cultured with Yac-1 cells in different E:T ratios (1:1, 10:1) for a further 24 hours. After harvesting, the cells were stained with an Annexin V Apoptosis Detection Kit APC (88-8007-74, eBioscience) and analyzed on the FACSCanto II.

3.2.8.2 *In vivo* stimulation

For *in vivo* assays, Grm1 mice were treated with pre-complexed IL-15; control mice did not receive the IL-15 treatment. After 4 days, spleen cells were harvested and NK cells were isolated with the aforementioned isolation kit. Again, Yac-1 cells were pre-stained with the proliferation dye followed by cultivation with NK cells in different E:T ratios (1:1, 10:1). After 24 hours, cells were harvested and stained with the apoptosis kit, as indicated above.

3.2.9 IncuCyte®

NK cells were isolated from spleens of Grm1 wt and B6 wt mice with the NK cell isolation kit (130-115-818, Miltenyi). Cells were either treated with pre-complexed IL-15 or only with medium o/n at 37°C and 5% CO_2. The next day, to later distinguish effector and target cells, NK cells were stained with the CellTrace Far Red Cell proliferation dye (C34564, ThermoFisher Scientific). Afterwards, pre-stained NK cells were cultured with Yac-1 lymphoma cells complemented with medium containing YOYO-1 iodide (Y3601, ThermoFisher Scientific); this dye stains dead cells by binding to the DNA of apoptotic cells. The cells were incubated for at least 24 hours in the Incucyte® machine (4647, Sartorius), taking fluorescence images every one to two

hours which can later be analyzed with the specific Incucyte® software (Sartorius). The program is able to distinguish red-colored cells demonstrating NK cells and green cells representing dead cells. An overlay of both colors reveals dead NK cells.

3.2.10 Analysis and sorting of immune cell subsets at different time points after IL-15 treatment in Grm1 wt and B6 wt mice

Grm1 mice were checked weekly for melanomas and characterized by the 6-point grading system (described in chapter 3.2.1). In the following scheme (Fig. 11) a timeline is given to show treatment of Grm1 mice with IL-15. Furthermore, different time points are shown where the analysis of immune cell subsets was performed (panels described in 3.2.7). Moreover, besides Grm1 mice, IL-15 treatment was given to B6 wt mice to evaluate differences between tumor-bearing and non-tumor-bearing mice.

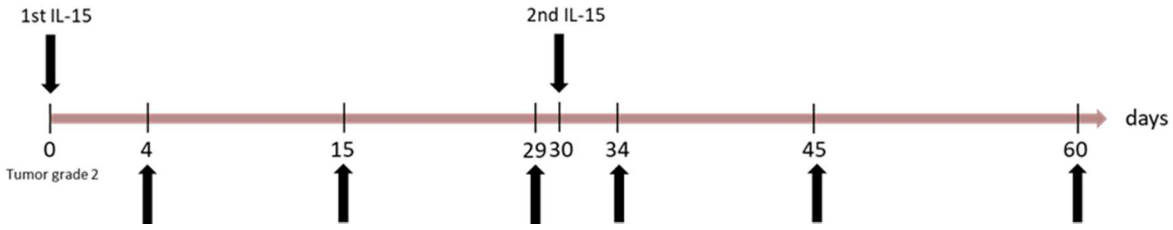

Figure 11: *Timeline for treatment and analysis of Grm1 and B6 wt (reference) mice*

In addition to surface and intracellular staining of different immune cell subsets, NK cells were sorted using a BD FACSAria sorter (BD Biosciences). Therefore, spleen cells were stained with the following panel: NK1.1-PE, NKp46-APC and CD3-APCCy7. 300 cells of NK cells were transferred into mTRAP lysis buffer containing tRNAs to avoid the degradation of mRNA. The cells were stored at -80°C until isolation of mRNA and amplification of cDNA in a whole transcriptome amplification (WTA) procedure.

3.2.11 Whole transcriptome amplification (WTA)

For subsequent RT^2 profiling, cDNA from sorted NK cells was isolated and amplified in a process called WTA according to protocols provided by AG Klein (Experimental Medicine, Regensburg). This method was performed by Jana Koch (Stuttgart, Germany). First, cells were lysed to release mRNA containing polyA tails. Biotinylated peptide nucleic acids (PNAs) were added which bind to polyA ends. mRNA was then fished by streptavidin-conjugated beads. Next, RT primers were hybridized to mRNA and cDNA was synthesized in a reverse transcription. After release of cDNA from beads, polyG tails were terminally added for following amplification of total cDNA with specific single CP2 primers. Obtained cDNA was finally quality control checked through PCR with WTA positive and negative controls, followed by re-amplification to gain enough material for a RT² profiler.

3.2.12 RT² Profiler and single qPCR

An RT² profiler assay is a multiplex PCR for detection of multiple different genes from different samples at the same time. For gene expression analysis from NK cells of the Grm1 timeline, isolated cDNA (obtained by WTA, described in chapter 3.2.11) from cells was added to 96-well plates pre-coated with primers for different genes which are listed in Table 4. Plates were ordered from Qiagen (RT^2 qPCR Primer Assay Plate, CLAM35809, Qiagen). A ready-to-use PCR master mix (RT² SYBR Green qPCR Mastermix, 330503, Qiagen) was added to the wells and a qPCR was run using the LightCycler® 480 Instrument II (05015278001, Roche). Qiagen was recommended the use of different housekeeper genes and other controls for a better analysis of data. As housekeepers we used: GAPDH (Gadph), beta-actin (Actb), HSP90AB1 (Hsp90ab1). The controls were: Genomic DNA control (GDC), Reverse Transcription control (RTC) and PCR positive control (PPC).
As control and confirmation of the RT² profiler assay, we additionally performed single qPCRs of samples with primers ordered from Qiagen:

1. Beta-actin: Mm_Actb_1_SG (# QT00095242)
2. Eomesodermin: Mm_Eomes_1_SG (#QT01074332)
3. NKG2D: Mm_Klrk1_1_SG (#QT00104363)

Table 4: Genes for RT2 profiler of NK cells

Gene	Gene name	Gene	Gene name
Interferon gamma (IFNγ)	Ifng	**NKG2A**	Klrc1
Granzyme B	Gzmb	**CD244**	Cd244
Perforin	Prf1	**FAS**	Fas
Bcl-2	Bcl2	**TNF receptor**	Tnfrsf1
NKG2D	Klrk1	**TIGIT**	Tigit
NKp46	Ncr1	**CTLA-4**	Ctla4
CXCR3	Cxcr3	**PD-1**	Pdcd1
Eomesodermin	Eomes	**Tbet**	Tbx21
KLRG1	Klrg1	**LAMP-1**	Lamp1

3.2.13 Transplantation of mammary glands of Balb-NeuT mice to Balb/c wt mice

The following operation was done by workers of AG Klein (Regensburg, Germany). Balb-NeuT donor mice were killed after the third to fifth week of life. Mammary glands of the right and left breasts were harvested and tissues were cut into 2x2x2 pieces that were stored in PBS until transplantation to recipient mice. Balb/c wt recipient mice were then anesthetized intraperitoneally with 5mg/kg Midazol, 0.05mg/kg Fentanyl and 0.5mg/kg Medetomidin. After shaving and disinfection of the affected area the upper skin layer at mammary glands was cut medially with a specific “V” section. Mammary glands were removed and replaced with mammary glands of the donor mouse. The wound was sewn with four to six stitches and mice received a subcutaneous injection of an antagonist mixture (Flumazenil 0.5 mg/kg, Atipamezol 2.5mg/kg, Naloxon 1.2 mg/kg) to awake them from anesthesia.

3.2.14 Monitoring of primary tumor development and curative surgery

Recipient mice were weekly monitored for tumor growth after transplantation of Balb-NeuT mammary glands. Breast tissue and the growing primary tumor were palpated and tumor growth was measured with a caliper. When the tumor reached ~ 1cm, it was removed in the same surgical procedure as the mammary glands transplanted as described above (chapter 3.2.13). Recipient mice were killed at different time points after this curative surgery (CS) for analysis. One set of mice was killed at the day of CS; a second set of mice was analyzed 5 weeks after CS and a third set of mice was killed 17 weeks after CS. For this experiment, spleen and lung were harvested for flow cytometry analysis to check NK and $CD8^+$ T cell subsets (chapter 3.2.15). A CD107a degranulation assay was performed to measure NK cell activity (chapter 3.2.16).

3.2.15 Phenotypical analysis of different immune cell subpopulations in the Balb-NeuT model

As mentioned above, NK cell and $CD8^+$ T cell subsets were analyzed at indicated time points (CS, CS+5 weeks, CS+17 weeks). The staining procedure is described in 3.2.7 and the following flow cytometry panels were used:

Table 5: Immune cell panels for flow cytometry analysis - surface staining

Flourophore	NK cells	$CD8^+$ T cells
FITC	-	CD8
PE	NKp46	gdTCR
PeCy7	CD27	CD44
APC	KLRG1	CD4
APCCy7	CD3	CD3
PacificBlue	CD11b	CD62L

3.2.16 CD107a degranulation assay

For the CD107a degranulation assay, 200,000 isolated splenocytes or lung cells were cultured with either medium (Table 6, Condition 1: “spontaneous”) or 7,500 A20 tumor cells (Table 6, Condition 2: “Kill”). CD107a-PE (558661, BD Biosciences) (2.5µl/ml EV) was added to each well followed by incubation at 37°C for 1.5h. Afterwards, GolgiPlug (1µl/ml EV, 555029, BD Biosciences) and GolgiStop (4µl/6ml EV, 554724, BD Biosciences) were added to each condition, then incubated for a further 4h at 37°C. For analysis, cells were harvested and stained with the Fixable Viability Dye eFluor506 (65-0866-14, eBioscience) diluted 1:1000 in PBS followed by staining with the following antibodies: CD8-FITC, CD27-PeCy7, NKp46-APC, CD3-APCCy7. Flow cytometry was performed using a FACSCanto II (BD Biosciences) and the data were analyzed using FlowJo software (Tree Star, Ashland, OR, USA).

Table 6: Pipette scheme of CD107a degranulation assay

Condition	Splenocytes/ Lung cells	Tumor cells	Medium	CD107a - PE	GolgiPLUG	GolgiSTOP
1	✓	-	✓	✓	✓	✓
2	✓	✓	-	✓	✓	✓

3.2.17 Measurement of glutamate concentrations in serum and skin samples of B6 wt and Grm1 Tbet$^{-/-}$ mice

Serum samples were collected from the blood of B6 wt and Grm1 Tbet$^{-/-}$ mice. Skin pieces from tails and ears of the aforementioned mice were collected as well and sent together with serum samples to the company MetaSysX (Potsdam-Golm, Germany), where they performed absolute quantification of glutamate concentrations. The samples were measured with an Agilent Technologies Gas Chromatography (GC) coupled to a Leco Pegasus HT mass spectrometer, which consists of an Electron Impact ionization source (EI), and a Time of Flight (TOF) mass analyzer.

3.2.18 Analysis of differentiation and proliferation of naïve CD8$^+$ T cells after addition of different concentrations of glutamate

Naïve CD8$^+$ T cells were isolated from splenocytes of B6 wt mice with an isolation kit (#130-096-543, Miltenyi) and stained with the cell proliferation dye eFluor670 (#65-0840-85, eBiosciences). 100,000 naïve CD8$^+$ T cells were pipetted into a 96-well plate pre-coated with anti-CD3 antibody (4µl/ml). A stimulation mix containing anti-CD28 antibody (1µl/ml), IL-2 (5µl/ml) and FasL (10µl/ml) was added. Moreover, the following different glutamate concentrations (final) were also added to wells: 0µM, 5µM, 10µM, 50µM, 100µM, 500µM, 1mM, 5mM, 10mM and 50mM. After 4 days, CD8$^+$ T cells were harvested and stained with the following antibodies to check for proliferation and differentiation: CD8-FITC, CD44-PeCy7, CD3-APCCy7 and CD62L-PB.

3.2.19 Calcium (Ca^{2+}) influx

$CD8^+$ T cells were isolated from splenocytes of B6 wt mice with an isolation kit (#130-104-075; Miltenyi). 100,000 $CD8^+$ T cells were pipetted into a 96-well plate pre-coated with an anti-CD3 antibody (10µl/ml). An anti-CD28 antibody (2µl/ml) was added followed by incubation for 3 days. After harvesting, cells were washed with Ringer buffer containing glycine. Magnesium was not added to the buffer because of possible interference with later calcium influx. Cells were then stained with 2µM of Ca^{2+} indicator Fura-2-AM (Thermo Fisher Scientific, Waltham, USA) and 0.05% pluronic F-127 (Thermo Fisher Scientific, Waltham, USA) for 30-45min at RT in the dark. After incubation, cells were washed once with Ringer solution and pipetted onto a glass coverslip. After attachment of cells for a few minutes, different glutamate concentrations were added and cells with increasing Ca^{2+} influx were monitored using a Zeiss inverted microscope (Axio Observer Z.1). Changes in intracellular free Ca^{2+} ($[Ca^{2+}]_i$) were recorded at 2-s intervals altering the wavelength of excitation light between 340 and 380 nm. Ca^{2+} images were acquired from 20-30 $CD8^+$ T cells using ZEN 2012 software (ZEISS, Jena, Germany) and analyzed with ImageJ.

3.2.20 Annexin V / PI assay

Naïve $CD8^+$ T cells were isolated from splenocytes of B6 wt mice with an isolation kit (#130-096-543, Miltenyi). 100,000 naïve $CD8^+$ T cells were added to a 96-well plate pre-coated with an anti-CD3 antibody (4µl/ml). A stimulation mix containing anti-CD28 antibody (1µl/ml), IL-2 (5µl/ml) and FasL (10µl/ml) was added. Moreover, the following different glutamate concentrations (final) were added to the wells: 0µM, 5µM, 10µM, 50µM, 100µM, 500µM, 1mM, 5mM, 10mM and 50mM. After 4, 24 and 48 hours, $CD8^+$ T cells were harvested and stained with an Annexin V Apoptosis Detection Kit APC (88-8007-74, eBioscience) followed by analysis of cell death using the FACSCanto II.

3.2.21 Analysis of activation marker expression of CD8$^+$ T cells after addition of different concentrations of glutamate

Naïve CD8$^+$ T cells were isolated from splenocytes of B6 wt mice with an isolation kit (#130-096-543, Miltenyi). 100,000 naïve CD8$^+$ T cells were added to a 96-well plate pre-coated with an anti-CD3 antibody (4µl/ml). A stimulation mix containing anti-CD28 antibody (1µl/ml), IL-2 (5µl/ml) and FasL (10µl/ml) was added. Moreover, the following different glutamate concentrations (final) were added to the wells: 0µM, 5µM, 10µM, 50µM, 100µM, 500µM, 1mM, 5mM, 10mM and 50mM. After 3 days of incubation, cells were harvested and stained with the Fixable Viability Dye eFluor506 (65-0866-14, eBioscience) diluted 1:1000 in PBS followed by staining with the following antibodies in different panels: CD28-FITC, CD69-FITC, CD25-PE, CD8-APC, CD3-APCCy7 and CD4-PB.

3.2.22 Analysis of Eomesodermin (Eomes) and Tbet expression of CD8$^+$ T cells after addition of different concentrations of glutamate

Naïve CD8$^+$ T cells were isolated from splenocytes of B6 wt mice with an isolation kit (#130-096-543, Miltenyi). 100,000 naïve CD8$^+$ T cells were added to a 96-well plate pre-coated with an anti-CD3 antibody (4µl/ml). A stimulation mix containing anti-CD28 antibody (1µl/ml), IL-2 (5µl/ml) and FasL (10µl/ml) was added. Moreover, the following different glutamate concentrations (final) were added to the wells: 0µM, 5µM, 10µM, 50µM, 100µM, 500µM, 1mM, 5mM, 10mM and 50mM. After 3 days, cells were harvested and stained with the Fixable Viability Dye eFluor506 (65-0866-14, eBioscience) diluted 1:1000 in PBS followed by staining with the following antibodies: Eomes-PE (IC stain), Tbet-PeCy7 (IC stain), CD8-APC, CD3-APCCy7 and CD4-PB.

3.2.23 Mixed leukocyte reaction (MLR) of B6 CD8$^+$ T cells and Balb/c splenocytes

Splenocytes of B6 wt and Balb/c wt mice were isolated as single cell suspensions. CD8$^+$ T cells were isolated from splenocytes of B6 wt mice with an isolation kit (#130-104-075; Miltenyi) and stained with a cell proliferation dye eFluor670 (#65-0840-85, eBiosciences). Stained B6 CD8$^+$ T cells and Balb/c splenocytes were mixed in a 1:1 ratio in a 96-well plate. The following different glutamate concentrations (final) were

added to wells: 0µM, 5µM, 10µM, 50µM, 100µM, 500µM, 1mM, 5mM, 10mM and 50mM. After 3 days, cells were harvested and stained with the Fixable Viability Dye eFluor506 (65-0866-14, eBioscience) diluted 1:1000 in PBS followed by staining with the following antibodies to check for proliferation and differentiation of $CD8^+$ T cells: CD8-FITC, CD4-PE, CD44-PeCy7, CD3-APCCy7 and CD62L-PB.

3.2.24 Analysis of activation marker expression of $CD4^+$ T cells after addition of different concentrations of glutamate

Naïve $CD4^+$ T cells were isolated from splenocytes of B6 wt mice with an isolation kit (#130-104-453, Miltenyi). 100,000 naïve $CD4^+$ T cells were added to a plate pre-coated with an anti-CD3 antibody (4µl/ml). A stimulation mix containing anti-CD28 antibody (1µl/ml) and IL-2 (5µl/ml) was added. The following different glutamate concentrations (final) were added to wells: 0µM, 5µM, 10µM, 50µM, 100µM, 500µM, 1mM, 5mM, 10mM and 50mM. After 2 days $CD4^+$ T cells were harvested and stained with the Fixable Viability Dye eFluor506 (65-0866-14, eBioscience) diluted 1:1000 in PBS followed by staining with the following antibodies: CD69-FITC, Foxp3-PE (IC stain), CD134-PeCy7, CD4-APC, CD3-APCCy7 and CD25-PB.

3.2.25 Statistics

All statistical analyses were performed using GraphPad Prism, version 7 (GraphPad Software, Inc., San Diego, CA, http://www.graphpad.com). Generally, differences with a p value ≤ 0.05 were considered to be statistically significant. However, the significance is further categorized dependent of the strength of significance:

- ns = $p > 0.05$,
- * = $p \leq 0.05$
- ** = $p \leq 0.01$
- *** = $p \leq 0.001$
- **** = $p \leq 0.0001$

Depending on each experiment, different statistical tests were applied. When we compared two groups, e.g. a control group (untreated/ unstimulated) and a test group (treated/ stimulated), a simple student's unpaired t-test was performed for statistical analysis. This test compares two mean values with each other and determines if they are significantly different. The influence of different categorically independent variables on one continuous dependent variable were analyzed using two-way ANOVA. Different post-hoc tests were performed depending on the problem of the experiment. Sidak´s multiple comparison test was used to calculate familywise error rates by comparing the mean values of different conditions of one group with mean values of the same conditions of another group. A Tukey´s multiple comparison test was used when we compared mean values of every treatment with the mean values of every other treatment. With a Dunnett´s multiple comparison test, we compared all means with the mean of a control group.

4 Results

4.1 Spontaneous melanoma mouse model - Grm1

4.1.1 Activity of Grm1 NK cells was similar to B6 wt NK cells

Since Grm1 mice spontaneously form tumors within their normal growth and development, we hypothesized that NK cells of tumor-bearing mice would be more active due to tumor antigen exposure compared to NK cells of B6 wt mice not developing tumors. To confirm this, we verified the amount of IFN-γ-producing NK cells isolated from B6 wt and Grm1 mice by an IFN-γ-Elispot (method section 3.2.2). At different E:T ratios, NK cells were cultivated with Yac-1 lymphoma cells for 24 hours. As negative controls, NK cells of both mouse strains were cultured only with medium. As expected, we observed that higher E:T ratios produced more positive spots (Fig.12), and IFN-γ-producing NK cells were only increased in the presence of tumor cells. Importantly, the number of IFN-γ-producing NK cells tended to be higher in Grm1 mice, but the difference was not significant at any of the ratios tested ($p>0.05$ for each comparison). Therefore, contrary to our expectations, Grm1 NK cells did not clearly show higher activity versus B6 wt NK cells.

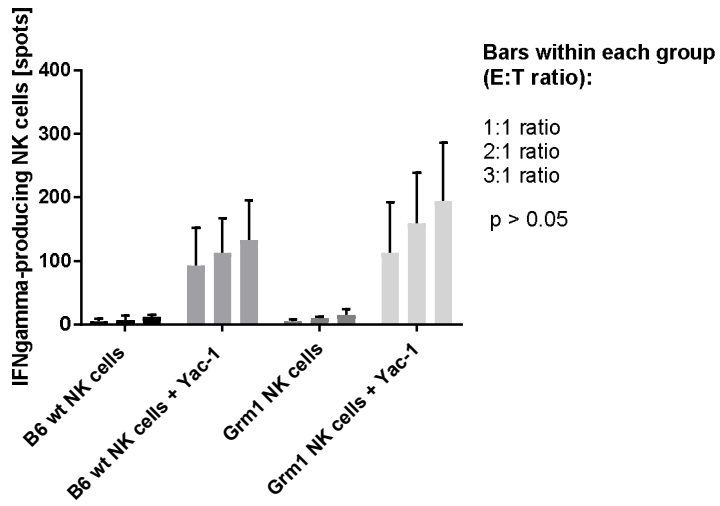

Figure 12: ***IFN-γ-Elispot of NK cells of B6 wt and Grm1 mice.*** **Isolated B6 wt and Grm1 NK cells were cultivated o/n either alone or in co-culture with Yac-1 lymphoma cells. Next day, IFN-γ-producing NK cells were detected and counted as spots on Elispot plates with specific Elispot software. Within each group different E:T ratios were set up (1:1, 2:1, 3:1). Statistical tests: Comparison of B6 wt and Grm1 (NK cells alone or cultivated with Yac-1 cells), n=2/each with triplicates, mean values with standard deviation (SD), two-way ANOVA, Sidak´s multiple comparisons test, p values > 0.05.**

4.1.2 NK cell depletion in Grm1 mice had no influence on tumor onset and tumor progression

In the previous experiment, we wanted to check the general activity of Grm1 NK cells against tumor cells *in vitro*. Since NK cells are a major part of tumor immune surveillance and control tumor onset and growth, we hypothesized that Grm1 mice depleted of NK cells would show an earlier tumor development and a faster tumor growth compared to immunocompetent mice. To confirm this, five-week-old Grm1 mice were repeatedly treated with the NK cell-depleting antibody PK136 (method section 3.2.3), until they reached tumor stage 2 (the day of first tumor appearance). Grm1 mice that did not receive this antibody served as control mice ("untreated"). The animals were checked weekly for tumor formation and progression by the 6-point grading system described in the methods section 3.2.1. However, as it is illustrated in Figure 13, mice which were treated with PK136 did not show significantly earlier tumor onset, although there was a tendency towards earlier tumor appearance (p=0.0726). Moreover, tumors of mice with missing NK cells did not grow faster compared to tumors of untreated mice (Fig. 14). Taken together, depletion of NK cells did not significantly reduce the time before tumor onset and tumor growth was not altered.

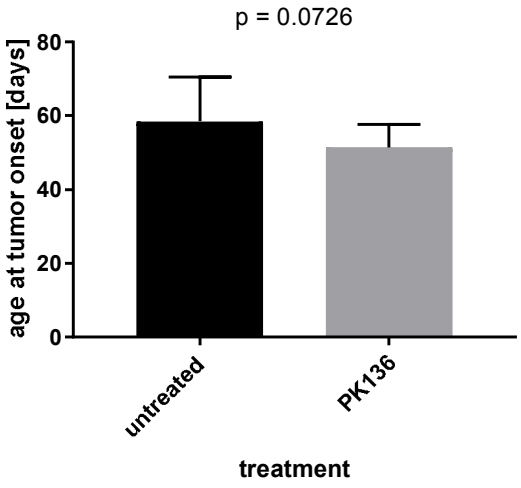

Figure 13: ***Tumor onset of untreated and PK136-treated Grm1 mice.*** **Grm1 mice repeatedly received a NK cell-depleting antibody PK136 until day of first tumor appearance. Untreated mice did not get antibody injection. Days until tumor onset were counted in both groups. No significant difference was observed. Statistical test: Comparison of untreated (n=19) and PK136-treated (n=12) Grm1 mice, mean values with SD, t-test; p=0.0726**

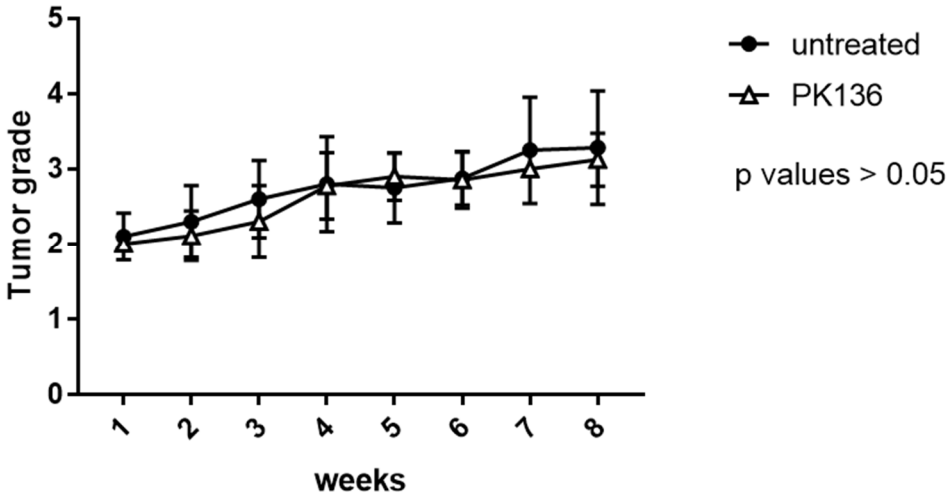

Figure 14: ***Tumor grade monitoring of untreated and PK136-treated Grm1 mice.*** **Grm1 mice repeatedly received a NK cell-depleting antibody PK136 until day of first tumor appearance. Untreated mice did not get antibody injection. Tumor grade was monitored for eight weeks after tumor onset (explanation of grades in chapter 3.2.1). No significant differences were observed at each time point. Statistical tests: Comparison of untreated and PK136-treated Grm1 mice at each time point, n=10, mean value with SD, Two-way ANOVA, Sidak´s multiple comparisons test, p values > 0.05.**

4.1.3 IL-15 treatment in Grm1 mice did not prevent tumor progression and metastasis formation

We have observed that NK cells alone had no clear influence on tumor onset and tumor growth in Grm1 mice. IL-15 is described as a cytokine boosting the immune system and enhancing anti-tumor immunity in mice. With regard to the potential prevention effect of IL-15 against tumor progression, we thought that treatment with this cytokine would lead to slower tumor growth in treated ("IL-15") mice in comparison to untreated mice. Moreover, we assumed a reduced metastasis formation in mice obtaining IL-15 immunotherapy. To test this, Grm1 mice were treated two times with IL-15 within 60 days (therapeutic schedule described in 3.2.5). Tumor growth was monitored by weekly classification of melanomas with the 6-point grading system (see chapter 3.2.1). Untreated mice were controlled over the same period. As shown in Fig. 15, tumor growth in IL-15-treated mice was similar to untreated mice with no significant differences. Moreover, after 60 days, metastasis formation was analyzed in liver and lung sections by immunohistochemistry (Fig. 16A). In liver, IL-15 treatment tended to reduce metastasis events, however not significantly.

In addition, in lungs the number of metastases increased with IL-15 treatment, but this difference was also not significant (Fig. 16B). Collectively, IL-15 treatment did not lead to slower tumor growth or less metastasis formation in Grm1 mice.

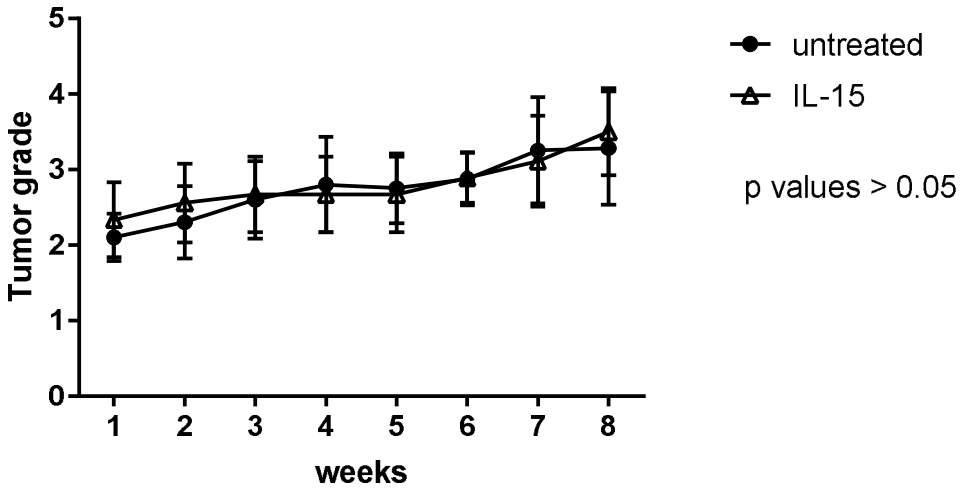

Figure 15: ***Tumor grade monitoring of untreated and IL-15 treated Grm1 mice.*** **Grm1 mice were untreated or treated with IL-15 from day of first tumor appearance (tumor grade 2). They were checked weekly for tumor progression and tumor stages were graded by a 6-point grading system (see chapter 3.2.1) over a time period of eight weeks after tumor formation. Statistical tests: Comparison of untreated and IL-15-treated Grm1 mice at each time point, n=10, mean value with SD, Two-way ANOVA, Sidak´s multiple comparisons test, p values > 0.05.**

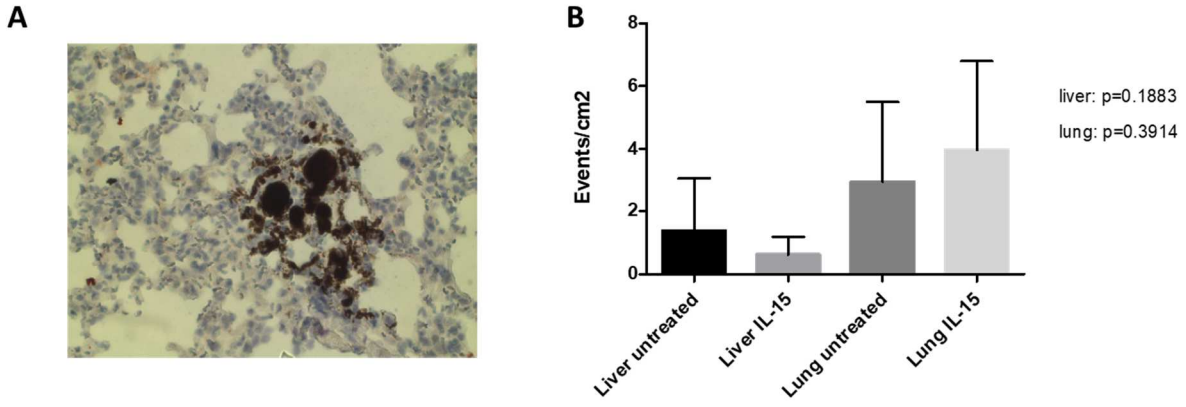

Figure 16: ***Investigation of liver and lung metastasis in untreated and IL-15 treated Grm1 mice on day 60.*** **A. Lung metastasis stained by immunohistochemistry (IHC) with an anti-mGluR1 antibody B: Counting of metastasis in liver and lung sections of untreated and IL-15-treated Grm1 mice. Events per cm² were calculated. Statistical test: Comparison of untreated and IL-15-treated mice, mean values with SD, Liver (UT: n=10; IL-15: n=11, p=0.1883) and lung (UT: n=10, IL-15: n=12, p=0.3914), t-test.**

4.1.4 IL-15 effects on CD8$^+$ T cells, but not NK cells, four days after treatment

Contrary to our expectation, IL-15 had no long-term effect on tumor progression and metastasis formation. To test if the therapy had any effect on immune cell subsets, CD8$^+$ T cells and NK cells were investigated by flow cytometry (staining panel described in 3.2.7) four days after first IL-15 application. CD8$^+$ T cell subpopulations changed significantly with IL-15 treatment, especially naïve CD8$^+$ T cells (TN) decreased and central memory T cells (TCM) increased markedly (Fig.17A). NK cell subsets in IL-15-treated animals showed no significant differences compared to untreated mice (Fig. 17B). However, expression of the NK cell activation marker KLRG1 was increased in CD27^{low} and CD27^{high} NK cells after treatment with the cytokine (Fig.17C). Taken together, IL-15 treatment for four days led to changes in CD8$^+$ T cell compartments and NK cell activity, but not in NK cell subset distribution.

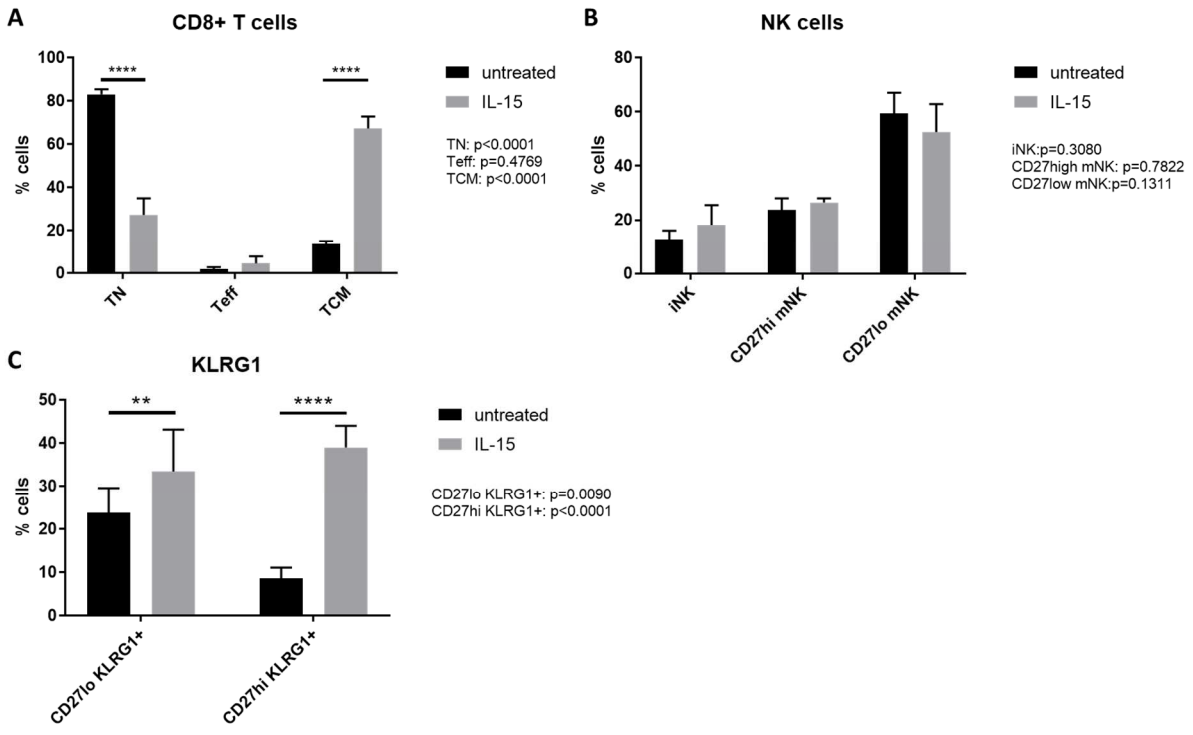

Figure 17: ***Effect of IL-15 on immune cells four days after treatment.*** **Immune cell subsets of Grm1 mice were analyzed by flow cytometry four days after IL-15 injection. Untreated mice did not get antibody injection. A. CD8$^+$ T cells subsets. B. NK cell subsets. C. KLRG1 expression of NK cells. Statistical tests: Comparison of untreated (n=9) and IL-15-treated (n=6) mice, mean values with SD, t-test, ** p ≤ 0.01, **** p ≤ 0.0001.**

4.1.5 IL-15 treatment induces significant changes in CD8$^+$ T cell and NK cell subsets 60 days after treatment

Single treatment of Grm1 mice with IL-15 showed significant changes only in the distribution of CD8$^+$ T cell subsets four days after injection of the cytokine. We analyzed immune cell subpopulations again after 60 days and two IL-15 applications (therapeutic schedule described in 3.2.5) to check if IL-15 has a longer-term effect on NK cells. CD8$^+$ T cells showed similar changes of subsets as found four days after IL-15 treatment. Naïve CD8$^+$ T cells were still diminished after the second IL-15 treatment and central memory T cells were still increased. Again, no significant changes were observed in the effector T cell subset (Fig. 18A). Contrary to day 4, NK cells showed significant changes in all three subpopulations on day 60. Immature NK (iNK) cells increased in contrast to mature NK cell (mNK) subsets that were decreased (Fig. 18B). KLRG1 expression tended to be reduced in CD27^{low} and CD27^{high} NK cells, but not significantly (Fig.18C). Collectively, 60 days after IL-15 treatment, changes in CD8$^+$ T cell and NK cell subsets were observed.

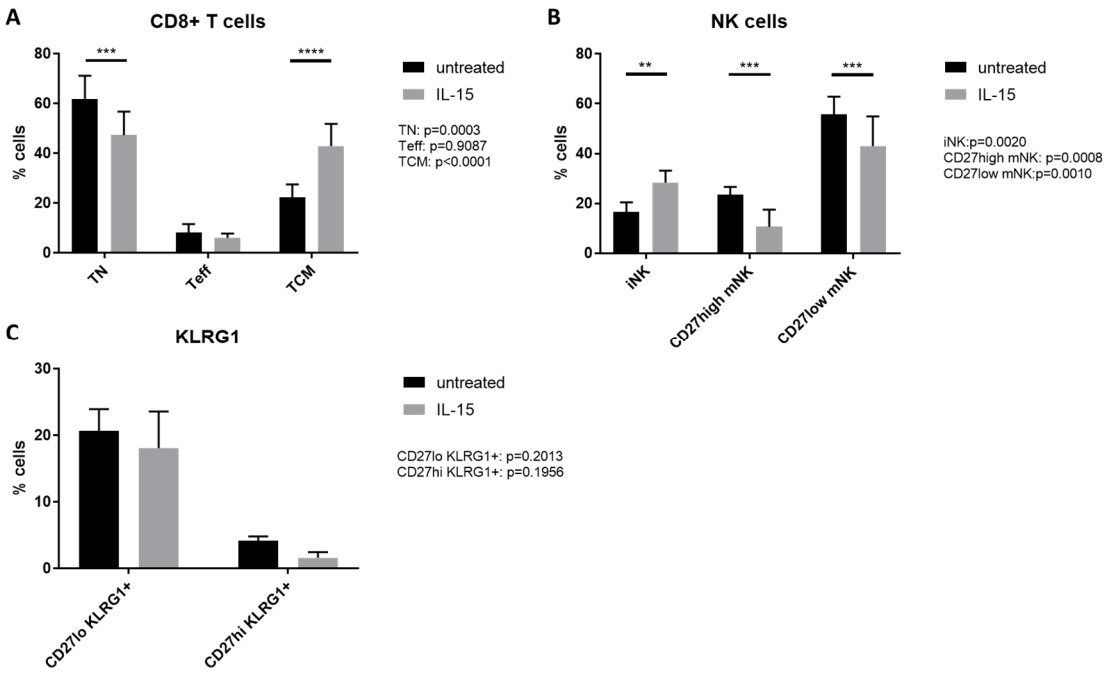

Figure 18: ***Effect of IL-15 on immune cells 60 days after treatment.*** **Immune cell subsets of Grm1 mice were analyzed by flow cytometry 60 days after IL-15 injection. Untreated mice did not get antibody injection. A. CD8$^+$ T cells subsets. B. NK cell subsets. C. KLRG1 expression of NK cells. Statistical tests: Comparison of untreated (n=9) and IL-15-treated (n=9) mice, mean values with SD, t-test, ** p ≤ 0.01, *** p ≤ 0.001, **** p ≤ 0.0001.**

4.1.6 IL-15 treatment led to higher NK cell cytotoxicity *in vitro* and *ex vivo*

In previous experiments we observed that IL-15 treatment led to changes in immune cell subset distribution and their activation. IL-15 is also described as a cytokine stimulating NK cell proliferation as well as cytotoxicity. The latter can be measured by a killing assay using Annexin V/PI staining. First, we investigated the effect of IL-15 on the killing capacity of NK cells *in vitro* (method section 3.2.8). Unstimulated or IL-15-stimulated NK cells were cultivated with Yac-1 lymphoma cells at different E:T ratios (1:1, 10:1). It was observed that IL-15 led to significantly higher NK cell activity compared to that of unstimulated NK cells. At both ratios, more dead tumor cells were observed when cultured with stimulated NK cells (Fig. 19A). NK cells of Grm1 mice, which were either untreated or stimulated with IL-15 for four days, were used in an *ex vivo* cytotoxicity assay (method section 3.2.8). NK cells were isolated from spleens and cultured with Yac-1 cells at different E:T ratios (1:1, 10:1). Again, NK cells that were stimulated with IL-15 *in vivo* showed higher cytotoxicity than NK cells isolated from mice that did not receive IL-15 treatment (Fig. 19B). Summarized, IL-15 treatment led to enhanced cytotoxicity of NK cells *in vitro* and *ex vivo.*

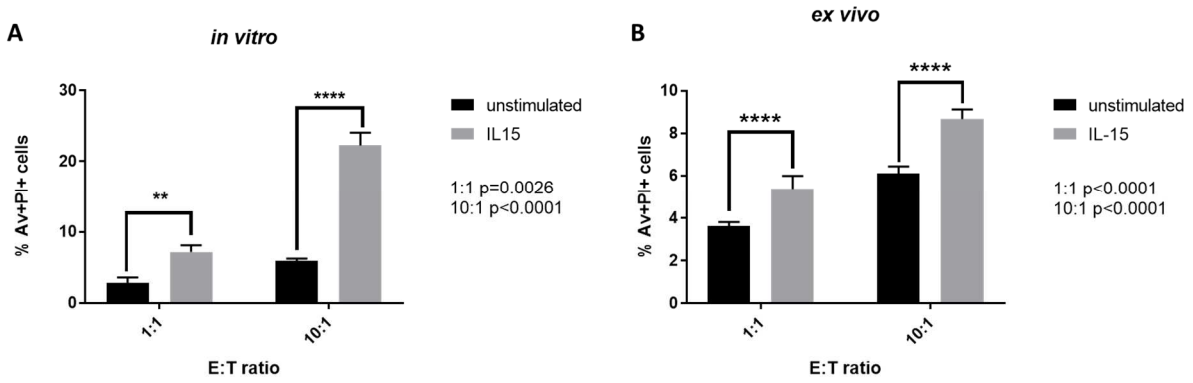

Figure 19: ***NK cell cytotoxicity assay in vitro and ex vivo.*** **A.** ***in vitro*** **assay: NK cells of Grm1 mice were isolated from spleens and stimulated over night with IL-15. Unstimulated NK cells were used as controls. NK cells were cultivated with Yac-1 lymphoma cells and killing capacity of NK cells was measured by AV/PI staining. B. ex** ***vivo*** **assay: Grm1 mice were treated with IL-15. After four days NK cells of spleens were isolated. NK cells of untreated mice were used as controls. NK cells were cultivated with Yac-1 lymphoma cells and killing capacity of NK cells was measured by AV/PI staining. Statistical tests: Comparison of untreated (in vitro: n=3; ex vivo n=5) and IL-15-treated (in vitro: n=3; ex vivo n=5) mice, mean values with SD, t-test, ** p ≤ 0.01, **** p ≤ 0.0001.**

4.1.7 IL-15-stimulated NK cells from Grm1 mice tended to have higher killing capacity compared to IL-15-stimulated NK cells of B6 wt mice

Flow cytometry analyses showed that NK cells of Grm1 mice, which were either stimulated with IL-15 *in vitro* or after IL-15 treatment of mice *in vivo,* had higher killing capacity against Yac-1 lymphoma cells compared to their control counterparts (unstimulated *in vitro* or untreated mice; see chapter 4.1.6). Moreover, we previously observed that Grm1 NK cells tended to be more active than NK cells of B6 wt mice (see chapter 4.1.1). In the following experiment, we used the Incucyte® technology of Sartorius to perform cytotoxicity assays on the basis of live cell imaging (method section 3.2.9). We compared the killing capacity of Grm1 and B6 wt NK cells towards Yac-1 cells. After isolation of NK cells from spleens of both mouse strains, we stimulated these immune cells with IL-15 o/n; unstimulated NK cells served as controls (-IL-15). Cytotoxicity of NK cells cultivated with Yac-1 cells were monitored for several days in the Incucyte® machine taking pictures every one to two hours. We repeated this experiment three times and in Fig. 20 one of the three experimental analyses is shown. Generally, we observed again a tendency that NK cells of Grm1 mice (Fig. 20, unfilled hexagon symbol and unfilled triangle symbol) have higher activity compared to NK cells of B6 wt mice (Fig. 20, filled hexagon symbol and filled triangle symbol) independent of stimulation with IL-15 (Fig. 20, unfilled or filled symbols). However, we could also see that IL-15 stimulation of NK cells led to a higher number of dead Yac-1 cells in both mouse strains. When we selected certain time points from all three experiments and compared the number of dead cells, we observed no significant differences between activity of NK cells isolated from Grm1 or B6 wt (Fig. 21), but the lack of significance was likely due to the high variability in results with the assay. Taken together, we confirmed that IL-15 enhanced the killing capacity of NK cells, however the activity of NK cells of Grm1 mice only showed a tendency to be higher compared to NK cells of B6 wt mice.

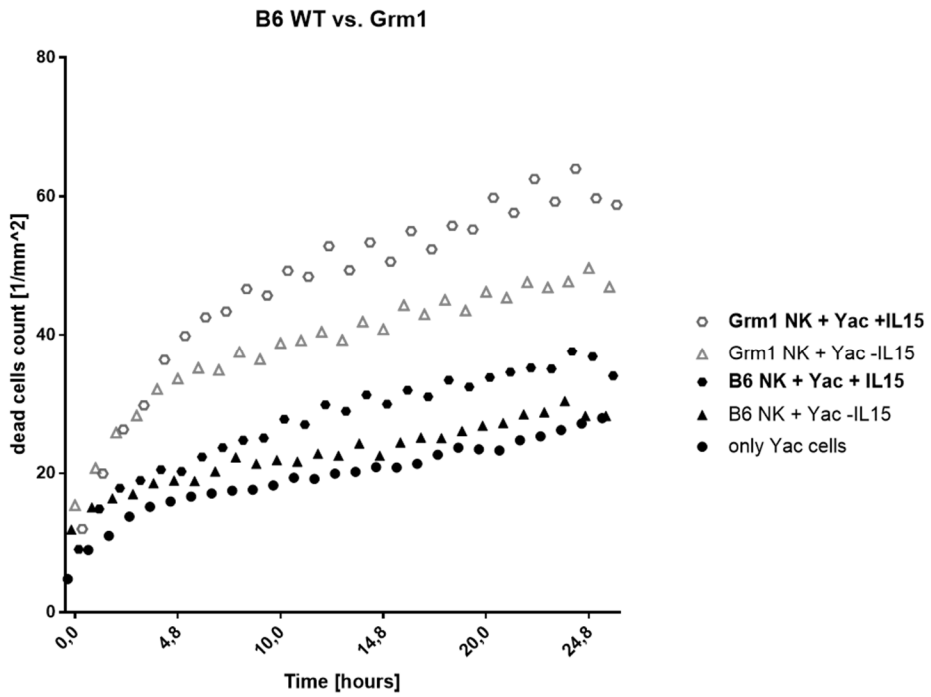

Figure 20: ***NK cell cytotoxicity assay of B6 wt and Grm1 mice monitored by Incucyte®.*** **NK cells of Grm1 and B6 wt mice were isolated from spleens and stimulated o/n with IL-15. Unstimulated NK cells were used as controls. Next day, NK cells were stained with the CellTrace Far Red dye and were then cultivated with Yac-1 cells for several hours. YOYO-1 dye was added to medium to identify dead cells by intercalating into DNA. The Incucyte® machine took pictures every one to two hours.**

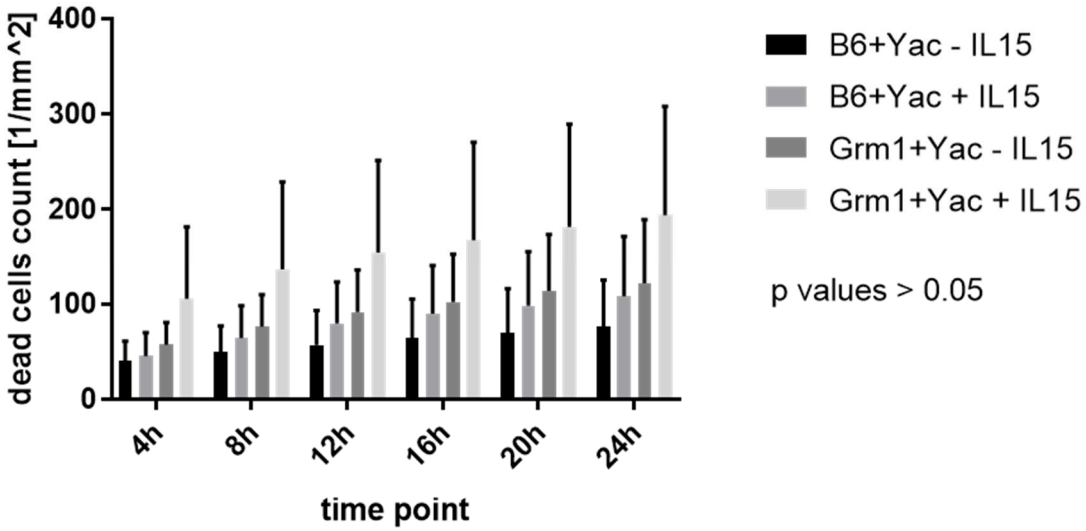

Figure 21: ***Comparison of the killing capacity of unstimulated and IL-15-stimulated NK cells of B6 wt and Grm1 mice at different time points.*** **The numbers of dead cells calculated by the Incucyte software were compared between B6 wt and Grm1 mice at certain time points. Statistical tests: Comparison of B6 wt and Grm1 mice +/- IL-15, mean values with SD, n=3, Two-way ANOVA, Tukey´s multiple comparisons test, p values > 0.05.**

4.1.8 IL-15 shortly boosted NK cells, but significantly reduced NK cell numbers after dual treatment

In previous experiments, we could see that IL-15 was generally able to enhance the anti-tumor activity of NK cells shortly after treatment and the cytokine increases cytotoxicity *in vitro* and *in vivo* (see chapter 4.1.6). However, no significant changes in subpopulations were observed four days after injection in Grm1 mice (see chapter 4.1.4). Only dual treatment of Grm1 mice with IL-15 led to significant changes in the NK cell subset monitored on day 60 (see chapter 4.1.5). Moreover, we could not observe slower tumor growth or lower numbers of metastases in Grm1 mice after cytokine treatment (see chapter 4.1.3). Hence, we again took a closer look at NK cells at different time points after IL-15 treatment. We set up a timeline in which Grm1 mice were treated with IL-15, like described above (chapter 3.2.5), and analyzed NK cells at various time points to observe changes during treatment. We hypothesized that IL-15 is indeed efficient in boosting NK cell numbers for a short time; however, it is not able to maintain this effect over a longer time interval, enabling tumors to eventually grow and spread into lung and liver. We also treated B6 wt mice in the same procedure to compare the effect of IL-15 in tumor-bearing versus non-tumor-bearing mice. We wanted to see if changes in NK cells are only due to IL-15 treatment or if the tumor itself influences these immune cells.

Firstly, we looked at total NK cells numbers in untreated and IL-15-treated Grm1 and B6 wt mice. A significant increase in total NK cell numbers was found four days after the first IL-15 injection, compared to untreated mice in both mouse strains ($p<0.05$). Within the first 29 days the amount of NK cells decreased and was enhanced again four days after the second administration of the IL-15 on day 30. However, on day 60 in both mouse strains, total NK cell numbers were markedly decreased in comparison to untreated mice ($p<0.05$, Fig. 22A and 22B). Therefore, we conclude that IL-15 only boosts NK cells for a short time after treatment.

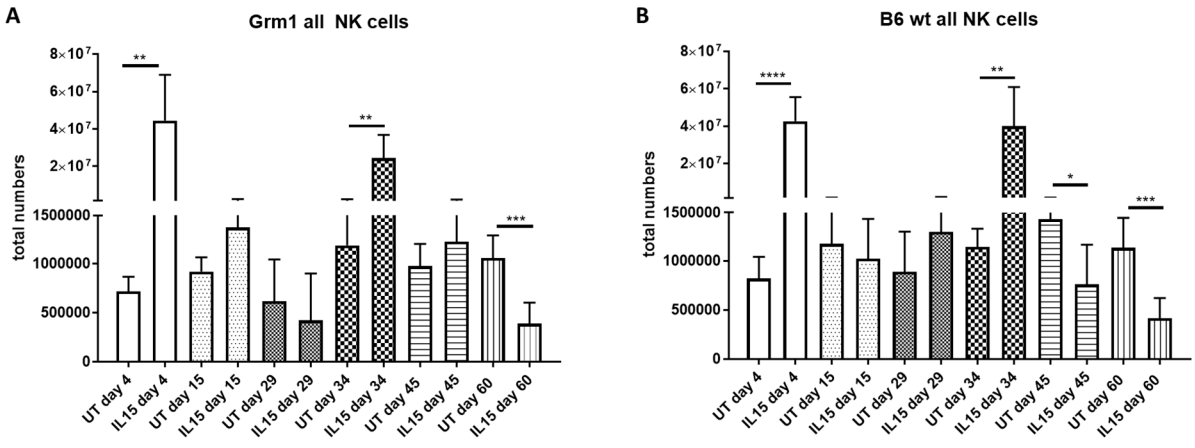

Figure 22: ***Total numbers of NK cells from untreated and IL-15-treated Grm1 (A) and B6 wt (B) mice at different time points of the Grm1 timeline.*** **Immune cells were isolated from spleens of Grm1 and B6 wt mice at different time points and NK cells were analyzed by flow cytometry. Total numbers were calculated by counting beads. Statistical tests: Comparison of untreated and IL-15-treated mice, mean values with SD, n=4-6, t-test; * $p \leq 0.05$, ** $p \leq 0.01$, *** $p \leq 0.001$, **** $p \leq 0.0001$.**

4.1.9 IL-15 led to a proportional shift to CD27^{low} mNK cells in Grm1 mice

After analysis of total NK cell numbers at different time points in the Grm1 timeline we further analyzed NK cell subsets. After the first IL-15 treatment, the percentage of immature NK cells (iNKs, CD11b^{neg}CD27^{high}) was not significantly increased in Grm1 or B6 wt mice and continued to be similar to untreated mice for further 29 days. After the second IL-15 injection, proportionally more iNKs were observed in IL-15-treated mice than in untreated mice in both strains (Fig. 23 A and B). In Grm1 mice, the percentage of iNKs decreased again to levels of iNKs of untreated mice during the next 30 days (Fig. 23A). In B6 wt mice, the percentage of iNKs continued to be significantly increased compared to Grm1 mice on day 60 (Fig 23B). Comparison of the total numbers of iNKs (Fig. 23C and D) showed a rise after both IL-15 applications, with decreasing numbers within the next 30 days. On day 60, the total numbers were decreased substantially due to the general decrease in all NK cells, as shown in Fig. 22.

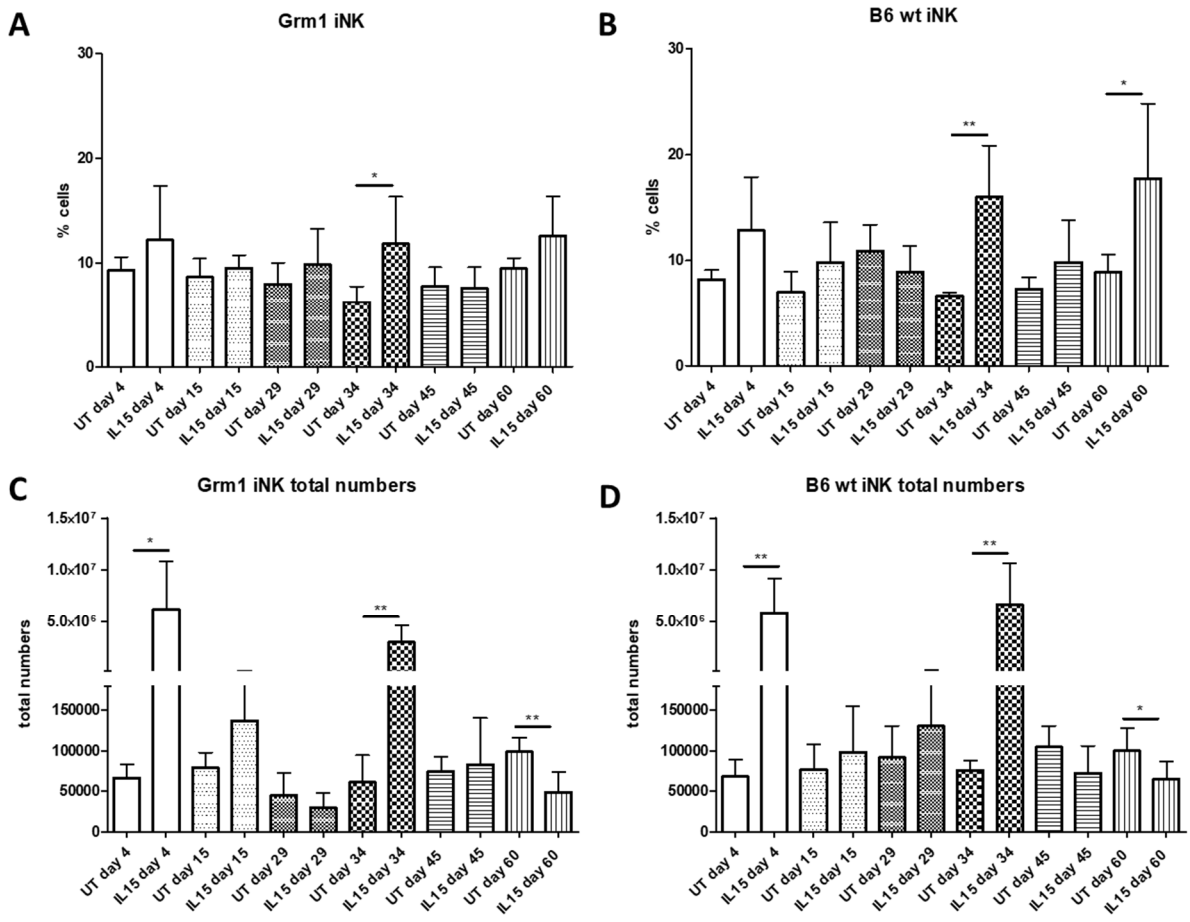

Figure 23: ***Percentages (A and B) and total absolute numbers (C and D) of immature NK cells (iNKs) in Grm1 (A, C) and B6 wt (B, D) mice at different time points of the Grm1 timeline.*** **Immune cells were isolated from spleens of Grm1 and B6 wt mice at different time points and immature NK cells were analyzed by flow cytometry. Total numbers were calculated by counting beads. Statistical tests: Comparison of untreated and IL-15-treated mice, mean values with SD, n=4-6, t-test, * $p \leq 0.05$, ** $p \leq 0.01$.**

As a percentage, we did not observe differences in CD27^{high} mature NK cells (CD27^{hi} mNKs) between untreated and IL-15-treated mice four days after applications of IL-15 (day 4 and day 34) in both mouse strains (Fig. 24 A and B). In Grm1 mice, we observed that several days after IL-15 application (day 29, 45 and 60), the proportion of CD27^{hi} mNKs was significantly decreased compared to untreated mice (Fig. 24A). In B6 wt mice, IL-15 did not affect the proportion of CD27^{hi} mNKs at each time point (Fig. 24B). Treatment of mice with IL-15 led to an increase in total numbers of CD27^{hi} mNKs in Grm1 and B6 wt mice, as observed on day 4 and day 34 (Fig. 24C and D).

Within the next 30 days, the absolute numbers of CD27^{hi} mNKs decreased below the levels of untreated mice, with substantial differences on day 60 in both mouse strains. (Fig. 24C and D).

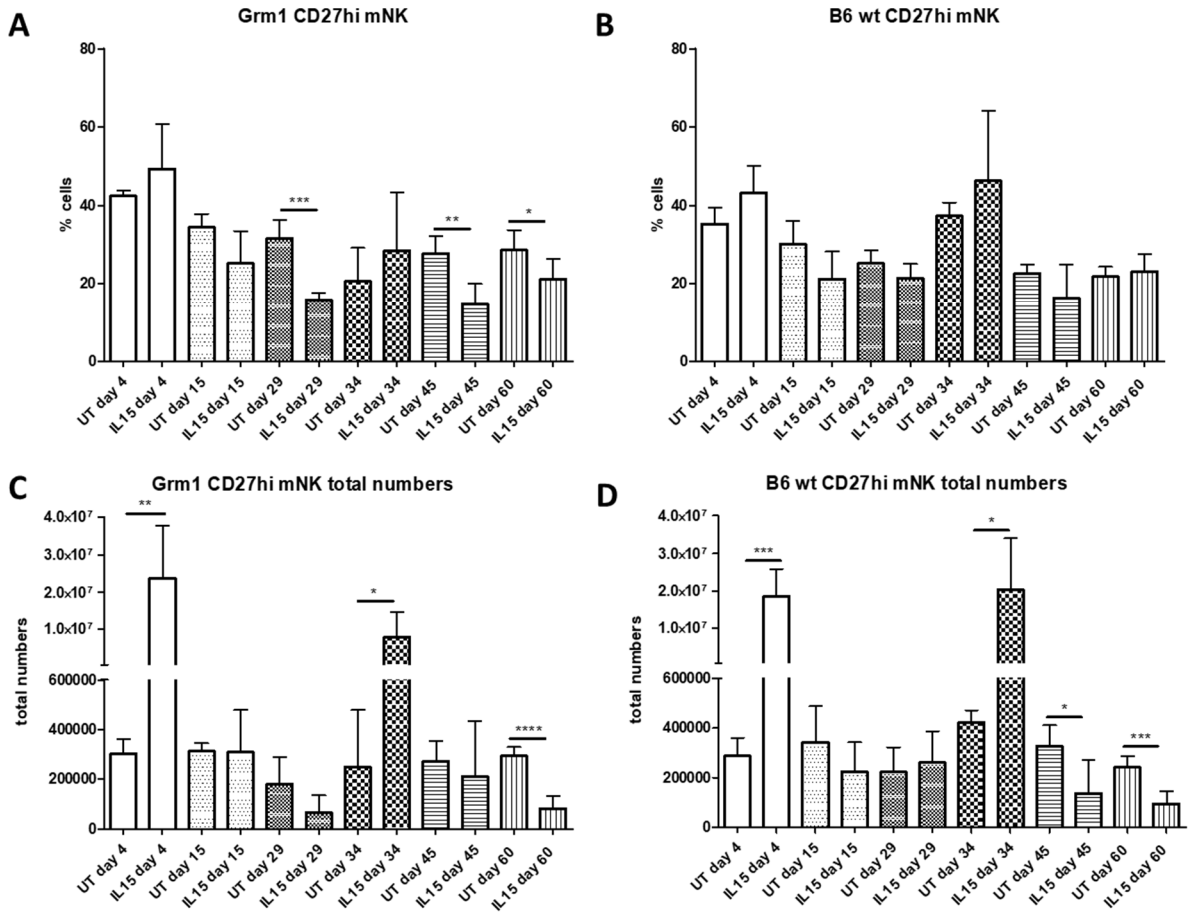

Figure 24: ***Percentages (A and B) and total absolute numbers (C and D) of CD27high mNK cells in Grm1 (A, C) and B6 wt (B, D) mice at different time points of the Grm1 timeline.*** **Immune cells were isolated from spleens of Grm1 and B6 wt mice at different time points and CD27^{hi}mNK cells were analyzed by flow cytometry. Total numbers were calculated by counting beads. Statistical tests: Comparison of untreated and IL-15-treated mice, mean values with SD, n=4-6, t-test, * p ≤ 0.05, ** p ≤ 0.01, *** p ≤ 0.001, **** p ≤ 0.0001.**

As a percentage, we did not observe differences in CD27^{low} mature NK cells (CD27^{lo} mNKs) cells between untreated and IL-15-treated mice four days after applications of IL-15 (day 4 and day 34) in both mouse strains (Fig. 25 A and B). In Grm1 mice, several days after IL-15 injection (day 29 and day 45), we observed proportionally more CD27^{lo} mNKs in IL-15-treated versus untreated mice.

On day 60 the numbers were still enhanced, but not significantly (Fig. 25A). In B6 wt mice we found more CD27^{lo} mNKs on day 29 in IL-15-treated mice, however on day 60, proportionally fewer CD27^{lo} mNKs were observed in IL-15-treated mice compared to untreated mice (Fig. 25B). Moreover, IL-15 treatment elevated the total numbers of CD27^{lo} mNKs on day 4 and day 34 and led to a marked decrease in numbers of these cells on day 60 in Grm1 and B6 wt mice (Fig. 25C and D). Collectively, while IL-15 treatment produced a short boost to NK cells, over the longer term there was a significantly reduced number of these cells after dual treatment.

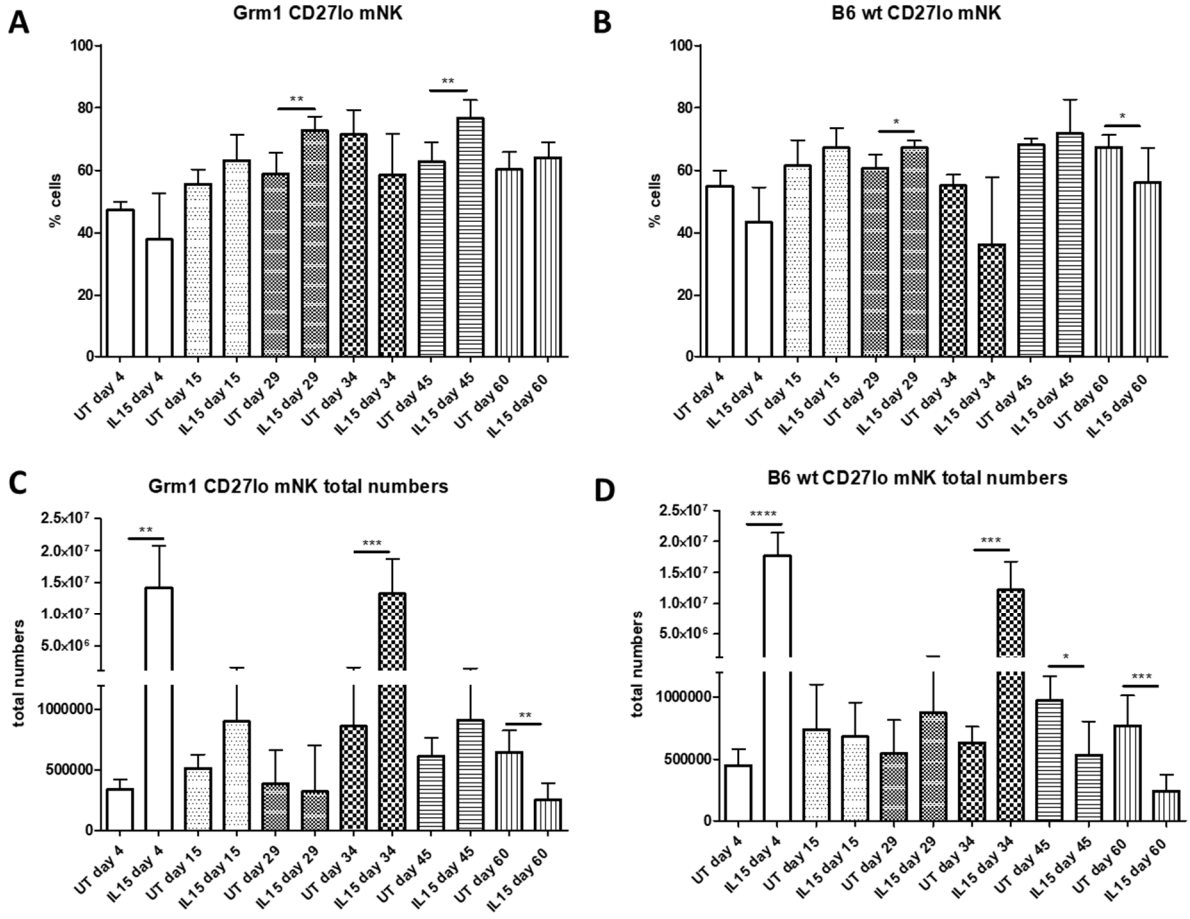

Figure 25: ***Percentages (A and B) and total numbers (C and D) of CD27low mNK cells in Grm1 (A, C) and B6 wt (B, D) mice at different time points of the Grm1 timeline.*** **Immune cells were isolated from spleens of Grm1 and B6 wt mice at different time points and CD27^{lo}mNK cells were analyzed by flow cytometry. Total numbers were calculated by counting beads. Statistical tests: Comparison of untreated and IL-15-treated mice, mean values with SD, n=4-6, t-test, * p ≤ 0.05, ** p ≤ 0.01, *** p ≤ 0.001, **** p ≤ 0.0001.**

4.1.10 IL-15 led to a significant increase in central memory CD8$^+$ T cells (TCMs)

Like NK cells, CD8$^+$ T cells contribute to tumor immune surveillance. Therefore, we had a closer look at CD8$^+$ T cell subpopulations at different time points during IL-15 treatment. Once more, we compared Grm1 mice with B6 wt mice to look for differences between animals with or without tumors. We were interested in seeing whether IL-15 is also only able to boost the adaptive part of the immune system for a short time, without durable effects. Like shown in Fig. 26A and B, IL-15 led to significantly greater total CD8$^+$ T cell number in Grm1 and B6 wt mice four days after treatment with IL-15 (day 4 and day 34). However, during the following 30 days after IL-15 injection, the CD8$^+$ T cell numbers were decreased again in both mouse strains almost to levels of untreated controls.

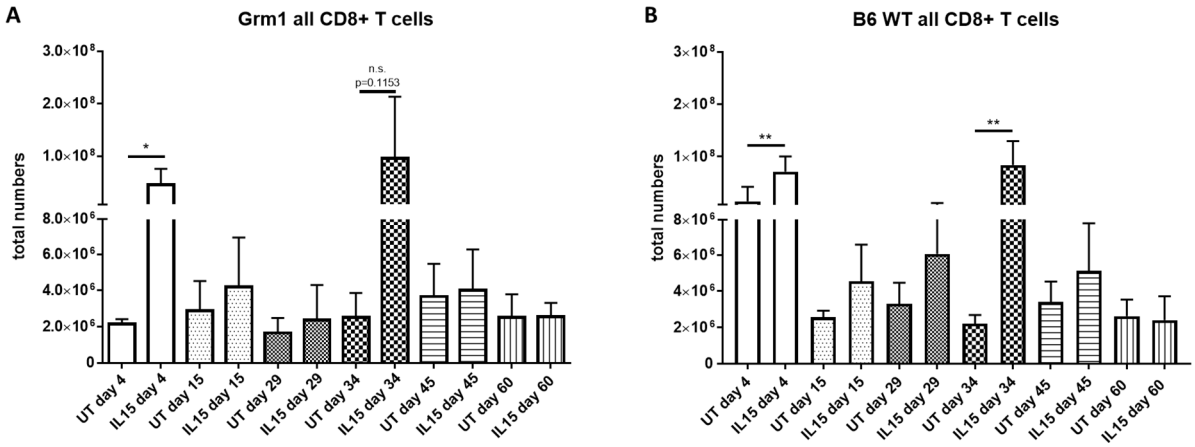

Figure 26: ***Total numbers of CD8$^+$ T cells from untreated and IL-15 treated Grm1 (A) and B6 wt (B) mice at different time points of the Grm1 timeline.*** **Immune cells were isolated from spleens of Grm1 and B6 wt mice at different time points and CD8$^+$ T cells were analyzed by flow cytometry. Total numbers were calculated by counting beads. Statistical tests: Comparison of untreated and IL-15-treated mice, mean values with SD, n=4-6, t-test, * $p \leq 0.05$, ** $p \leq 0.01$.**

In both strains, the proportion of naïve CD8$^+$ T cells (TNs) was significantly diminished in mice treated with IL-15 compared to untreated mice, almost over the whole period of treatment (Fig. 27A and B). Only day 15 in Grm1 (Fig. 27A) and day 15 and day 29 in B6 wt mice (Fig. 27B) showed no significant differences between untreated and IL-15 treated mice. The total number of TNs was substantially enhanced in both mouse strains at day 4 and day 34 (Fig. 27C and D), In B6 wt we observed also significantly elevated levels at day 15, 29 and 45 (Fig. 27D).

During treatment, the total number of TNs of Grm1 mice declined approximately to levels of T cell numbers of untreated mice (Fig. 27C).

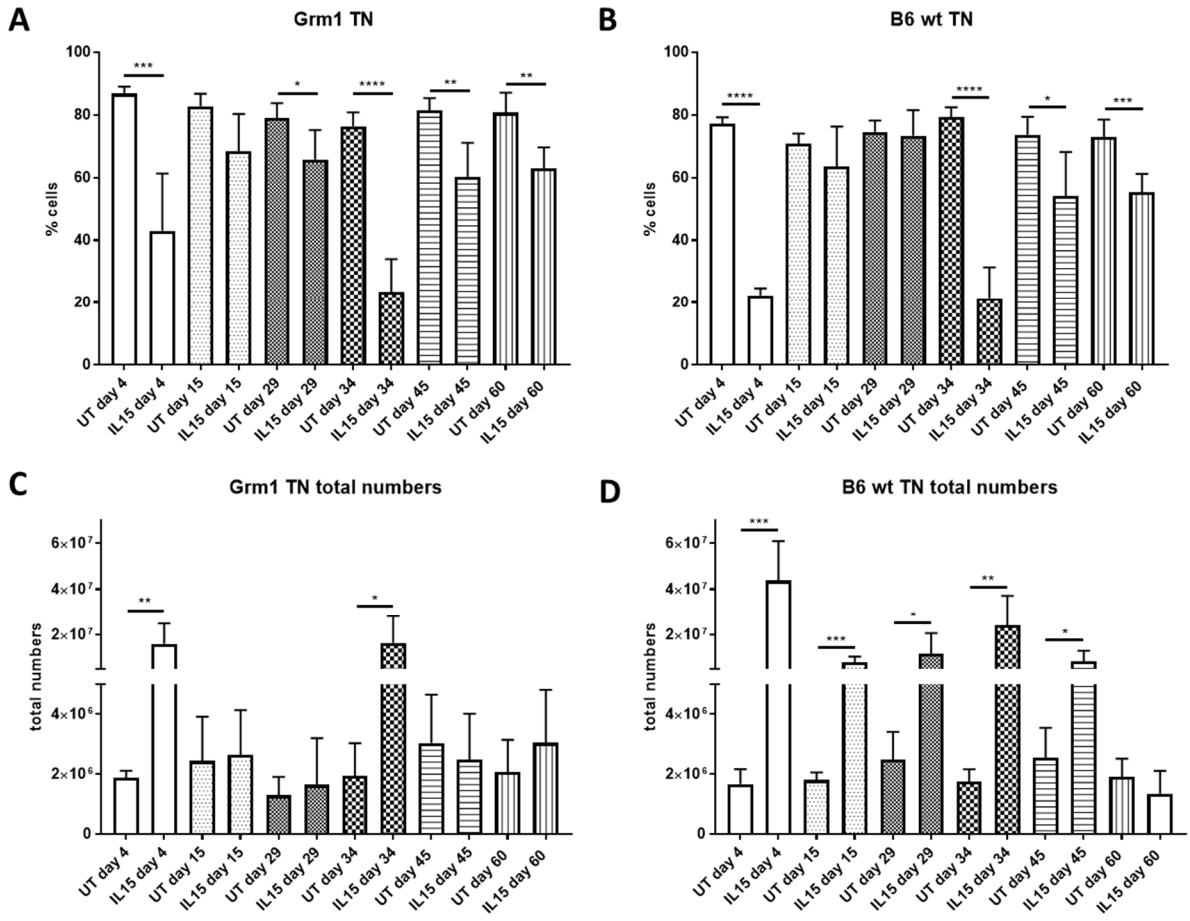

Figure 27: ***Percentages (A and B) and total numbers (C and D) of naïve CD8⁺ T cells (TNs) in Grm1 (A, C) and B6 wt (B, D) mice at different time points of the Grm1 timeline.*** **Immune cells were isolated from spleens of Grm1 and B6 wt mice at different time points and TNs were analyzed by flow cytometry. Total numbers were calculated by counting beads. Statistical tests: Comparison of untreated and IL-15-treated mice, mean values with SD, n=4-6, t-test, * p ≤ 0.05, ** p ≤ 0.01, *** p ≤ 0.001, **** p ≤ 0.0001.**

Percentages of effector T cells (Teffs) only increased shortly after IL-15 injection, however it seemed that this cell subset was unaffected by the cytokine during whole treatment. We observed similar proportions of Teffs in untreated and in IL-15-treated mice after several days of IL-15 injections (Fig. 28A and B). The same observation was made in total numbers of Teffs. After both IL-15 treatments, the total numbers increased significantly and decrease again to levels of Teffs from untreated mice in both muse strains (Fig. 28C and D).

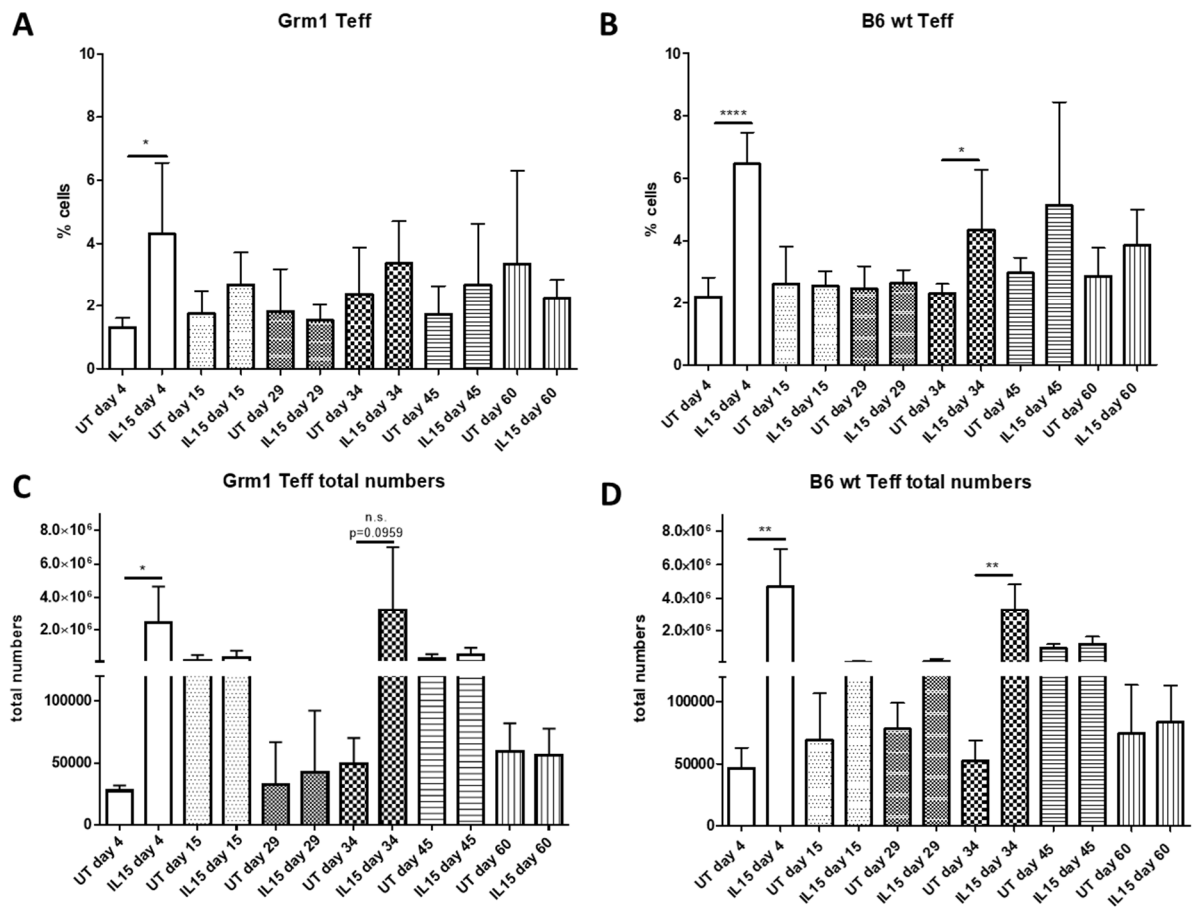

Figure 28: : *Percentages (A and B) and total numbers (C and D) of effector CD8⁺ T cells (Teffs) in Grm1 (A, C) and B6 wt (B, D) mice at different time points of the Grm1 timeline.* Immune cells were isolated from spleens of Grm1 and B6 wt mice at different time points and Teffs were analyzed by flow cytometry. Total numbers were calculated by counting beads. * p ≤ 0.05, ** p ≤ 0.01, **** p ≤ 0.0001

The significant decrease in the percentages of TNs (Fig. 27A and B) was correlated with a substantial increase in the percentages of central memory CD8⁺ T cells (TCMs) cells in both mouse strains directly after IL-15 treatment (Fig. 29A and B). This high proportion of TCMs stayed until day 60. Moreover, the total numbers of TCMs were increased with IL-15 treatment on day 4 and day 34 (Fig. 29C and D). In Grm1 mice (Fig. 29C) the total number of TCMs was still significantly elevated on day 60 in comparison to B6 wt mice (Fig. 29D) in which the total numbers of TCMs were similar in untreated and IL-15-treated mice. Taken together, IL-15 is able to shortly boost CD8⁺ T cell numbers and leads to the development of TCMs.

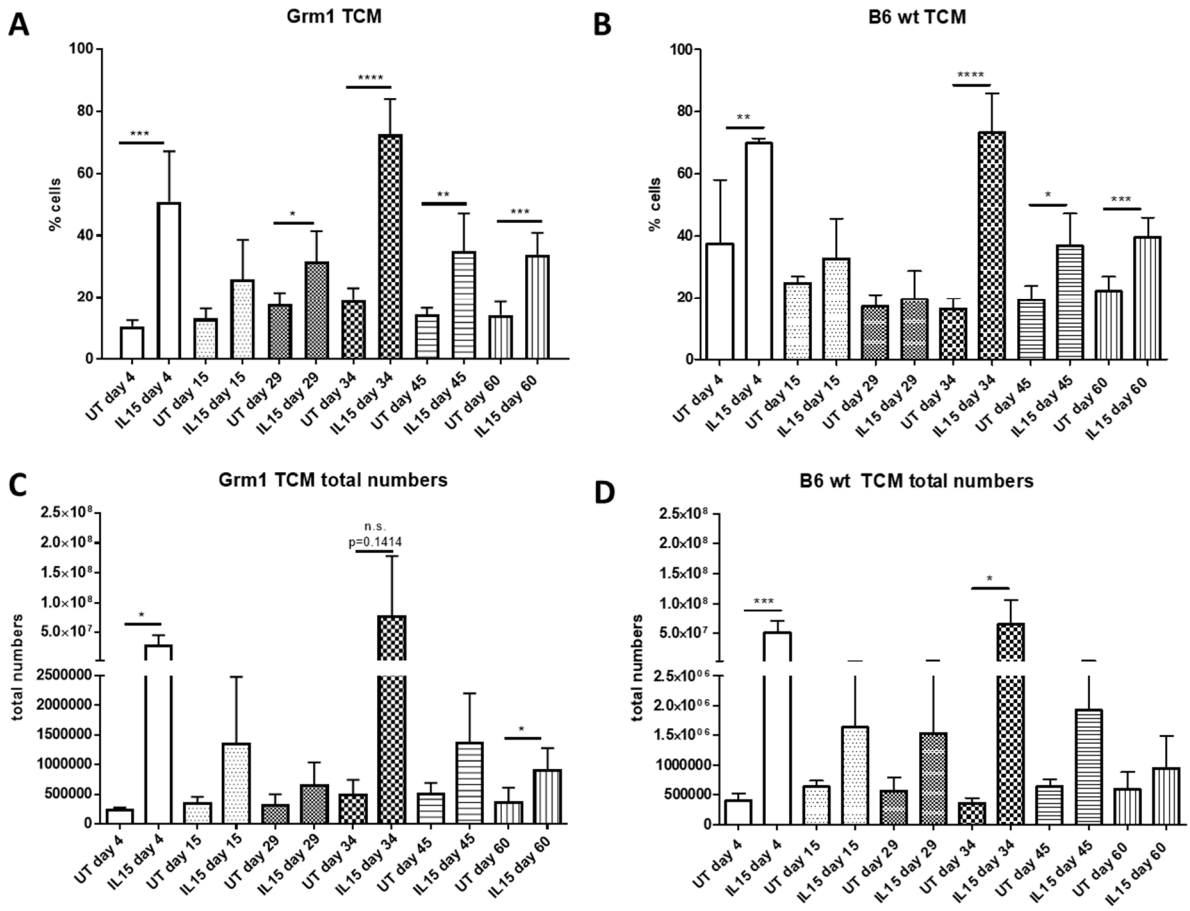

Figure 29: ***Percentages (A and B) and total numbers (C and D) of central memory CD8⁺ T cells (TCMs) in Grm1 (A, C) and B6 wt (B, D) mice at different time points of the Grm1 timeline.*** **Immune cells were isolated from spleens of Grm1 and B6 wt mice at different time points and central memory CD8⁺ T cells were analyzed by flow cytometry. Total numbers were calculated by counting beads. Statistical tests: Comparison of untreated and IL-15-treated mice, mean values with SD, n=4-6, t-test, * p ≤ 0.05, ** p ≤ 0.01, *** p ≤ 0.001, **** p ≤ 0.0001**

4.1.11 IL-15 treatment led to decreased expression of Eomes and NKG2D in NK cells several days after stimulation

In previous flow cytometry analyses we observed that IL-15 was able to induce short immune boosts to NK cells, however without durable effects after dual treatment of mice with this cytokine. Moreover, we did not see that IL-15 treatment inhibited tumor progression and metastasis formation. To better understand the marked decrease in NK cell numbers at the endpoint of analysis (day 60) and the lack of an effect on tumors, we investigated the gene expression of several genes related to NK cell development, maturation, activity, apoptosis and exhaustion at different time points during IL-15 treatment of Grm1 and B6 wt mice (genes listed in 3.2.12).

Therefore, through a collaboration with PD Dr. Philipp Renner (Robert-Bosch-Krankenhaus, Stuttgart, Germany), cDNA was isolated from 300 sorted NK cells by whole transcriptome amplification (WTA). Before starting a multiplex PCR analysis called RT^2 profiler (see method section 3.2.11 and 3.2.12), we had to exclude samples because of poor cDNA, as checked by quality control after cDNA isolation. Unfortunately, most of the genes were not ultimately analyzed because the housekeeping genes could not be determined, the CT values were out of range, or we did not get usable CT values for the genes of interest. The need to exclude samples using the RT^2 profiler approach created the problem that a full set of expression results was not available at each time point (day 4, 29, 34 and 60). Therefore, we decided to run single qPCRs with primers for the housekeeping gene β-actin and only the specific genes of interest, Eomes and NKG2D, as the literature indicates that exhausted NK cells showed reduced expression of those particular genes[214]. We hoped to get more information compared to the RT^2 profiler because of the higher specificity of primers and PCR cycle conditions in the single qPCRs. We picked out two time points (day 4 and day 29) including one time point directly after treatment with IL-15 and a subsequent time point several days after treatment (Fig.30A-D). In both mouse strains, IL-15 treatment led to an upregulation of Eomes, as well as NKG2D, directly after injection (day 4). However, several days after treatment (day 29), the expression of those genes tended to be reduced compared to day 4. The difference was only significant in B6 wt mice for the expression of NKG2D (Fig. 30D). Additional samples have to be included to confirm the differences in the expression of Eomes and NKG2D, because the lack of significance is likely due to the limited numbers of available samples and the varying CT values within the groups resulting in high standard deviations. Due to time restrictions, these follow-up experiments were not performed as part of this thesis project.

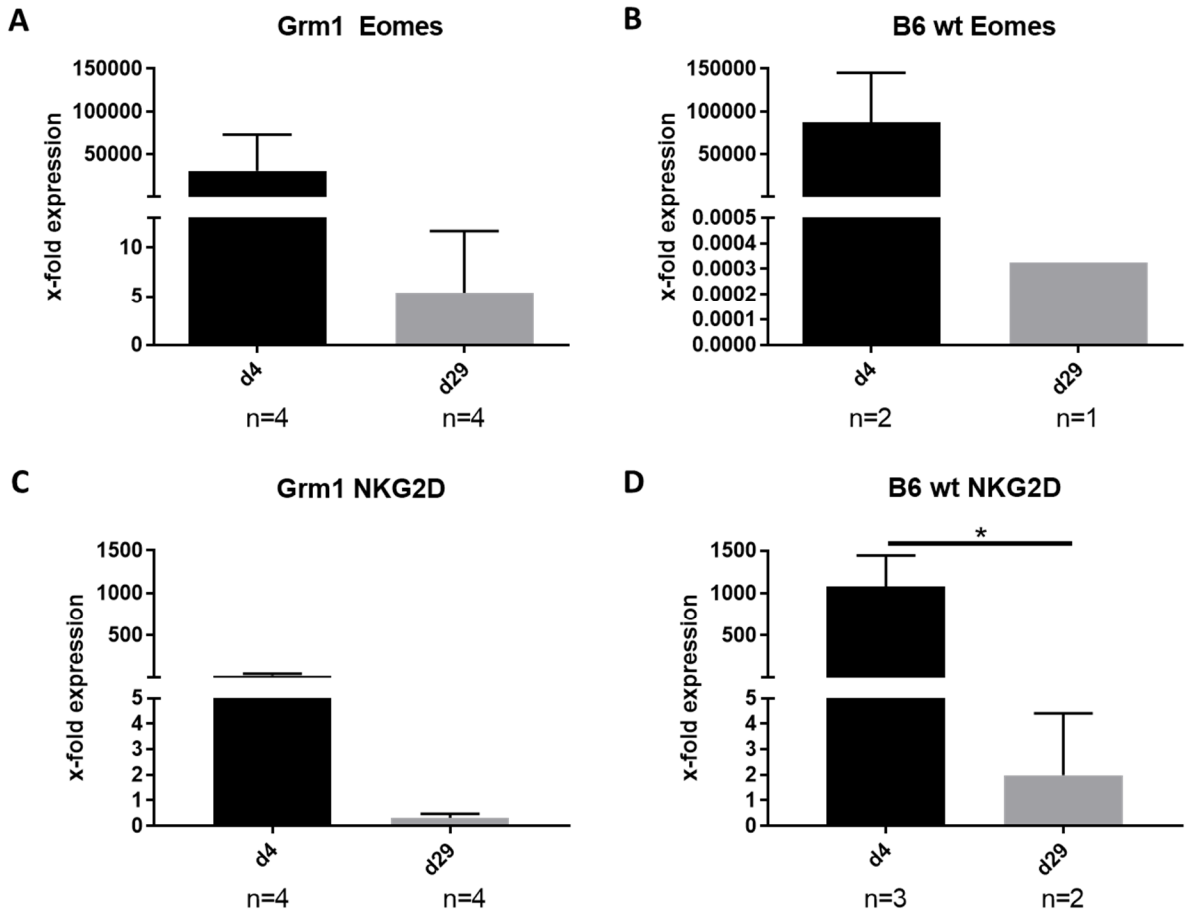

Figure 30: ***x-fold expression of Eomes (A, B) and NKG2D (C, D) in IL-15-treated mice compared to untreated mice on day 4 and day 29.*** **NK cells of Grm1 (A, C) and B6 wt (B,D) mice were sorted at different time points during the IL-15 treatment and cDNA was isolated by WTA. With the help of qPCRs, the x-fold expression of Eomes and NKG2D was calculated. Statistical tests: Comparison of the expression of IL-15-treated mice compared to untreated mice, mean values with SD, n=1-4, t-test, * $p \leq 0.05$. Statistical tests were only performed where there were multiple values available.**

4.2 BalbNeuT model

Our work with the Grm1 model suggests that NK cells are an important immune cell type in tumor immune surveillance. Interestingly, we observed that $CD8^+$ T cells alone are not able to kill primary tumors or prevent the formation of metastases when NK cells are exhausted after immunotherapy. We considered using another mouse model to confirm the importance of immune cells in tumor destruction and to investigate the special role of immune cells in immunoediting. Therefore, we investigated the possible usefulness of the BalbNeuT mammary gland transplantation model, which allows for complete removal of the primary tumor so that factors not related to the primary tumor can be investigated (see chapter 2.7). For this purpose, BalbNeuT mammary glands with neoplastic potential were transplanted into Balb/c wt mice by the Prof. C. Klein group as part of the FOR 2127 consortium (University of Regensburg). We did manage to monitor for immune cell changes in the wt mice during primary tumor development and then after metastases formation; these results are shown and described below. However, the eventual goal of these experiments after baseline testing in wt mice was to transplant mammary glands into immunodeficient mice to be able to dissect the specific role of each immune cell type that could be transferred to these mice. Unfortunately, there were long-term difficulties in getting the studies in immunodeficient mice approved by the authorities, so the experiments could not be performed in the limited time of this thesis project. For completeness, however, the results of the experiments in Balb/c wt mice that were performed during my thesis work period are provided in the following sections.

4.2.1 Monitoring of primary tumor growth and curative surgery in Balb/c wt mice transplanted with BalbNeuT mammary glands

With the BalbNeuT model, we wanted to investigate immunoediting processes. We transplanted mammary glands of BalbNeuT mice into Balb/c wt mice to change the microenvironment of the tumor (method section 3.2.13). The idea was to observe, if the cells with neoplastic potential are able to adapt to the new host and form primary tumors (PTs). First, we checked the time until primary tumors reached a size of ~ 1 cm. To monitor tumor growth, mice were inspected weekly and the tumors were measured by palpation and with a caliper.

15 of 19 Balb/c wt mice transplanted with mammary glands needed 22.7 (+/- 5.364) weeks to form primary tumors reaching a size of 1cm (Fig. 31). Four mice did not develop tumors and were excluded from further analysis.

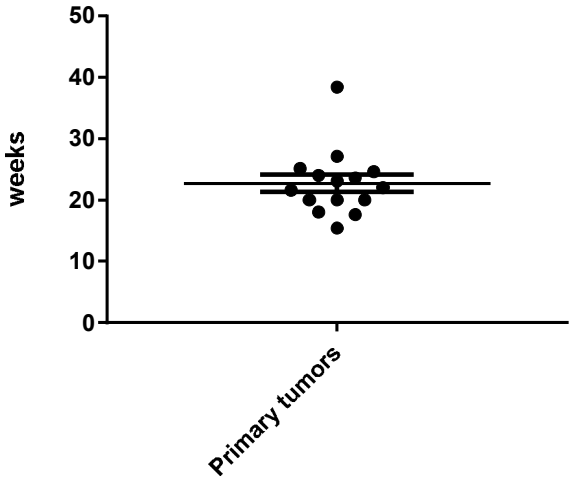

Figure 31: ***Time between transplantation of mammary glands and curative surgery*** **(PT ~1 cm). Mammary glands from four-week old BalbNeuT mice were transplanted into four-week old Balb/c wt mice. Primary tumor development was monitored until the tumor size reached ~1cm. n=15 (19 mice were transplanted, 4 mice were excluded from data because of missing primary tumor onset). Mean values with SD.**

4.2.2 Transplanted mice developed lung metastases after curative surgery of the primary tumor

After monitoring the primary tumor development in Balb/c wt mice transplanted with BalbNeuT mammary glands, we divided the mice into three different groups depending on further analysis time after curative surgery. Mice were analyzed for immune cell changes (described in sections below) or for metastasis formation either at day of curative surgery (CS), five weeks or 17 weeks after CS (CS+5 weeks; CS+17 weeks). Balb/c wt mice can develop lung metastases after transplantation of BalbNeuT mammary glands and subsequent development of primary tumors. In the following figure, numbers of visible lung metastases are shown (Fig. 32). As mentioned above, some mice did not develop primary tumors in two of the groups (CS and CS+17 weeks) and were excluded from this analysis. At the time of CS, no metastases were visible. Two mice developed lung metastases five weeks after CS and one mouse showed six identifiable metastases 17 weeks after removal of the primary tumor.

In this latter group we could only show one mouse (Fig. 32) because three out of five transplanted mice did not develop any primary tumor and therefore no metastases; another mouse died before analysis.

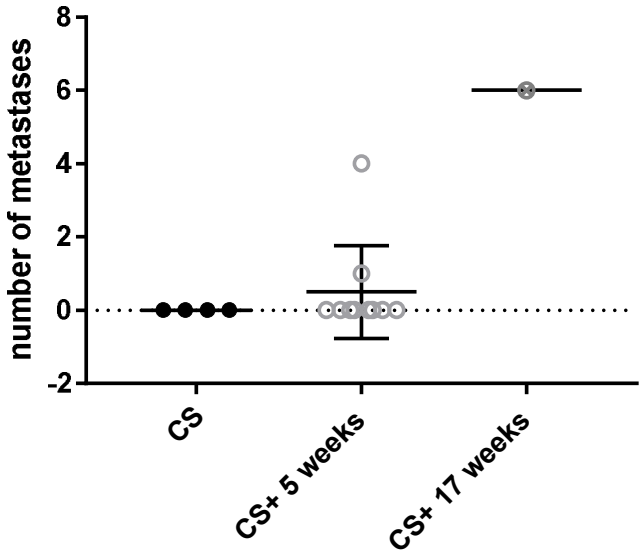

Figure 32: ***Numbers of lung metastases at different time points after curative surgery of the primary tumor.*** **Mammary glands of BalbNeuT mice were transplanted into Balb/c wt mice. After primary tumor development, mice were analyzed for metastasis formation at three different time points after curative surgery (CS, CS+5 weeks, CS+17 weeks). Mean values with SD**

4.2.3 Presence of primary breast tumors or lung metastasis did not lead to a rise of effector immune cells in spleen

$CD8^+$ T cells and NK cells are part of immune surveillance and control primary tumor growth and metastasis formation. Therefore, we hypothesized that immune cell subsets in spleen change during tumor progression and this predicted that the numbers of effector NK and $CD8^+$ T cells would increase with tumor development (time point "CS"). After removal of the primary tumor for five weeks (time point "CS+5 weeks), we predicted that immune cell subsets would re-adjust to normal levels similar to their control group. During metastasis formation (time point "CS+17 weeks"), we hypothesized a renewed increase of effector immune cell subsets. To confirm our hypotheses, immune cells of Balb/c wt mice transplanted with BalbNeuT mammary glands were analyzed at the aforementioned time points. Mice, that did not receive transplanted mammary glands, were included as controls ("ctrl CS", "ctrl CS+5 weeks",

"ctrl CS+17 weeks"). "Untransplanted" mice were four-week-old animals that were investigated before transplantation and they served as a comparison group to monitor immune cell changes due to natural development and aging. Notably, in the following experiment, a statistical analysis of time point "CS+17 weeks" was not possible because only one transplanted animal was included, other animals did not develop primary tumors. Generally, we observed an increase in Teffs and TCMs in correlation with a decrease in TNs within natural development of mice (comparison of "untransplanted" mice and "ctrl" mice). However, during primary tumor development and metastasis formation, all three $CD8^+$ T cell subsets did not change significantly compared to control mice (Fig. 33). Moreover, during development of mice, there tended to be fewer iNKs and $CD27^{hi}$ mNKs and more $CD27^{lo}$ mNKs were observed (comparison of "untransplanted" mice and "ctrl" mice), but any change was likely related to immunological maturation of the mice and not to tumor development. Like in $CD8^+$ T cell subsets, no significant changes in subpopulations were observed in transplanted mice compared to control mice (Fig. 34). To sum up, the presence of primary breast tumors or lung metastases did not lead to the predicted increase in immune surveillance relevant immune cells in spleen.

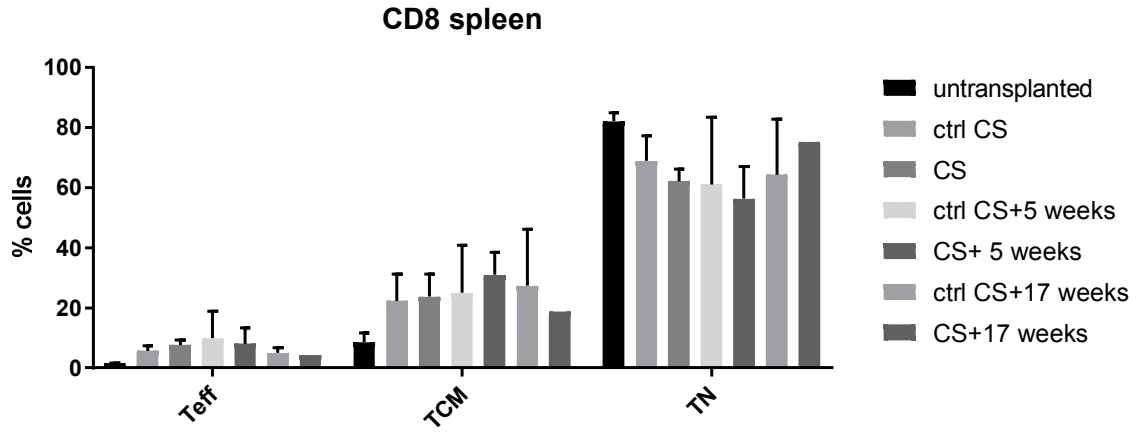

Figure 33: ***$CD8^+$ T cell subsets in spleen at different time points of tumor progression and metastasis formation.*** **Mammary glands of BalbNeuT mice were transplanted into Balb/c wt mice. After primary tumor development and curative surgery, $CD8^+$ T cell subsets were analyzed by flow cytometry. Mice that were not transplanted with mammary glands were used as control mice. There were no significant changes between control mice and transplanted mice. Statistical tests: Comparison of control mice and transplanted mice, mean values with SD, n=5-10, t-test, $p > 0.05$ for all comparisons.**

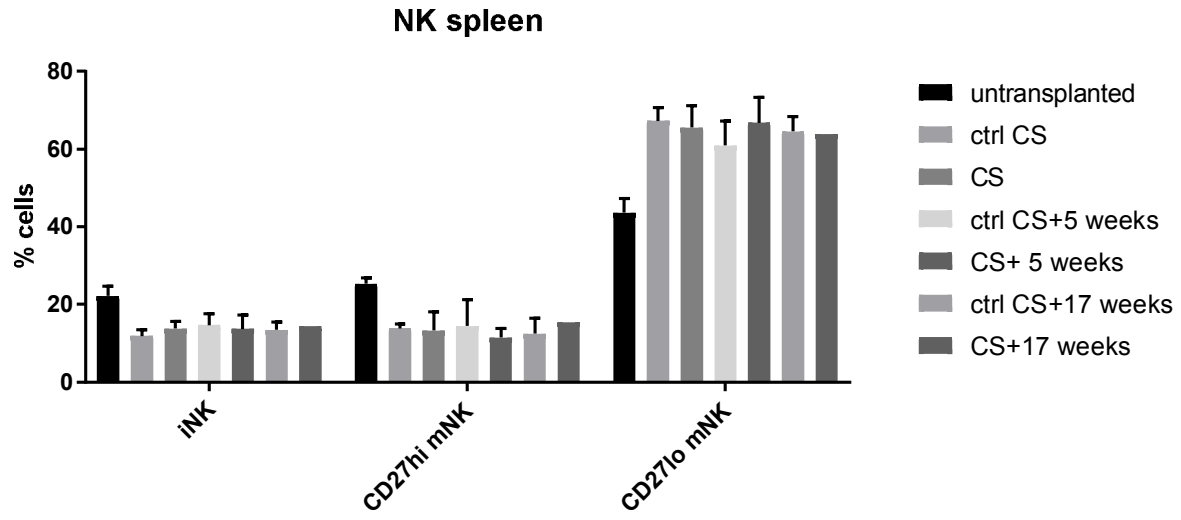

Figure 34: ***NK cell subsets in spleen at different time points of tumor progression and metastasis formation.*** **Mammary glands of BalbNeuT mice were transplanted into Balb/c wt mice. After primary tumor development and curative surgery, NK cell subsets were analyzed by flow cytometry. Mice that were not transplanted with mammary glands were used as control mice. There were no significant changes between control mice and transplanted mice. Statistical tests: Comparison of control mice and transplanted mice, mean values with SD, n=5-10, t-test, p > 0.05 for all comparisons.**

4.2.4 Changes in NK cell subsets were observed in lungs five weeks after curative surgery of the primary tumor

In previous experiments, no changes in immune cell subsets were observed during primary tumor growth and metastasis formation in spleens. Since metastases arise in lungs in the BalbNeuT model, we had a closer look at immune cells in this organ. We hypothesized that the subsets change in lungs in response to direct interaction with tumor cells. Like observed in spleens, Teffs and TCMs increased and TNs decreased when mice matured. Again, no significant changes were observed in each T cell subset in lung compared to transplanted and control mice (Fig. 35). When we looked at NK cell subsets in the lung, we initially could see significant differences between control mice and transplanted mice. Five weeks after curative surgery of the primary tumor, a correlating decrease in $CD27^{hi}$ mNKs with an increase of $CD27^{lo}$ mNKs was detected. In the group “CS+17 weeks” we observed the same trend of NK cell distribution changes, however any differences were small and a statistical analysis was again not possible because only one transplanted animal was available due to other animals not developing primary tumors (Fig. 36).

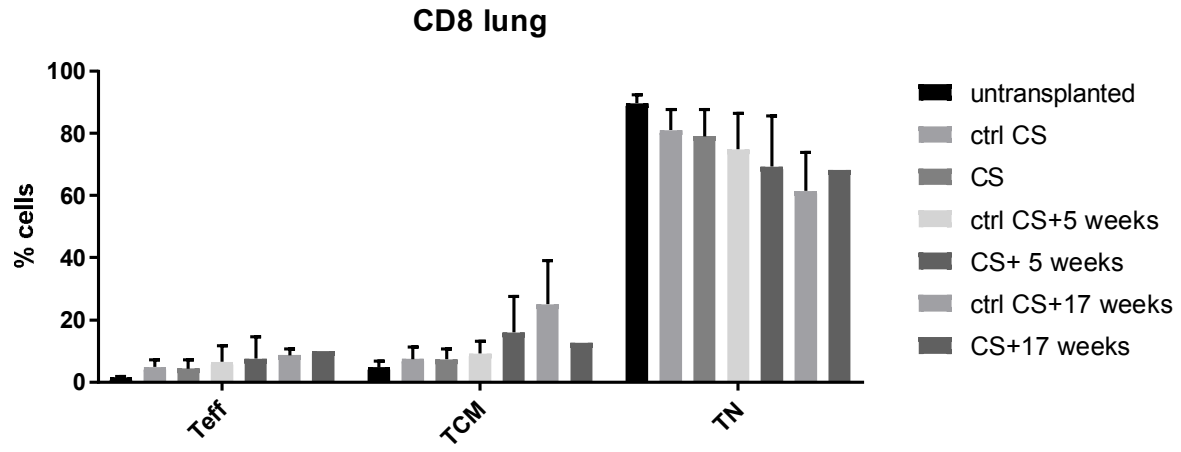

Figure 35: ***CD8⁺ T cell subsets in lung at different time points of tumor progression and metastasis formation.*** **Mammary glands of BalbNeuT mice were transplanted in Balb/c wt mice. After primary tumor development and curative surgery, CD8⁺ T cell subsets were analyzed by flow cytometry. Mice that were not transplanted with mammary glands were used as control mice. No significant changes between control mice and transplanted mice were apparent. Statistical tests: Comparison of control mice and transplanted mice, mean values with SD, n=5-10, t-test, p > 0.05 for all comparisons.**

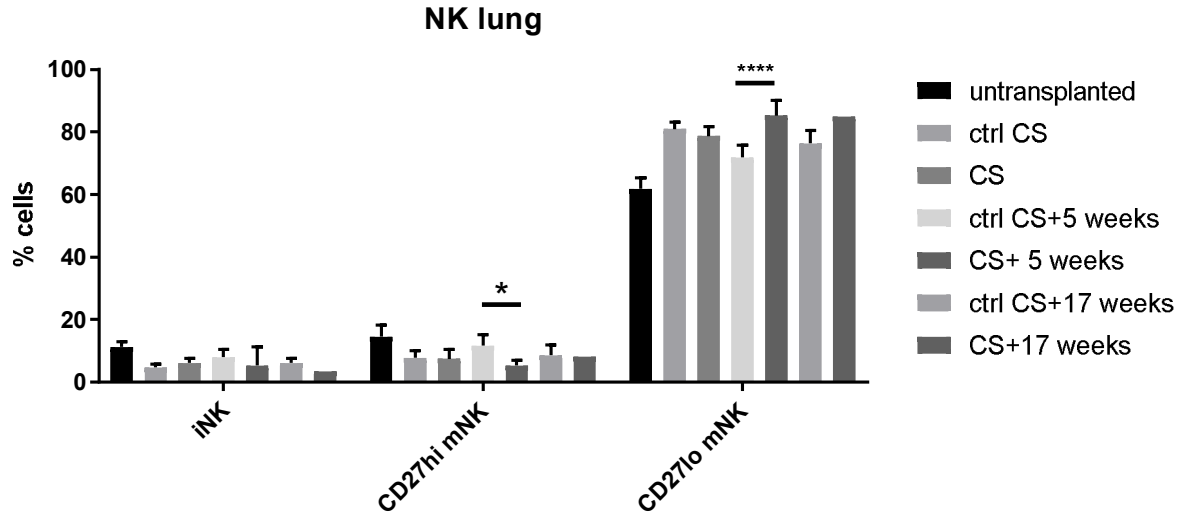

Figure 36: ***NK cell subsets in lung at different time points of tumor progression and metastasis formation.*** **Mammary glands of BalbNeuT mice were transplanted into Balb/c wt mice. After primary tumor development and curative surgery, NK cell subsets were analyzed by flow cytometry. Mice that were not transplanted with mammary glands were used as control mice. Statistical tests: Comparison of control mice and transplanted mice, mean values with SD, n=5-10, t-test, * p ≤ 0.05, **** p ≤ 0.0001.**

4.2.5 NK cell activity was enhanced in the presence of primary tumors

CD107a is a marker for degranulation and therefore functional activity of NK cells. To get an impression of the activity of NK cells during tumor progression we performed a CD107a degranulation assay at each time point (method description in chapter 3.2.16). We were predicting a higher NK cell activity in the presence of primary tumors in transplanted mice (CS). With removal of tumors (CS+5 weeks), we assumed a lower activity of NK cells similar to their control groups followed by reactivation during metastasis formation (CS+17 weeks). We observed at the time of curative surgery (CS) that the expression of CD107a was enhanced in transplanted mice, compared to control mice in both culture conditions ["spontaneous" (splenocytes/lung cells+ medium) and "kill" (splenocytes/lung cells + A20 tumor cells)] in spleen and lung. Moreover, in cultures with A20 tumor cells ("kill" condition), NK cells of transplanted mice showed significantly more degranulation than NK cells of control mice ($p<0.05$). A significant change was not observed in cultures of NK cells with only culture medium ("spontaneous") (Fig.37). Five weeks after removal of the primary tumor (CS+5 weeks), the expression of CD107a was not significantly increased in transplanted mice compared to control mice in both organs, neither in the "spontaneous" nor in the "kill" condition. In lung, the expression of CD107a tended to be lower in transplanted mice compared to control mice, when lung cells were cultured with A20 tumor cells ("kill" condition); however; the standard deviation is relatively high in the group of transplanted mice (Fig. 38). 17 weeks after CS, NK cells of transplanted mice tended to have more degranulation in spleen, compared to their control groups in the "spontaneous" as well as in the "kill" condition. However, statistical analyses were not possible due to the lack of mice with primary tumor formation; only one transplanted mouse was included in the analyses (Fig. 39). In lung, we observed similar results as shown in the lung five weeks after the curative surgery (shown in Fig. 38). Immune cells in the lung from transplanted mice tended to have less degranulation when cultured with A20 tumor cells ("kill" condition). Taken together, development of primary tumors (and probably metastases) leads to stimulation of NK cell activity.

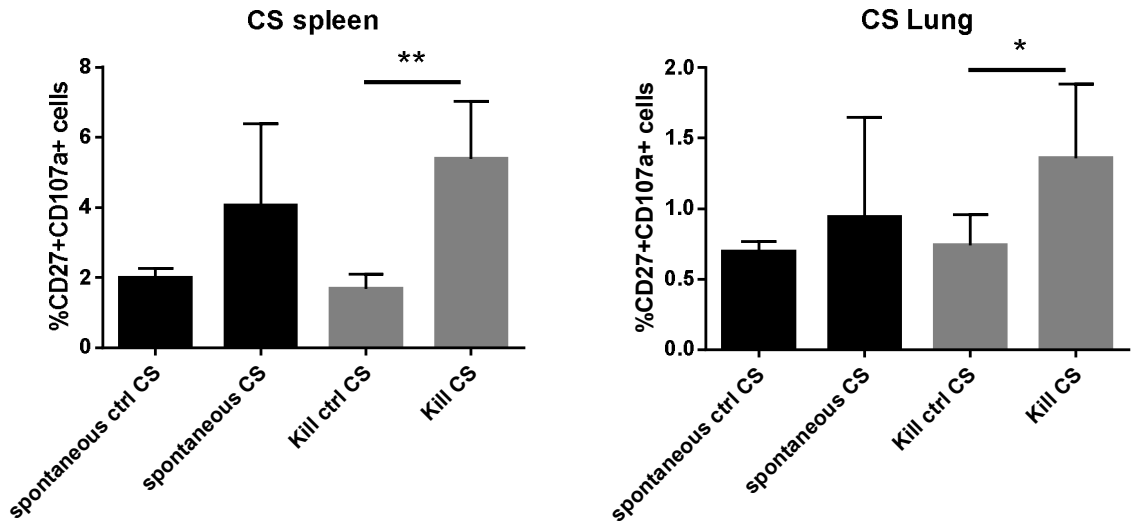

Figure 37: *CD107a degranulation assay at time point "CS" in spleen and lung.* Mammary glands of BalbNeuT mice were transplanted into Balb/c wt mice. After primary tumor development and curative surgery, the CD107a-degranulation marker was analyzed by flow cytometry. Mice that were not transplanted with mammary glands were used as control mice. Statistical tests: Comparison of transplanted and control mice in the "spontaneous" and "kill" condition, mean values with SD, t-test, n=5-10, *≤ 0.05, p ** p ≤ 0.01.

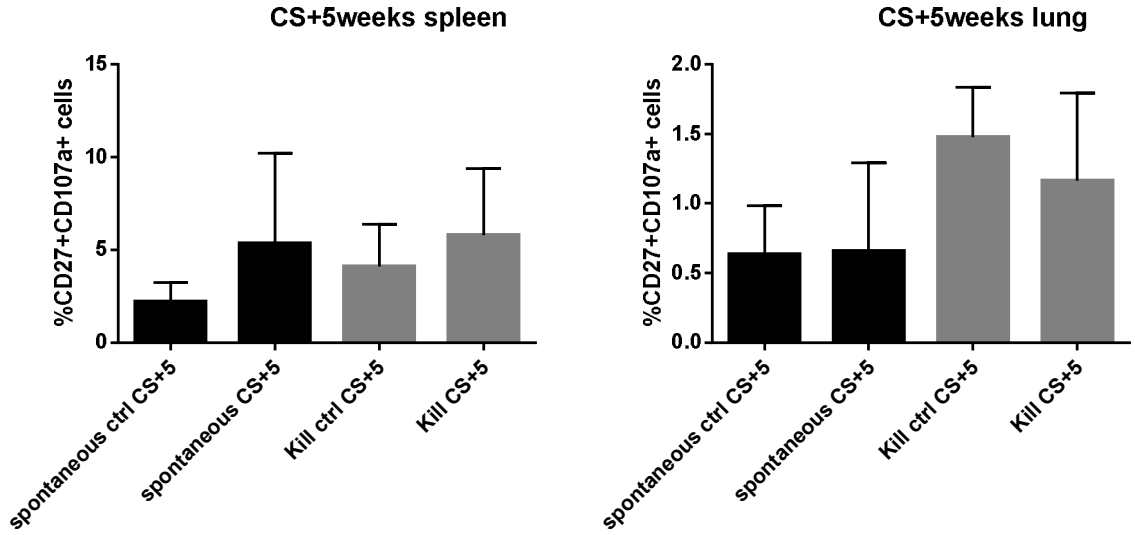

Figure 38: *CD107a degranulation assay at time point "CS+5 weeks" in spleen and lung.* Mammary glands of BalbNeuT mice were transplanted into Balb/c wt mice. After primary tumor development and curative surgery, the CD107a-degranulation marker was analyzed by flow cytometry. Mice that were not transplanted with mammary glands were used as control mice. Statistical tests: Comparison of transplanted and control mice in the "spontaneous" and "kill" condition, mean values with SD, t-test, n=5-10.

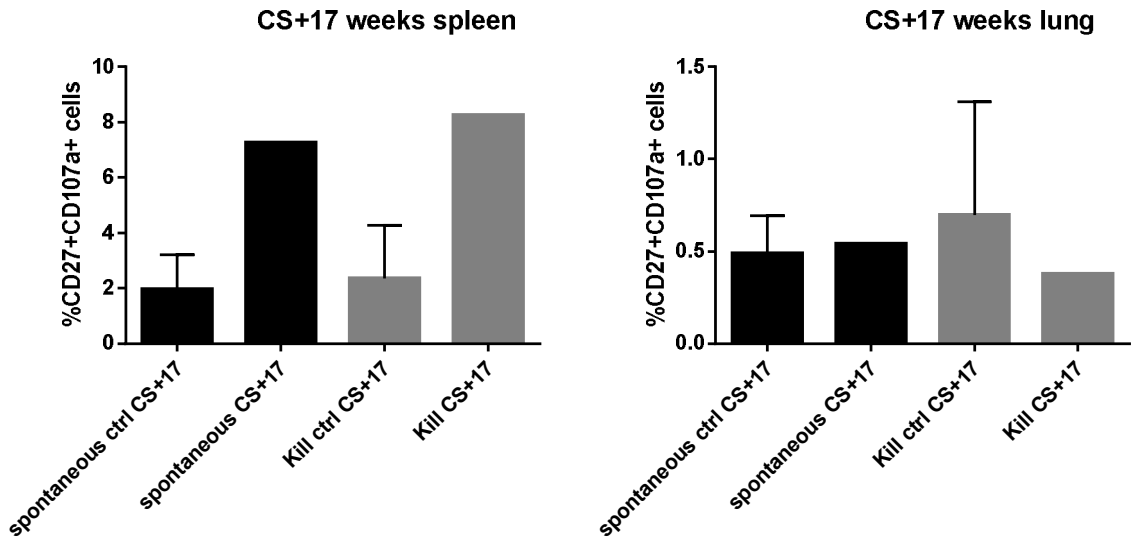

Figure 39: ***CD107a degranulation assay at time point "CS+17 weeks" in spleen and lung*****. Mammary glands of BalbNeuT mice were transplanted into Balb/c wt mice. After primary tumor development and curative surgery, the CD107a-degranulation marker was analyzed by flow cytometry. Mice that were not transplanted with mammary glands were used as control mice. Statistical tests: Comparison of transplanted and control mice in the "spontaneous" and "kill" condition, mean values with SD, n=5-10, no t-test possible.**

4.3 Glutamate

4.3.1 Grm1 Tbet$^{-/-}$ mice did not show higher glutamate concentrations in serum and skin samples compared to B6 wt mice

Namkoong and colleagues discovered increased glutamate release by melanoma cells with constitutively activated Grm1 receptors *in vitro*. Moreover, Shah *et al.* recently showed a higher glutamate concentration in blood plasma of mice with aberrant Grm1 expression in melanocytes (~50mM). As we observed lower numbers of effector and especially memory T cells in Grm1 Tbet$^{-/-}$ mice in comparison to B6 wt and B6 Tbet$^{-/-}$ mice, we hypothesized that Grm1 Tbet$^{-/-}$ mice have elevated levels of glutamate that could have negative effects on the differentiation of CD8^{+} T cells. To test this we measured glutamate concentrations in serum of B6 wt and Grm1 Tbet$^{-/-}$ mice via the company MetaSysX (Potsdam, Germany). However, as shown in the left part of Fig. 40, the concentration turned out to actually be significantly lower in serum of Grm1 Tbet$^{-/-}$ mice (~50µM). Moreover, glutamate concentrations in our samples were 1000-fold lower than in plasma of mice mentioned in Shah´s paper. Since Grm1 mice carry the mutation only in melanocytes, we thought that the glutamate concentration may only be different in skin tissues. However, when tested glutamate levels in the skin of B6 wt versus Grm1 Tbet$^{-/-}$ mice, no significant differences were observed (Fig. 40, right). Collectively, our Grm1 Tbet$^{-/-}$ mice did not show elevated concentrations of glutamate in serum or skin samples.

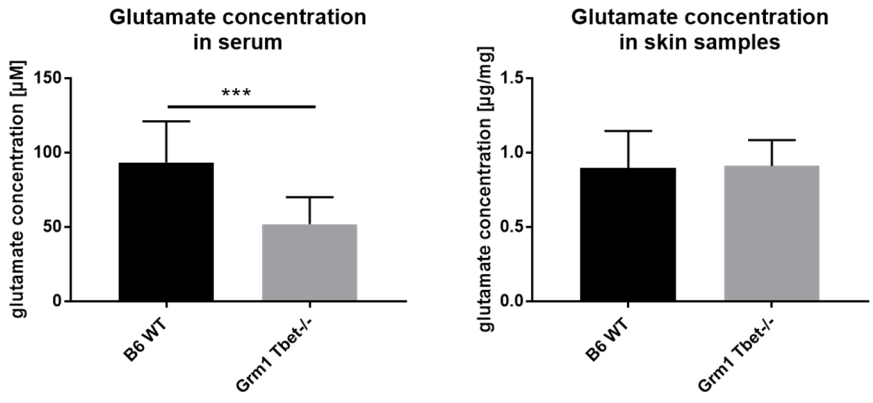

Figure 40: ***Concentration of glutamate in serum and skin samples of B6 wt and Grm1 Tbet$^{-/-}$ mice.*** **The company MetaSysX measured glutamate concentrations in serum (µM) and in skin samples (µg/mg) from B6 wt and Grm1 Tbet-/- mice. Statistical tests: Comparison of B6 wt and Grm1 Tbet$^{-/-}$ mice, mean values with SD, n=10, t-test, *** p ≤ 0.001**

4.3.2 High glutamate concentrations led to impaired differentiation of naïve CD8$^+$ T cells

Despite the unexpected results of the glutamate measurement in serum and skin of our Grm1 Tbet$^{-/-}$ mice, and the differences to results of Shah *et al.*, it is likely that local effects (around melanocytes producing glutamate in Grm1 mice) of glutamate could influence immune cells, such as CD8$^+$ T cells. We hypothesized that higher glutamate concentrations in local tissues with melanocytes impair differentiation of naïve CD8$^+$ T cells after general T cell stimulation. Therefore, naïve CD8$^+$ T cells were isolated from splenocytes of B6 wt mice and stimulated for four days with a specific mixture of antibodies and cytokines (anti-CD3/ anti-CD28/ IL-2/ FasL, see chapter 3.2.18); effector and memory CD8$^+$ T cell subsets (TCMs and Teffs) were measured by flow cytometry. Into these cultures, we added different concentrations of glutamate to test for an effect on cell differentiation. As can be seen in the left part of Fig. 41, from concentrations ≥ 500µM, the number of TCMs was significantly diminished compared to samples without glutamate (w/o Glu). Moreover, the number of Teffs was decreased at higher concentrations of glutamate with significant differences at concentrations of 10mM and 50mM (Fig. 41, right). Taken together, increasing glutamate concentration had dose-dependent effects on differentiation of naïve CD8$^+$ T cells after stimulation.

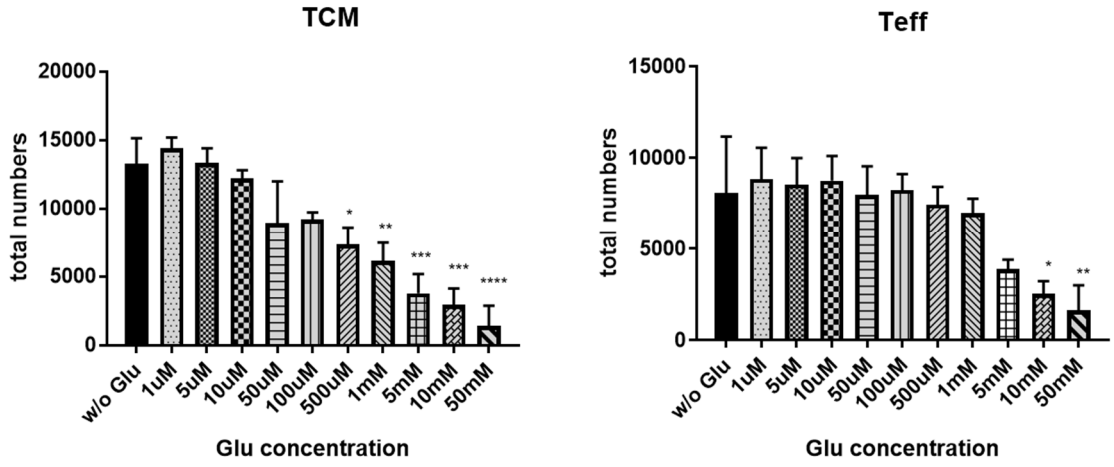

Figure 41: ***Total numbers of central memory and effector T cells after stimulation of naive CD8$^+$ T cells with different concentrations of glutamate.*** **Naïve CD8$^+$ T cells were isolated from spleen and incubated for 4 days with a mixture of anti-CD3/anti-CD28/IL-2/FasL and different concentrations of glutamate. Cells were analyzed by flow cytometry. Statistical test: Comparison of cells incubated with glutamate and samples incubated without glutamate, mean values with SD, n=2, two-way Anova, Dunnett´s multiple comparisons test, * p ≤ 0.05, ** p ≤ 0.01, *** p ≤ 0.001, **** p ≤ 0.0001.**

4.3.3 High glutamate concentrations led to impaired proliferation of naïve CD8$^+$ T cells after stimulation

Stimulation and differentiation of cells is partially connected to proliferation of these cells. Therefore, we predicted that besides the effect of glutamate on differentiation of CD8$^+$ T cells, the proliferation of TCM and Teff subsets might also be influenced by higher concentrations of glutamate. Like in the previous experiment, we isolated naïve CD8$^+$ T cells from splenocytes of B6 wt mice. Cells were stimulated for four days with a specific mixture of antibodies and cytokines (anti-CD3/ anti-CD28/ IL-2/ FasL, see chapter 3.2.18) followed by measurement of TCMs and Teffs; different concentrations of glutamate were added to these cultures. As predicted, significantly fewer TCMs proliferate at glutamate concentrations ≥5mM compared to samples without added glutamate (Fig. 42, left). The numbers of proliferating Teffs also declined at these concentrations, due to high variability in the two experiments, these differences were not significant (Fig. 42, right). Taken together, increasing glutamate concentrations had dose-dependent effects on CD8$^+$ T cell proliferation.

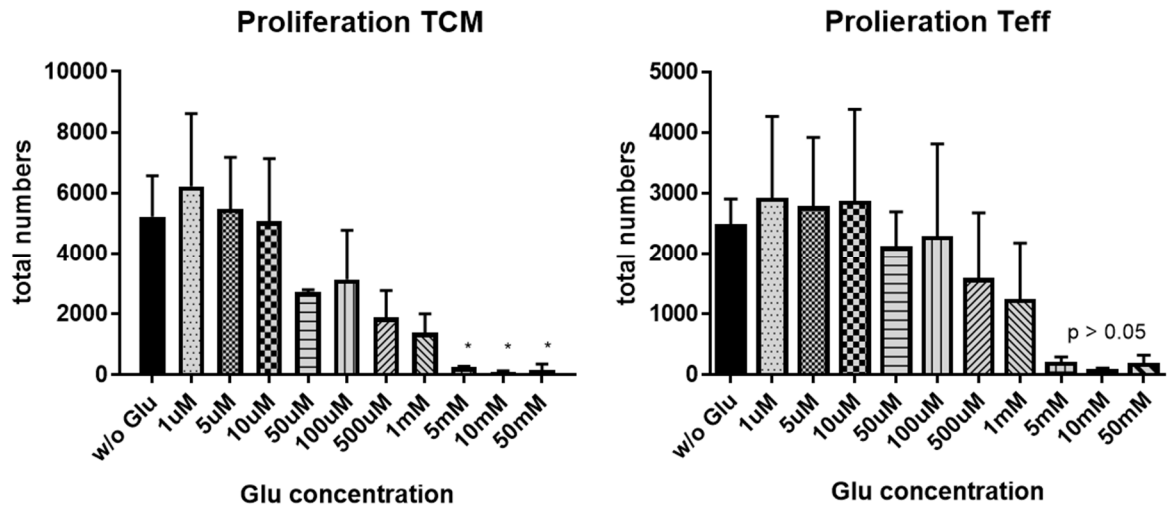

Figure 42: ***Total numbers of proliferating central memory and effector T cells after stimulation of naive CD8$^+$ T cells with different concentrations of glutamate.*** **Naïve CD8$^+$ T cells were isolated from spleens of B6 wt mice and incubated for 4 days with a mixture of anti-CD3/anti-CD28/IL-2/FasL and different concentrations of glutamate. Cells were analyzed by flow cytometry. Statistical test: Comparison of cells incubated with glutamate and samples incubated without glutamate, mean values with SD, n=2, two-way Anova, Dunnett´s multiple comparisons test, * p ≤ 0.05.**

4.3.4 $Ca2^{+}$ influx after addition of different glutamate concentrations

Calcium (Ca^{2+}) influx into cytoplasm is often associated with apoptosis of cells. To exclude the fact that the aforementioned effects of glutamate on differentiation and proliferation is due to apoptosis of cells we performed a Ca^{2+} influx assay (described in method section 3.2.19) in stimulated $CD8^{+}$ T cells after addition of three different concentrations of glutamate (10µM, 100µM and 1mM). At each concentration, a mixture of responding and non-responding cells was observed. Furthermore, there were cells that spontaneously died, resulting in calcium influx signals before adding glutamate (summary in Fig. 43 A). In Fig. 43B, one reacting cell was picked out of the analysis to show the signal increase after addition of glutamate (red line). We also observed that Ca^{2+} influx occurred after only a few minutes of glutamate exposure, but not immediately. To sum up, addition of glutamate led to Ca^{2+} influx in $CD8^{+}$ T cells, which could be a sign for apoptosis in these immune cells. To confirm that, we have done a further Annexin V/ PI staining which is described in the next section (chapter 4.3.5).

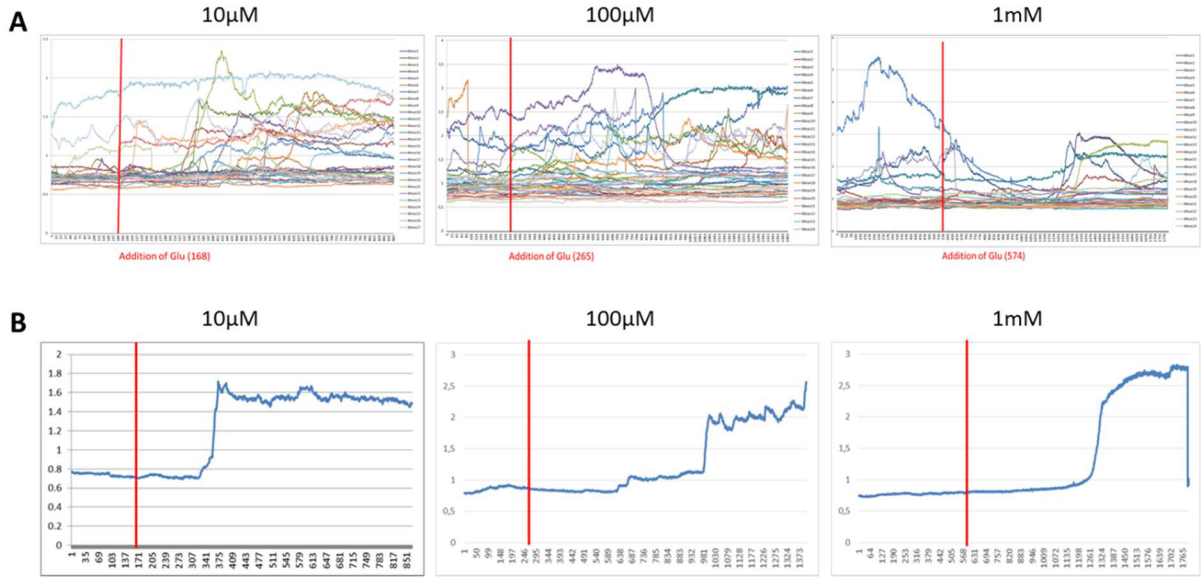

Figure 43: *Ca^{2+} influx assay of $CD8^{+}$ T cells with different concentrations of glutamate*. $CD8^{+}$ T cells were isolated from spleens of B6 wt mice and incubated for three days with anti-CD3/anti-CD28 antibodies. A Ca^{2+} influx assay was performed and monitored by fluorescence microscopy after addition of different concentrations of glutamate (time point of addition is illustrated by the red lines). A. Overview of all monitored signals. B. fluorescence change of one single $CD8^{+}$ T cell after addition of different concentrations of glutamate.

4.3.5 Cell death is not responsible for effects of glutamate on CD8$^+$ T cells

Besides apoptosis, Ca^{2+} is involved in many other signaling pathways in the cell. To confirm that addition of glutamate actually leads to cell death in CD8$^+$ T cells potentially associated with Ca^{2+} and that this is the reason for the observed effects in differentiation and proliferation (chapter 4.3.2 and 4.3.3), we performed an Annexin V/ PI staining. 4h, 24h and 48h after addition of glutamate we monitored the amount of dead cells among unstimulated and stimulated CD8$^+$ T cells. We observed that the amount of dead CD8$^+$ T cells, which were not stimulated, increased over an extended period of time. Stimulated cells did not show increased cell death at higher glutamate concentrations compared to cells without glutamate over time (Fig. 44). Therefore, the effect on differentiation and proliferation was not likely related to cell death at higher glutamate concentrations and Ca^{2+} likely plays a different role that is not related to our hypothesis and further experiments.

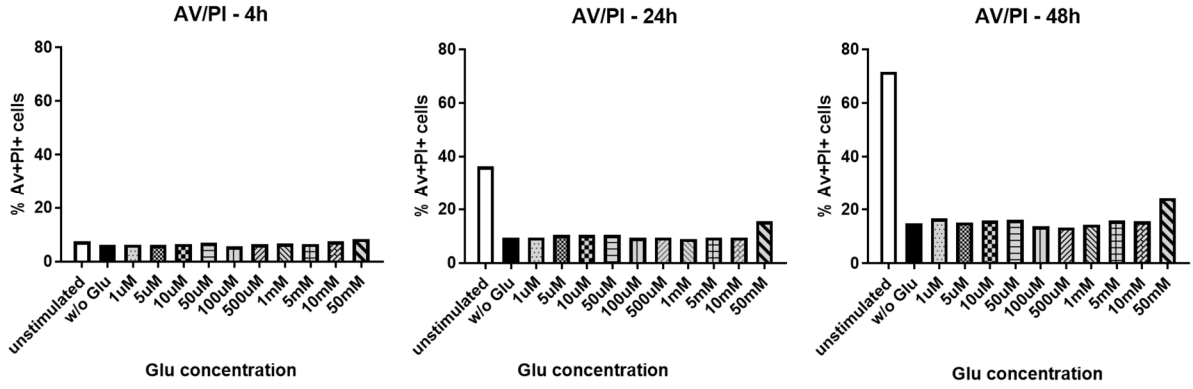

Figure 44: ***Annexin V/PI staining of unstimulated or stimulated CD8$^+$ T cells treated with or without glutamate.*** **Naïve CD8$^+$ T cells were isolated from spleens of B6 wt mice and incubated with a mixture of anti-CD3/anti-CD28/IL-2/FasL and different concentrations of glutamate. An Annexin V/PI staining was performed 4 hours, 24 hours and 48 hours after addition of glutamate and analyzed by flow cytometry.**

4.3.6 Higher glutamate concentrations led to decreased expression of transcription factors Eomes and Tbet

Eomes and Tbet are key transcription factors involved in the differentiation of naïve CD8$^+$ T cells to effector (Teffs) and central memory (TCMs) CD8$^+$ T cells. In wt mice, expression of Tbet leads to generation of Teffs and expression of Eomes leads to development of TCMs. In the following experiments, we tested whether glutamate has effects on expression of these transcription factors.

We hypothesized that higher glutamate concentrations reduce the expression of Eomes and Tbet and therefore the differentiation into cell subsets is impaired. For this experiment, we isolated naïve CD8$^+$ T cells from splenocytes of B6 wt mice. We stimulated them for three days with a specific mixture of antibodies and cytokines (anti-CD3/ anti-CD28/ IL-2/ FasL, see chapter 3.2.18) and added different concentrations of glutamate. Afterwards, we measured the expression of Eomes and Tbet by flow cytometry. Data in Fig. 45 show that stimulation of CD8$^+$ T cells generally led to clear expression of both transcription factors, compared to unstimulated cells. With increasing glutamate concentrations, the expression of Eomes went down with a significant difference at a glutamate concentration of 10mM. Tbet expression was affected at even lower glutamate concentrations; from 5mM, the expression was substantially diminished compared to cells without glutamate. Taken together, higher concentrations of glutamate decrease the expression of key transcription factors responsible for generation of TCM and Teff.

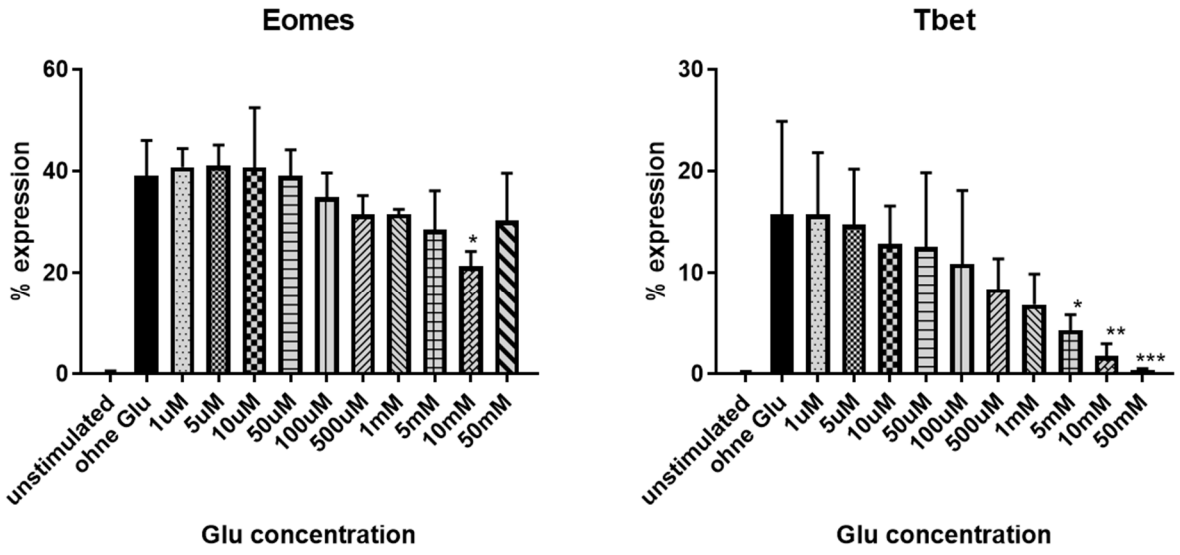

Figure 45: ***Eomes and Tbet expression of CD8$^+$ T cells after addition of glutamate for 3 days.*** **Naïve CD8$^+$ T cells were isolated from spleens of B6 wt mice and incubated for 4 days with a mixture of anti-CD3/anti-CD28/IL-2/FasLand different concentrations of glutamate. Cells were analyzed by flow cytometry. Statistical test: Comparison of cells incubated with glutamate and samples incubated without glutamate, mean values with SD, n=4-5, two-way Anova, Dunnett´s multiple comparisons test, * p ≤ 0.05, ** p ≤ 0.01, *** p ≤ 0.001.**

4.3.7 Expression of different activation markers in CD8$^+$ T cells is decreased with higher glutamate concentrations

In previous experiments we observed that higher concentrations of glutamate had negative effects on the differentiation and proliferation of CD8$^+$ T cells. We also discovered that these observations were not likely due to cell death. In the following experiments, we wanted to check if glutamate has any influence on classic proteins involved in the stimulation or activation of CD8$^+$ T cells. We suspected that the expression of these markers might decrease with higher glutamate concentrations, resulting in impaired activation of CD8$^+$ T cell differentiation and proliferation. Again, we isolated naïve CD8$^+$ T cells from splenocytes of B6 wt mice. We stimulated them for three days with the same specific mixture of antibodies and cytokines as used previously ± different concentrations of glutamate. Afterwards, we measured the expression of the T cell activation markers CD28, CD69 and CD25. As shown in Fig. 46, CD28 expression was significantly decreased with glutamate concentrations of 10mM and 50mM. Moreover, at same concentrations, CD25 expression was also diminished substantially. Looking at the early activation marker CD69, a higher glutamate concentration of 50mM resulted in decreased expression.

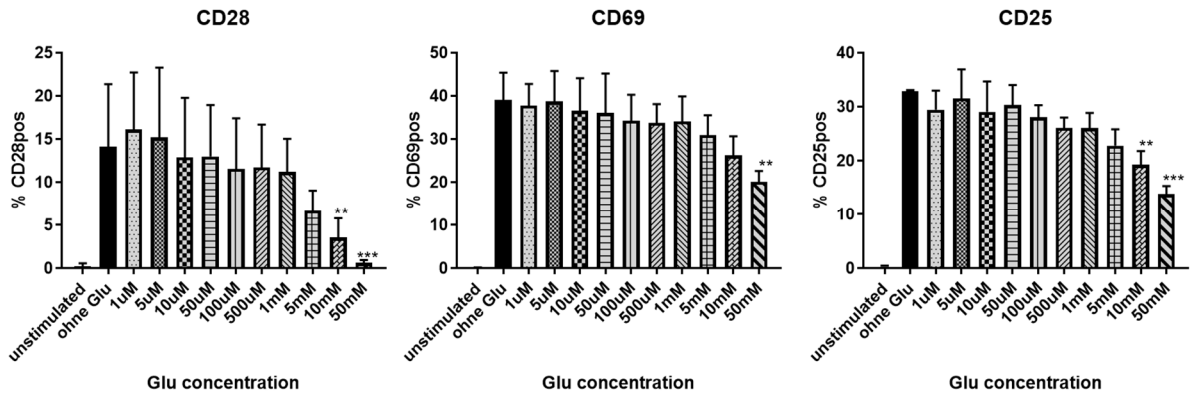

Figure 46: ***Expression of CD28, CD69 and CD25 of CD8$^+$ T cells after addition of glutamate for 3 days.*** **Naïve CD8$^+$ T cells were isolated from spleens of B6 wt mice and incubated for 4 days with a mixture of anti-CD3/anti-CD28/IL-2/FasL and different concentrations of glutamate. Cells were analyzed by flow cytometry. Statistical test: Comparison of cells incubated with glutamate and samples incubated without glutamate, mean values with SD, n=2-6, two-way Anova, Dunnett´s multiple comparisons test, ** p ≤ 0.01, *** p ≤ 0.001.**

4.3.8 Higher glutamate concentrations impaired alloreaction of CD8$^+$ T cells

Besides the differentiation and proliferation of CD8$^+$ T cells, we wanted to know if the activity of CD8$^+$ T cells was comprised. We performed a mixed leucocyte reaction (MLR) with B6 wt CD8$^+$ T cells and fully MHC allogeneic splenocytes of Balb/c wt mice ± glutamate (method section 3.2.23). We predicted that at the highest glutamate concentrations the stimulation of responder CD8$^+$ T cells by stimulator cells (Balb/c) would be impaired, resulting in reduced proliferation of these responder cells. As shown in Fig. 47, proliferation of B6 wt CD8$^+$ T cells was enhanced after addition of Balb/c wt splenocytes to wells in comparison to unstimulated CD8$^+$ T cells. Glutamate concentrations above 5mM resulted in a significant decrease in proliferation of responder cells. This means, that higher glutamate concentrations impaired alloreaction of CD8$^+$ T cells, as predicted.

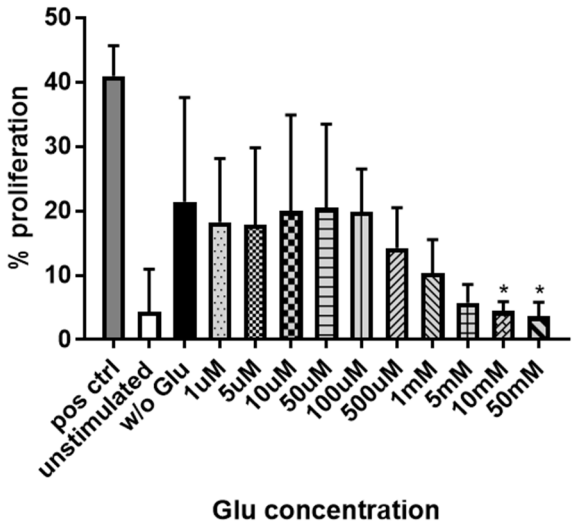

Figure 47: ***MLR of B6 wt CD8$^+$ T cells with Balb/c splenocytes*** **(1:1) after addition of glutamate. B6 wt CD8$^+$ T cells were isolated from spleens and cultivated with Balb/c wt splenocytes and different concentrations of glutamate for 5 days. Cell proliferation was analyzed by flow cytometry with the Fixable Viability Dye eFluor506. Statistical test: Comparison of stimulated cells incubated with glutamate and stimulated cells incubated without glutamate, mean values with SD, n=4, two-way Anova, Dunnett´s multiple comparisons test, * p ≤ 0.05.**

4.3.9 Glutamate does not affect expression of CD4$^+$ T cell activation markers

We already observed that high glutamate concentrations had inhibitory effects on activation and activity of CD8$^+$ T cells. Next, we were interested to know if this amino acid influences the activation of CD4$^+$ T cells as well. Therefore, we isolated naïve CD4$^+$ T cells, stimulated them similarly to CD8$^+$ T cells ± different glutamate concentrations. After two days we measured the expression of three different activation markers. Expression of CD69 and CD25 was not changed after addition of glutamate. When we looked at the expression of CD134, we detected a downward trend at higher glutamate concentrations above 5mM, however, no significant alterations compared to samples without glutamate were observed. Taken together, we summarize that glutamate does not affect the activation of CD4$^+$ T cells.

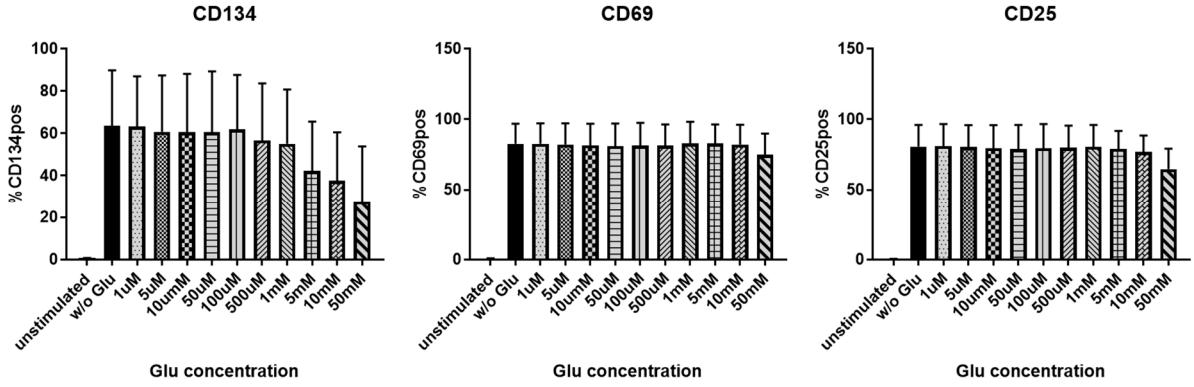

Figure 48: ***Expression of CD134, CD69 and CD25 of CD4$^+$ T cells after addition of glutamate for 2 days.*** **Naïve CD4$^+$ T cells were isolated from spleens of B6 wt mice and incubated for 4 days with a mixture of anti-CD3/anti-CD28/IL-2 and different concentrations of glutamate. Cells were analyzed by flow cytometry. Statistical test: Comparison of cells incubated with glutamate and cells incubated without glutamate, mean values with SD, n=5, two-way Anova, Dunnett´s multiple comparisons test.**

In these experiments, we observed that high concentrations of glutamate have impairing effects on differentiation, proliferation and activity of CD8$^+$ T cells, but do not affect CD4$^+$ T cells.

5 Discussion

NK cells and $CD8^+$ T cells are thought to be important immune cells in tumor immune surveillance. They normally are capable of recognizing tumor cells and killing them by different mechanisms. However, cells with neoplastic potential can develop mechanisms to evade immune destruction and adapt to the host´s microenvironment, resulting in uncontrolled tumor growth and metastasis formation[67,68]. During this doctoral thesis work, using different mouse models that were specifically selected to mimic “natural” tumor development and metastasis, we showed the importance of NK cells and $CD8^+$ T cells and the existence of immunoediting processes during natural tumor progression. More precisely, we showed that natural development of tumors in mice leads to stimulation of immune cell differentiation and activity. Not necessarily expectedly, this initial response ultimately resulted in the accumulation of terminally-differentiated NK cells and $CD8^+$ T cells that had reduced anti-tumor activities. Therefore, our results suggest that the immune response to developing tumors reduces over time, allowing metastases to eventually expand uncontrollably. Since we and others have previously shown in simple tumor implantation models that IL-15 induces these immune cells to attack tumors, we tried to enhance the anti-tumor effect *in vivo* by administering IL-15 at the time of tumor onset. Unexpectedly, however, we found that tumor development and metastasis was not decreased with IL-15 treatment and moreover may have resulted in reduced NK cell and $CD8^+$ T cell activity directed against tumor progression. Our work highlights the crucial differences between the formerly published tumor mouse models, in which tumors or tumor cells were simply transferred to mice, and the spontaneous natural development of tumors with regard to the role of the immune system and immunoediting processes by tumors. Furthermore, we show that immune cells of mice that were stimulated with IL-15 did not overcome these immunoediting processes, and rather likely induce immune exhaustion several days after treatment.

A number of aspects of my research project are worth discussing in more detail. First, as mentioned above, previous work from other investigators in our research group have shown the important role for NK cells in tumor immune surveillance, but only in

tumor implantation or tumor seeding (intravenous infusion) mouse models[211]. For example, by using these well-known adoptive-transfer tumor mouse models, they showed that a lack of mature NK cells leads to the development of lung metastases after intravenous injection of colon carcinoma cells in mice. A marked reduction of metastasis formation was observed after adoptive transfer of these missing NK cell populations. Furthermore, IL-15 treatment of mice completely prevented the formation of lung metastasis after seeding of tumor cells by stimulating NK cell differentiation and activity[211]. Indeed, these experiments showed the importance of potential anti-tumor activities of NK cells and the beneficial effect of IL-15 in immunotherapy. However, critically, these experiments were conducted with tumor cells that did not develop naturally in the animals; rather, the implantation or seeding was performed with already fully developed human or mouse cancer cells, thus omitting the natural tumor development process. A major goal of my thesis work was therefore to extend these previous experiments by studying the role of NK cells and $CD8^+$ T cells in mouse models that mimic the natural (e.g. spontaneous) tumor evolution process. For this purpose, we selected a melanoma mouse model where mice developed tumors a few weeks after birth because of the overexpression of Grm1 receptors in melanocytes[185]. Some experiments were also performed in the BalbNeuT model, where mammary glands with neoplastic potential were transplanted into wt mice at a very young age from which breast tumors are formed after several weeks[194]. Therefore, mice from the two different models typify, at least to some degree, natural development of primary tumors and the metastasis formation process. These models were the basis for my investigations.

Considering this basis, I begin the discussion by first analyzing an innate part of the immune system, which in my thesis was essentially NK cells. Since NK cells are able to recognize and kill neoplastic cells without prior sensitization, we hypothesized that the natural development of tumors in our mice would lead to activation of NK cells. As it is described in the literature, one mechanism for tumors to evade recognition and killing by the immune system is via downregulation of MHC class I molecules on tumor cell surfaces that are normally necessary for the activation of cytotoxic $CD8^+$ T cells[121,215]. Since MHC class I is also a ligand for inhibitory NK cell receptors, the

downregulation of these molecules, and additional signals for activating receptors on NK cells, could therefore lead to the activation of NK cells in our spontaneous tumor-forming mice[215]. Indeed, with the help of the BalbNeuT model, we could clearly see that the presence of tumor cells leads to increased activity of NK cells. We observed that NK cells of mice with existing primary tumors (and probably also with metastases) have higher expression of CD107a, which is described as a functional marker for NK cell activity[216], compared to mice in which primary tumors were removed in a curative surgery. Thus, we have shown that NK cells were activated by naturally developing tumors. IN the furture, our observations should be further substantiated by examining the MHC class I expression on tumor cells. In addition, it will be critical to test whether activating receptors on NK cells are upregulated during tumor development and metastasis formation.

To perform the previously described cytotoxic activities, immature NK cells (iNKs) have to be stimulated to proliferate and differentiate into effector immune cells. We assumed that natural tumor development would lead to accumulation of mature NK cells with high anti-tumor capacities. Mature NK cells can be further divided in $CD27^{high}$ and $CD27^{low}$ NK cells ($CD27^{hi}$ and $CD27^{lo}$ mNKs). These NK cell subsets differ in their cytotoxicity and cytokine production. $CD27^{hi}$ mNKs are highly cytotoxic and have the capacity to produce cytokines like IFN-γ; they might even have the ability to kill tumor cells which express MHC class I, because of the reduced levels of inhibitory receptors for MHC class I molecules[110]. In comparison, $CD27^{lo}$ mNKs are characterized as the NK cell subset with reduced capacity to proliferate, lower cytotoxicity and decreased cytokine production[114]. So, we predicted that natural tumor progression would lead to development of $CD27^{hi}$ mNKs. However, in our mice (Grm1 and BalbNeuT model) we observed that $CD27^{lo}$ mNKs represented the largest subpopulation at each indicated time point. In Grm1 mice, we started to investigate NK cell subsets only after the first tumors were visible, therefore we cannot make clear statements about NK cell changes before versus after malignant transformation. On the other hand, in the BalbNeuT model, we additionally investigated NK cells before transplantation of mammary glands and at a very young age of mice. We observed that natural aging generally leads to increased numbers of $CD27^{lo}$ mNKs; however, at the time of primary tumor

development (or shortly after removal of primary tumors), mice showed significantly enhanced numbers of this NK cell subset. This could be explained by the activation of NK cells by tumor cells and the subsequent differentiation of iNKs and $CD27^{hi}$ into $CD27^{lo}$ mNKs. Therefore, our experiments indicate that NK cells do show evidence of responding to the presence of developing tumors.

We hypothesized at the beginning of our study that immune cells, like NK cells, are able to recognize and kill malignant cells to prevent tumor development or at least metastasis formation. However, the observed long-term elevation in levels of those terminally-differentiated $CD27^{lo}$ mNKs that have lower anti-tumor capacities could help to explain the substantial primary tumor and metastasis burden in our Grm1 mice. Moreover, the apparent dominance of $CD27^{lo}$ mNKs could lead to reduced tumor immune surveillance in the longer-term and would help to explain the development of breast tumors and lung metastases in mice transplanted with BalbNeuT mammary glands. However, we also observed that not all recipient mice developed tumors within the time-frame of our experiment. Different reasons are possible for this phenomenon. One possibility is that errors during the mammary gland transplantation procedure could lead to false positioning of the glands resulting in a lack of tumor development. Furthermore, it is conceivable that not all BalbNeuT mice are equally perfect donors for mammary glands. It is also possible that the immune system of some mice overcame immunoediting processes and is so powerful that malignant cells could be destroyed before development of primary tumors. Taken together, prevention of tumor development and metastasis formation can only be guaranteed by effector immune cells with high anti-tumor capacities. To further confirm our findings, future experiments should evolve transplanting BalbNeuT mammary glands into immunodeficient mice to check if tumors can rise more frequently and grow faster when distinct immune cell types, like NK cells, are missing.

As alluded to before, researchers from our group have previously reported that IL-15 treatment of mice prevented metastasis formation in lungs after the adoptive transfer of tumors using the a tumor cell “seeding” model. They observed in these earlier experiments that IL-15 treatment led to the development of immature NK cells and

mostly CD27^{hi} mNKs[211]. Since, these latter NK cells are a subset characterized by their high cytotoxicity, and cytokine production, the prevention of metastases in this model makes scientific sense. In my thesis work, we wanted to confirm these results in mice with naturally developing tumors. We hypothesized that IL-15 treatment would stimulate the accumulation of CD27^{hi} mNKs with strong anti-tumor capacities, leading to reduced primary tumor and metastasis burden. In my thesis work, we observed initially that IL-15 treatment of Grm1 mice with natural tumor development boosted total NK cell numbers and increased their killing capacities *in vitro* and *in vivo* for a limited time; however, in the long run, it unexpectedly rather resulted in significantly increased levels of NK cells with less anti-tumor activities (CD27^{lo} mNKs)[217]. Consistent with this result, IL-15 treatment in the spontaneous (natural) tumor model did not lead to slower tumor growth or less liver and lung metastases. The different outcome in tumor progression observed in past and present experiments could be explained by the different settings of these two tumor models ("seeding" model versus natural tumor development). One consideration in this respect is that in the "seeding" model, IL-15 was injected into mice before injection of tumor cells. Therefore, CD27^{hi} mNKs were not under the influence of tumor editing processes and therefore were able to kill subsequently infused tumor cells. In contrast, in the mice with the natural tumor development, IL-15 was first given when tumors became visible initially. Since it takes time to recognize the first tumors in this melanoma model, and they only become visible once they are firmly established, it is possible that cells such as NK cells, but also other immune cells responsible for tumor immune surveillance, like CD8^{+} T cells (discussed later), have already been immune-edited to some degree and the IL-15 treatment is no longer effective. Our results would therefore support the hypothesis that tumors evolve the ability to alter the effects of e.g. IL-15 treatment on NK cell differentiation via immunoediting. Another interesting possibility to explain the lack of anti-tumor effect in the Grm1 mouse model could relate to the preferential expansion of the CD27^{lo} mNKs under the influence of early spontaneous tumor development. Interestingly, our use of IL-15 treatment after tumor establishment could actually have further enhanced the disproportional expansion of these less effective tumor-killing cells. A further indication that natural tumor development could influence the effect of IL-15 on NK cells is the comparison of our experiments in Grm1 versus B6 wt mice. Consistent with this idea,

IL-15 treatment in Grm1 mice led to significantly more $CD27^{lo}$ mNKs compared to the development of $CD27^{hi}$ mNKs in B6 wt mice. Therefore, my thesis work shows that IL-15 treatment is inefficient in mice with natural tumor development, at least when applied after tumors have already developed, and this may be related to selective expansion of CD27lo mNKs that are not effective at preventing further tumor growth and metastasis formation. These results may have implications in humans, when considering treatment with IL-15 to boost anti-tumor effects.

When we treated the Grm1 mice with IL-15, we assumed that the repeated administration of the cytokine would lead to a permanently increased level of NK cells. However, we actually made the observation that repeated IL-15 treatment in Grm1 mice, as well as in B6 wt mice, led to significantly decreased total numbers of NK cells over time. Our results are consistent with a study by Felices *et al*., showing that besides initial proliferation and expansion of NK cells, multiple treatment with IL-15 can decrease the viability of NK cells and reduce tumor control[218]. With our observation, we then hypothesized that stimulation with IL-15 results in the exhaustion of NK cells and probably their clearance by apoptosis. Alvarez and colleagues recently showed that NK cells exhaust after sustained proliferation, which impairs anti-tumor activity that is associated with a downregulation of the transcription factor Eomes and the activating NK cell receptor NKG2D[214]. With, albeit, a small number of samples, our hypothesis of NK cell exhaustion is supported by gene expression analyses of these genes showing the downregulation several days after IL-15 treatment. Taken together, we have shown that natural tumor development influences the maturation and activity of NK cells leading to terminally-differentiated cells with a reduced capacity to kill tumor cells. Furthermore, IL-15 treatment of mice shows exhaustion effects on NK cells rather than beneficial effects on anti-tumor activities.

Besides NK cells we also investigated the adaptive part of the immune system. We studied the role of $CD8^+$ T cells in the context of natural tumor development. Since we assumed that immunoediting processes take place in mice with natural tumor growth, we hypothesized that the presence of malignant cells does not activate $CD8^+$ T cells. As mentioned above, one mechanism is the downregulation of MHC class I molecules

on tumors cell surfaces resulting in a lack of stimulation of $CD8^+$ T cell activity. Moreover, tumor cells can express ligands for immune checkpoint proteins on $CD8^+$ T cells, leading to inactivation and exhaustion of these immune cells[28,219]. Like expected, we observed that the development of tumors in our mice did not change the proportions of $CD8^+$ T cell subsets. We have seen in both of our mouse models that naïve $CD8^+$ T cells are the predominant subpopulation over time. Thus, $CD8^+$ T cells did not overcome immunoediting processes to be activated to kill naturally developing tumor cells. In future experiments, we could further investigate and confirm immunoediting processes, e.g. by gene expression analyses of tumor and immune cells. For instance, on tumor cells, we could check the expression of MHC class I molecules or immune checkpoint ligands (e.g. PD-L1) at different time points during tumor development and IL-15 treatment. Furthermore, immunosuppressive molecules released by tumor cells could be determined in the tumor microenvironment. Additionally, on immune cells, the expression of the corresponding immune checkpoint proteins or the expression of "death" receptors (Fas, TRAIL) could be investigated[220]. Another point that we must consider in this discussion is that the assumed "tumor antigens" in our spontaneous cancer models may simply not be immunogenic, thus not stimulating a $CD8^+$ T cell response. If this is the case, then we would need to consider to use other models where different tumor-specific antigens are expressed and known to stimulate $CD8^+$ T cells.

It is described in the literature, that $CD8^+$ T cells migrate away from tumors to the spleen or lymph nodes after activation within the tumor microenvironment and lose their capacity to proliferate (until they were stimulated with exogenous compounds)[221]. Considering the possibility, we treated our Grm1 mice with IL-15 and hypothesized that the treatment stimulates $CD8^+$ T cells to proliferate, differentiate into effector immune cells and perform anti-tumor activities. We observed that administration of IL-15 led to proliferation of $CD8^+$ T cells, which was evident by the significant increase in total T cell numbers. Moreover, after IL-15 treatment the proportion of naïve $CD8^+$ T cells decreased simultaneously with an increase in central memory $CD8^+$ T cells (TCMs). Other research groups have also made this same observation[64,144,222,223]. TCMs are, similar to $CD27^{lo}$ mNKs, terminally-differentiated cells with reduced anti-tumor activities. This could further help to explain why tumors and metastases are eventually

able to grow uncontrollably in Grm1 mice. O summarize, tumors appear to develop mechanisms to escape immune recognition and killing by $CD8^+$ T cells through different immunoediting processes, especially in the models we used where the immune system is exposed to the entire natural neoplasm development process. As already discussed for NK cells, IL-15 treatment of mice did not overcome these evasive mechanisms, and may even result in the development of terminally-differentiated TCMs that have reduced anti-tumor capacities.

Glutamate is the natural ligand of the Grm1 receptor and is released in higher amounts by melanocytes that show overexpression of this receptor[188,210]. During experiments with Grm1 $Tbet^{-/-}$ mice, we coincidentally observed that these mice showed reduced numbers of effector (Teffs), and especially central memory (TCMs) $CD8^+$ T cells compared to B6 wt and B6 $Tbet^{-/-}$ mice. We used Tbet-deficient mice because this transcription factor is normally involved in the differentiation of NK cells and $CD8^+$ T cells and we originally wanted to study tumor progression in mice with altered immune cell differentiation. Nonetheless, we hypothesized that glutamate concentrations would be elevated in our Grm1 $Tbet^{-/-}$ mice, which could possibly affect the development of $CD8^+$ T cells and consequently their killing capacity against melanoma cancer cells. However, measurements of glutamate concentrations in serum and skin samples of B6 wt and Grm1 $Tbet^{-/-}$ mice did not show increased *in vivo* levels of glutamate. Since during measurements the company that performed the testing informed us that they had some problems in determining the glutamate concentrations, we took a critical look at the authenticity of the measured concentrations. This was especially interesting to us because measurements in the Grm1 mice mentioned in Shah´s paper from 2019 showed 1000-fold higher glutamate concentrations[210]. The only potential explanation we could find is that Shah *et al.* measured glutamate in plasma versus serum in our experiments. Unfortunately, we have not been able to determine the cause for this discrepancy, and did not have the opportunity to repeat the measurements in plasma instead of serum.

Nonetheless, we continue to assume despite our inability to see higher systemic glutamate levels in Grm1 mice, that at least local tissue concentrations of glutamate

around areas of melanocytes must be higher in these mice and could be influencing the immune response to melanoma tumor cells. Therefore, we remained interested in the potential general effect of glutamate on $CD8^+$ T cells. To examine this aspect, we tested a wide range of glutamate concentrations with immune cells from B6 wt mice in *in vitro* experiments. In general, to be sure that we could be sensitive to all possible effects, we added glutamate in a wide range of concentrations (0µM – 50mM). In those experiments, we observed that high concentrations of glutamate do impair the differentiation and proliferation of $CD8^+$ T cells. We found that these concentrations led to reduced numbers of TCMs and Teffs, which could be associated with the reduced expression of the activation markers CD25, CD28 and CD69 at higher glutamate concentrations. We also observed that $CD8^+$ T cells that were cultured with high glutamate concentrations showed a decreased response towards fully MHC disparate splenocytes from allogeneic mice; therefore, glutamate also impairs typical allogeneic immune response activity, which could be relevant in the case where cancers are expressing tumor-specific antigens. Moreover, differentiation of $CD8^+$ T cells depends on key transcription factors like Eomes, and we found that the expression of this gene was decreased at higher glutamate concentrations. The question remains whether these results could contribute to the end-effect of lower numbers of Teffs and TCMs in Grm1 $Tbet^{-/-}$ mice (assuming that the Grm1 mutation leads to high glutamate concentrations surrounding melanocytes in these mice). In addition to these experiments, we also tested whether glutamate affects in the activation of $CD4^+$ T cells, but no effect was detected. We therefore conclude from these experiments with glutamate that high concentrations of this amino acid have the ability to interfere with the maturation and activity of $CD8^+$ T cells, but not $CD4^+$ T cells. Further analyses of experiments in Grm1 $Tbet^{-/-}$ mice could show if the impairment of $CD8^+$ T cells leads to altered tumor progression and metastasis formation. However, these *in vivo* experiments are very time consuming and therefore beyond the scope of my thesis work. Nonetheless, since Grm1 mutations are found in different human cancer types, our findings are relevant and help to better understand the potential role and actions of the immune system, especially of $CD8^+$ T cells, in these cancer patients in the context of increase glutamate levels.

In summary, in my doctoral thesis I investigated and confirmed a role for NK cells and $CD8^+$ T cells in tumor immune surveillance and showed that there is a difference in this role depending on whether the tumor and immune system evolved in the setting of “natural” tumor development. This work supports the hypothesis that immunoediting processes do likely occur during natural tumor development. Moreover, I demonstrated that IL-15 treatment in mice with natural tumor development does not show beneficial effects over the long-term, which is contrary to what has been reported in adoptive-transfer tumor models. This research provides insight into how innate and adaptive immune responses may affect the growth and metastasis of cancer.

6 Sources

1. WorldHealthOrganization. Noncommunicable diseases. Published 2018, June. Accessed.
2. WorldHealthOrganization. GLOBOCAN 2018. Published 2018. Accessed.
3. Chakraborty S, Rahman T. The difficulties in cancer treatment. *Ecancermedicalscience.* 2012;6:ed16.
4. Hanahan D, Weinberg RA. The hallmarks of cancer. *Cell.* 2000;100(1):57-70.
5. Hanahan D, Weinberg RA. Hallmarks of cancer: the next generation. *Cell.* 2011;144(5):646-674.
6. Wyckoff JB, Jones JG, Condeelis JS, Segall JE. A critical step in metastasis: in vivo analysis of intravasation at the primary tumor. *Cancer Res.* 2000;60(9):2504-2511.
7. Kalluri R, Weinberg RA. The basics of epithelial-mesenchymal transition. *J Clin Invest.* 2009;119(6):1420-1428.
8. Chambers AF, Groom AC, MacDonald IC. Dissemination and growth of cancer cells in metastatic sites. *Nat Rev Cancer.* 2002;2(8):563-572.
9. Poste G, Fidler IJ. The pathogenesis of cancer metastasis. *Nature.* 1980;283(5743):139-146.
10. Fidler IJ. Metastasis: quantitative analysis of distribution and fate of tumor emboli labeled with 125 I-5-iodo-2'-deoxyuridine. *J Natl Cancer Inst.* 1970;45(4):773-782.
11. Sai B, Xiang J. Disseminated tumour cells in bone marrow are the source of cancer relapse after therapy. *J Cell Mol Med.* 2018;22(12):5776-5786.
12. Paget S. The distribution of secondary growths in cancer of the breast. 1889. *Cancer Metastasis Rev.* 1989;8(2):98-101.
13. Akhtar M, Haider A, Rashid S, Al-Nabet ADMH. Paget's "Seed and Soil" Theory of Cancer Metastasis: An Idea Whose Time has Come. *Adv Anat Pathol.* 2019;26(1):69-74.
14. Klein CA. Parallel progression of primary tumours and metastases. *Nat Rev Cancer.* 2009;9(4):302-312.
15. Qian CN, Mei Y, Zhang J. Cancer metastasis: issues and challenges. *Chin J Cancer.* 2017;36(1):38.
16. Dimberu PM, Leonhardt RM. Cancer immunotherapy takes a multi-faceted approach to kick the immune system into gear. *Yale J Biol Med.* 2011;84(4):371-380.
17. https://www.cancerresearchuk.org/about-cancer/cancer-in-general/treatment/immunotherapy/types/monoclonal-antibodies. Monoclonal antibodies. Published 2019. Accessed 17.09.2019.

18. Adams GP, Weiner LM. Monoclonal antibody therapy of cancer. *Nat Biotechnol.* 2005;23(9):1147-1157.

19. Harbeck N, Penault-Llorca F, Cortes J, et al. Breast cancer. *Nat Rev Dis Primers.* 2019;5(1):66.

20. Slamon DJ, Leyland-Jones B, Shak S, et al. Use of chemotherapy plus a monoclonal antibody against HER2 for metastatic breast cancer that overexpresses HER2. *N Engl J Med.* 2001;344(11):783-792.

21. Azoury SC, Straughan DM, Shukla V. Immune Checkpoint Inhibitors for Cancer Therapy: Clinical Efficacy and Safety. *Curr Cancer Drug Targets.* 2015;15(6):452-462.

22. Rudd CE, Taylor A, Schneider H. CD28 and CTLA-4 coreceptor expression and signal transduction. *Immunol Rev.* 2009;229(1):12-26.

23. Leach DR, Krummel MF, Allison JP. Enhancement of antitumor immunity by CTLA-4 blockade. *Science.* 1996;271(5256):1734-1736.

24. Wolchok JD, Hodi FS, Weber JS, et al. Development of ipilimumab: a novel immunotherapeutic approach for the treatment of advanced melanoma. *Ann N Y Acad Sci.* 2013;1291:1-13.

25. Cameron F, Whiteside G, Perry C. Ipilimumab: first global approval. *Drugs.* 2011;71(8):1093-1104.

26. Brown JA, Dorfman DM, Ma FR, et al. Blockade of programmed death-1 ligands on dendritic cells enhances T cell activation and cytokine production. *J Immunol.* 2003;170(3):1257-1266.

27. Latchman Y, Wood CR, Chernova T, et al. PD-L2 is a second ligand for PD-1 and inhibits T cell activation. *Nat Immunol.* 2001;2(3):261-268.

28. Ahmadzadeh M, Johnson LA, Heemskerk B, et al. Tumor antigen-specific CD8 T cells infiltrating the tumor express high levels of PD-1 and are functionally impaired. *Blood.* 2009;114(8):1537-1544.

29. Hino R, Kabashima K, Kato Y, et al. Tumor cell expression of programmed cell death-1 ligand 1 is a prognostic factor for malignant melanoma. *Cancer.* 2010;116(7):1757-1766.

30. Kim JW, Nam KH, Ahn SH, et al. Prognostic implications of immunosuppressive protein expression in tumors as well as immune cell infiltration within the tumor microenvironment in gastric cancer. *Gastric Cancer.* 2016;19(1):42-52.

31. Ribas A, Hamid O, Daud A, et al. Association of Pembrolizumab With Tumor Response and Survival Among Patients With Advanced Melanoma. *JAMA.* 2016;315(15):1600-1609.

32. Larkin J, Hodi FS, Wolchok JD. Combined Nivolumab and Ipilimumab or Monotherapy in Untreated Melanoma. *N Engl J Med.* 2015;373(13):1270-1271.

33. Larkin J, Chiarion-Sileni V, Gonzalez R, et al. Five-Year Survival with Combined Nivolumab and Ipilimumab in Advanced Melanoma. *N Engl J Med.* 2019;381(16):1535-1546.

34. Dong H, Strome SE, Salomao DR, et al. Tumor-associated B7-H1 promotes T-cell apoptosis: a potential mechanism of immune evasion. *Nat Med.* 2002;8(8):793-800.

35. Lee SK, Seo SH, Kim BS, et al. IFN-gamma regulates the expression of B7-H1 in dermal fibroblast cells. *J Dermatol Sci.* 2005;40(2):95-103.

36. Butte MJ, Keir ME, Phamduy TB, Sharpe AH, Freeman GJ. Programmed death-1 ligand 1 interacts specifically with the B7-1 costimulatory molecule to inhibit T cell responses. *Immunity.* 2007;27(1):111-122.

37. Deng R, Bumbaca D, Pastuskovas CV, et al. Preclinical pharmacokinetics, pharmacodynamics, tissue distribution, and tumor penetration of anti-PD-L1 monoclonal antibody, an immune checkpoint inhibitor. *MAbs.* 2016;8(3):593-603.

38. Stewart R, Morrow M, Hammond SA, et al. Identification and Characterization of MEDI4736, an Antagonistic Anti-PD-L1 Monoclonal Antibody. *Cancer Immunol Res.* 2015;3(9):1052-1062.

39. Boyerinas B, Jochems C, Fantini M, et al. Antibody-Dependent Cellular Cytotoxicity Activity of a Novel Anti-PD-L1 Antibody Avelumab (MSB0010718C) on Human Tumor Cells. *Cancer Immunol Res.* 2015;3(10):1148-1157.

40. Chmielewski M, Hombach AA, Abken H. Antigen-Specific T-Cell Activation Independently of the MHC: Chimeric Antigen Receptor-Redirected T Cells. *Front Immunol.* 2013;4:371.

41. https://www.cancerresearchuk.org/about-cancer/cancer-in-general/treatment/immunotherapy/types/CAR-T-cell-therapy. CAR T cell therapy. Published 2019. Accessed 17.09.2019.

42. Golubovskaya V, Wu L. Different Subsets of T Cells, Memory, Effector Functions, and CAR-T Immunotherapy. *Cancers (Basel).* 2016;8(3).

43. Sadelain M, Rivière I, Brentjens R. Targeting tumours with genetically enhanced T lymphocytes. *Nat Rev Cancer.* 2003;3(1):35-45.

44. Hombach A, Wieczarkowiecz A, Marquardt T, et al. Tumor-specific T cell activation by recombinant immunoreceptors: CD3 zeta signaling and CD28 costimulation are simultaneously required for efficient IL-2 secretion and can be integrated into one combined CD28/CD3 zeta signaling receptor molecule. *J Immunol.* 2001;167(11):6123-6131.

45. Rosenberg SA, Dudley ME. Adoptive cell therapy for the treatment of patients with metastatic melanoma. *Curr Opin Immunol.* 2009;21(2):233-240.

46. Muranski P, Boni A, Wrzesinski C, et al. Increased intensity lymphodepletion and adoptive immunotherapy--how far can we go? *Nat Clin Pract Oncol.* 2006;3(12):668-681.

47. Maude SL, Frey N, Shaw PA, et al. Chimeric antigen receptor T cells for sustained remissions in leukemia. *N Engl J Med.* 2014;371(16):1507-1517.

48. Turtle CJ, Hanafi LA, Berger C, et al. Immunotherapy of non-Hodgkin's lymphoma with a defined ratio of CD8+ and CD4+ CD19-specific chimeric antigen receptor-modified T cells. *Sci Transl Med.* 2016;8(355):355ra116.

49. Kochenderfer JN, Dudley ME, Kassim SH, et al. Chemotherapy-refractory diffuse large B-cell lymphoma and indolent B-cell malignancies can be effectively treated with autologous T cells expressing an anti-CD19 chimeric antigen receptor. *J Clin Oncol.* 2015;33(6):540-549.

50. Pettitt D, Arshad Z, Smith J, Stanic T, Holländer G, Brindley D. CAR-T Cells: A Systematic Review and Mixed Methods Analysis of the Clinical Trial Landscape. *Mol Ther.* 2018;26(2):342-353.

51. Lee S, Margolin K. Cytokines in cancer immunotherapy. *Cancers (Basel).* 2011;3(4):3856-3893.

52. Berraondo P, Sanmamed MF, Ochoa MC, et al. Cytokines in clinical cancer immunotherapy. *Br J Cancer.* 2019;120(1):6-15.

53. Waldmann TA. Cytokines in Cancer Immunotherapy. *Cold Spring Harb Perspect Biol.* 2018;10(12).

54. Basham TY, Bourgeade MF, Creasey AA, Merigan TC. Interferon increases HLA synthesis in melanoma cells: interferon-resistant and -sensitive cell lines. *Proc Natl Acad Sci U S A.* 1982;79(10):3265-3269.

55. Dolei A, Capobianchi MR, Ameglio F. Human interferon-gamma enhances the expression of class I and class II major histocompatibility complex products in neoplastic cells more effectively than interferon-alpha and interferon-beta. *Infect Immun.* 1983;40(1):172-176.

56. Zhang S, Kohli K, Black RG, et al. Systemic Interferon-γ Increases MHC Class I Expression and T-cell Infiltration in Cold Tumors: Results of a Phase 0 Clinical Trial. *Cancer Immunol Res.* 2019;7(8):1237-1243.

57. Trepiakas R, Pedersen AE, Met O, Svane IM. Addition of interferon-alpha to a standard maturation cocktail induces CD38 up-regulation and increases dendritic cell function. *Vaccine.* 2009;27(16):2213-2219.

58. Siegal FP, Kadowaki N, Shodell M, et al. The nature of the principal type 1 interferon-producing cells in human blood. *Science.* 1999;284(5421):1835-1837.

59. Tsuruoka N, Sugiyama M, Tawaragi Y, et al. Inhibition of in vitro angiogenesis by lymphotoxin and interferon-gamma. *Biochem Biophys Res Commun.* 1988;155(1):429-435.

60. Wagner TC, Velichko S, Chesney SK, et al. Interferon receptor expression regulates the antiproliferative effects of interferons on cancer cells and solid tumors. *Int J Cancer.* 2004;111(1):32-42.

61. Indraccolo S. Interferon-alpha as angiogenesis inhibitor: learning from tumor models. *Autoimmunity.* 2010;43(3):244-247.

62. Waldmann TA. The interleukin-2 receptor on normal and malignant lymphocytes. *Adv Exp Med Biol.* 1987;213:129-137.

63. McNally A, Hill GR, Sparwasser T, Thomas R, Steptoe RJ. CD4+CD25+ regulatory T cells control CD8+ T-cell effector differentiation by modulating IL-2 homeostasis. *Proc Natl Acad Sci U S A.* 2011;108(18):7529-7534.

64. Berard M, Brandt K, Bulfone-Paus S, Tough DF. IL-15 promotes the survival of naive and memory phenotype CD8+ T cells. *J Immunol.* 2003;170(10):5018-5026.

65. Marks-Konczalik J, Dubois S, Losi JM, et al. IL-2-induced activation-induced cell death is inhibited in IL-15 transgenic mice. *Proc Natl Acad Sci U S A.* 2000;97(21):11445-11450.

66. Yee C, Thompson JA, Byrd D, et al. Adoptive T cell therapy using antigen-specific CD8+ T cell clones for the treatment of patients with metastatic melanoma: in vivo persistence, migration, and antitumor effect of transferred T cells. *Proc Natl Acad Sci U S A.* 2002;99(25):16168-16173.

67. Burnet FM. The concept of immunological surveillance. *Prog Exp Tumor Res.* 1970;13:1-27.

68. Dunn GP, Bruce AT, Ikeda H, Old LJ, Schreiber RD. Cancer immunoediting: from immunosurveillance to tumor escape. *Nat Immunol.* 2002;3(11):991-998.

69. Schreiber RD, Old LJ, Smyth MJ. Cancer immunoediting: integrating immunity's roles in cancer suppression and promotion. *Science.* 2011;331(6024):1565-1570.

70. Matzinger P. Tolerance, danger, and the extended family. *Annu Rev Immunol.* 1994;12:991-1045.

71. Brentville VA, Atabani S, Cook K, Durrant LG. Novel tumour antigens and the development of optimal vaccine design. *Ther Adv Vaccines Immunother.* 2018;6(2):31-47.

72. Ehx G, Perreault C. Discovery and characterization of actionable tumor antigens. *Genome Med.* 2019;11(1):29.

73. Guerra N, Tan YX, Joncker NT, et al. NKG2D-deficient mice are defective in tumor surveillance in models of spontaneous malignancy. *Immunity.* 2008;28(4):571-580.

74. Takeda K, Hayakawa Y, Smyth MJ, et al. Involvement of tumor necrosis factor-related apoptosis-inducing ligand in surveillance of tumor metastasis by liver natural killer cells. *Nat Med.* 2001;7(1):94-100.

75. Smyth MJ, Thia KY, Street SE, MacGregor D, Godfrey DI, Trapani JA. Perforin-mediated cytotoxicity is critical for surveillance of spontaneous lymphoma. *J Exp Med.* 2000;192(5):755-760.

76. Teng MW, Swann JB, Koebel CM, Schreiber RD, Smyth MJ. Immune-mediated dormancy: an equilibrium with cancer. *J Leukoc Biol.* 2008;84(4):988-993.

77. Eyles J, Puaux AL, Wang X, et al. Tumor cells disseminate early, but immunosurveillance limits metastatic outgrowth, in a mouse model of melanoma. *J Clin Invest.* 2010;120(6):2030-2039.

78. Koebel CM, Vermi W, Swann JB, et al. Adaptive immunity maintains occult cancer in an equilibrium state. *Nature.* 2007;450(7171):903-907.

79. Marincola FM, Jaffee EM, Hicklin DJ, Ferrone S. Escape of human solid tumors from T-cell recognition: molecular mechanisms and functional significance. *Adv Immunol.* 2000;74:181-273.

80. Spiotto MT, Yu P, Rowley DA, et al. Increasing tumor antigen expression overcomes "ignorance" to solid tumors via crosspresentation by bone marrow-derived stromal cells. *Immunity.* 2002;17(6):737-747.

81. Ochsenbein AF, Klenerman P, Karrer U, et al. Immune surveillance against a solid tumor fails because of immunological ignorance. *Proc Natl Acad Sci U S A.* 1999;96(5):2233-2238.

82. von Bernstorff W, Voss M, Freichel S, et al. Systemic and local immunosuppression in pancreatic cancer patients. *Clin Cancer Res.* 2001;7(3 Suppl):925s-932s.

83. Kim R, Emi M, Tanabe K, Arihiro K. Tumor-driven evolution of immunosuppressive networks during malignant progression. *Cancer Res.* 2006;66(11):5527-5536.

84. Dunn GP, Old LJ, Schreiber RD. The three Es of cancer immunoediting. *Annu Rev Immunol.* 2004;22:329-360.

85. Smyth MJ, Hayakawa Y, Takeda K, Yagita H. New aspects of natural-killer-cell surveillance and therapy of cancer. *Nat Rev Cancer.* 2002;2(11):850-861.

86. Barry M, Heibein JA, Pinkoski MJ, et al. Granzyme B short-circuits the need for caspase 8 activity during granule-mediated cytotoxic T-lymphocyte killing by directly cleaving Bid. *Mol Cell Biol.* 2000;20(11):3781-3794.

87. Voskoboinik I, Whisstock JC, Trapani JA. Perforin and granzymes: function, dysfunction and human pathology. *Nat Rev Immunol.* 2015;15(6):388-400.

88. Kägi D, Ledermann B, Bürki K, et al. Cytotoxicity mediated by T cells and natural killer cells is greatly impaired in perforin-deficient mice. *Nature.* 1994;369(6475):31-37.

89. Onyilagha C, Kuriakose S, Ikeogu N, Kung SKP, Uzonna JE. NK Cells Are Critical for Optimal Immunity to Experimental. *J Immunol.* 2019;203(4):964-971.

90. Mandal A, Viswanathan C. Natural killer cells: In health and disease. *Hematol Oncol Stem Cell Ther.* 2015;8(2):47-55.

91. Smyth MJ, Cretney E, Kelly JM, et al. Activation of NK cell cytotoxicity. *Mol Immunol.* 2005;42(4):501-510.

92. Screpanti V, Wallin RP, Ljunggren HG, Grandien A. A central role for death receptor-mediated apoptosis in the rejection of tumors by NK cells. *J Immunol.* 2001;167(4):2068-2073.

93. Blanchard DK, Michelini-Norris MB, Djeu JY. Production of granulocyte-macrophage colony-stimulating factor by large granular lymphocytes stimulated with Candida albicans: role in activation of human neutrophil function. *Blood.* 1991;77(10):2259-2265.

94. Angiolillo AL, Sgadari C, Taub DD, et al. Human interferon-inducible protein 10 is a potent inhibitor of angiogenesis in vivo. *J Exp Med.* 1995;182(1):155-162.

95. Pende D, Falco M, Vitale M, et al. Killer Ig-Like Receptors (KIRs): Their Role in NK Cell Modulation and Developments Leading to Their Clinical Exploitation. *Front Immunol.* 2019;10:1179.

96. Wight A, Mahmoud AB, Scur M, et al. Critical role for the Ly49 family of class I MHC receptors in adaptive natural killer cell responses. *Proc Natl Acad Sci U S A.* 2018;115(45):11579-11584.

97. Campbell KS, Purdy AK. Structure/function of human killer cell immunoglobulin-like receptors: lessons from polymorphisms, evolution, crystal structures and mutations. *Immunology.* 2011;132(3):315-325.

98. Schenkel AR, Kingry LC, Slayden RA. The ly49 gene family. A brief guide to the nomenclature, genetics, and role in intracellular infection. *Front Immunol.* 2013;4:90.

99. Long EO, Burshtyn DN, Clark WP, et al. Killer cell inhibitory receptors: diversity, specificity, and function. *Immunol Rev.* 1997;155:135-144.

100. Le Dréan E, Vély F, Olcese L, et al. Inhibition of antigen-induced T cell response and antibody-induced NK cell cytotoxicity by NKG2A: association of NKG2A with SHP-1 and SHP-2 protein-tyrosine phosphatases. *Eur J Immunol.* 1998;28(1):264-276.

101. Robbins SH, Nguyen KB, Takahashi N, Mikayama T, Biron CA, Brossay L. Cutting edge: inhibitory functions of the killer cell lectin-like receptor G1 molecule during the activation of mouse NK cells. *J Immunol.* 2002;168(6):2585-2589.

102. Ito M, Maruyama T, Saito N, Koganei S, Yamamoto K, Matsumoto N. Killer cell lectin-like receptor G1 binds three members of the classical cadherin family to inhibit NK cell cytotoxicity. *J Exp Med.* 2006;203(2):289-295.

103. Bryceson YT, March ME, Ljunggren HG, Long EO. Synergy among receptors on resting NK cells for the activation of natural cytotoxicity and cytokine secretion. *Blood.* 2006;107(1):159-166.

104. Sutherland CL, Chalupny NJ, Schooley K, VandenBos T, Kubin M, Cosman D. UL16-binding proteins, novel MHC class I-related proteins, bind to NKG2D

and activate multiple signaling pathways in primary NK cells. *J Immunol.* 2002;168(2):671-679.

105. Costello RT, Sivori S, Marcenaro E, et al. Defective expression and function of natural killer cell-triggering receptors in patients with acute myeloid leukemia. *Blood.* 2002;99(10):3661-3667.

106. Sivori S, Vitale M, Morelli L, et al. p46, a novel natural killer cell-specific surface molecule that mediates cell activation. *J Exp Med.* 1997;186(7):1129-1136.

107. Pende D, Parolini S, Pessino A, et al. Identification and molecular characterization of NKp30, a novel triggering receptor involved in natural cytotoxicity mediated by human natural killer cells. *J Exp Med.* 1999;190(10):1505-1516.

108. Nimmerjahn F, Ravetch JV. Antibodies, Fc receptors and cancer. *Curr Opin Immunol.* 2007;19(2):239-245.

109. Cooper MA, Fehniger TA, Turner SC, et al. Human natural killer cells: a unique innate immunoregulatory role for the CD56(bright) subset. *Blood.* 2001;97(10):3146-3151.

110. Hayakawa Y, Huntington ND, Nutt SL, Smyth MJ. Functional subsets of mouse natural killer cells. *Immunol Rev.* 2006;214:47-55.

111. Langers I, Renoux VM, Thiry M, Delvenne P, Jacobs N. Natural killer cells: role in local tumor growth and metastasis. *Biologics.* 2012;6:73-82.

112. Sharma P, Kumar P, Sharma R. Natural Killer Cells - Their Role in Tumour Immunosurveillance. *J Clin Diagn Res.* 2017;11(8):BE01-BE05.

113. Bryceson YT, March ME, Ljunggren HG, Long EO. Activation, coactivation, and costimulation of resting human natural killer cells. *Immunol Rev.* 2006;214:73-91.

114. Hayakawa Y, Smyth MJ. CD27 dissects mature NK cells into two subsets with distinct responsiveness and migratory capacity. *J Immunol.* 2006;176(3):1517-1524.

115. Kim S, Iizuka K, Kang HS, et al. In vivo developmental stages in murine natural killer cell maturation. *Nat Immunol.* 2002;3(6):523-528.

116. Huntington ND, Tabarias H, Fairfax K, et al. NK cell maturation and peripheral homeostasis is associated with KLRG1 up-regulation. *J Immunol.* 2007;178(8):4764-4770.

117. Boulanger MJ, Garcia KC. Shared cytokine signaling receptors: structural insights from the gp130 system. *Adv Protein Chem.* 2004;68:107-146.

118. Smyth MJ, Taniguchi M, Street SE. The anti-tumor activity of IL-12: mechanisms of innate immunity that are model and dose dependent. *J Immunol.* 2000;165(5):2665-2670.

119. Ljunggren HG, Kärre K. Host resistance directed selectively against H-2-deficient lymphoma variants. Analysis of the mechanism. *J Exp Med.* 1985;162(6):1745-1759.

120. Kärre K, Ljunggren HG, Piontek G, Kiessling R. Selective rejection of H-2-deficient lymphoma variants suggests alternative immune defence strategy. 1986. *J Immunol.* 2005;174(11):6566-6569.

121. Khanna R. Tumour surveillance: missing peptides and MHC molecules. *Immunol Cell Biol.* 1998;76(1):20-26.

122. Morvan MG, Lanier LL. NK cells and cancer: you can teach innate cells new tricks. *Nat Rev Cancer.* 2016;16(1):7-19.

123. Bauer S, Groh V, Wu J, et al. Activation of NK cells and T cells by NKG2D, a receptor for stress-inducible MICA. *Science.* 1999;285(5428):727-729.

124. Shankaran V, Ikeda H, Bruce AT, et al. IFNgamma and lymphocytes prevent primary tumour development and shape tumour immunogenicity. *Nature.* 2001;410(6832):1107-1111.

125. Smyth MJ, Thia KY, Cretney E, et al. Perforin is a major contributor to NK cell control of tumor metastasis. *J Immunol.* 1999;162(11):6658-6662.

126. Bi J, Tian Z. NK Cell Dysfunction and Checkpoint Immunotherapy. *Front Immunol.* 2019;10:1999.

127. Sakamoto N, Ishikawa T, Kokura S, et al. Phase I clinical trial of autologous NK cell therapy using novel expansion method in patients with advanced digestive cancer. *J Transl Med.* 2015;13:277.

128. Ishikawa E, Tsuboi K, Saijo K, et al. Autologous natural killer cell therapy for human recurrent malignant glioma. *Anticancer Res.* 2004;24(3b):1861-1871.

129. Parkhurst MR, Riley JP, Dudley ME, Rosenberg SA. Adoptive transfer of autologous natural killer cells leads to high levels of circulating natural killer cells but does not mediate tumor regression. *Clin Cancer Res.* 2011;17(19):6287-6297.

130. Davies JOJ, Stringaris K, Barrett AJ, Rezvani K. Opportunities and limitations of natural killer cells as adoptive therapy for malignant disease. *Cytotherapy.* 2014;16(11):1453-1466.

131. Wang W, Erbe AK, Hank JA, Morris ZS, Sondel PM. NK Cell-Mediated Antibody-Dependent Cellular Cytotoxicity in Cancer Immunotherapy. *Front Immunol.* 2015;6:368.

132. Kruschinski A, Moosmann A, Poschke I, et al. Engineering antigen-specific primary human NK cells against HER-2 positive carcinomas. *Proc Natl Acad Sci U S A.* 2008;105(45):17481-17486.

133. Glienke W, Esser R, Priesner C, et al. Advantages and applications of CAR-expressing natural killer cells. *Front Pharmacol.* 2015;6:21.

134. Hu W, Wang G, Huang D, Sui M, Xu Y. Cancer Immunotherapy Based on Natural Killer Cells: Current Progress and New Opportunities. *Front Immunol.* 2019;10:1205.

135. Kaech SM, Cui W. Transcriptional control of effector and memory CD8+ T cell differentiation. *Nat Rev Immunol.* 2012;12(11):749-761.

136. Pennock ND, White JT, Cross EW, Cheney EE, Tamburini BA, Kedl RM. T cell responses: naive to memory and everything in between. *Adv Physiol Educ.* 2013;37(4):273-283.

137. Alberts B, Johnson A, Lewis J, Raff M, Walter P. *Molecular Biology of the Cell , 4th edition.* 2002.

138. Schluns KS, Williams K, Ma A, Zheng XX, Lefrançois L. Cutting edge: requirement for IL-15 in the generation of primary and memory antigen-specific CD8 T cells. *J Immunol.* 2002;168(10):4827-4831.

139. Hamann D, Baars PA, Rep MH, et al. Phenotypic and functional separation of memory and effector human CD8+ T cells. *J Exp Med.* 1997;186(9):1407-1418.

140. Sallusto F, Geginat J, Lanzavecchia A. Central memory and effector memory T cell subsets: function, generation, and maintenance. *Annu Rev Immunol.* 2004;22:745-763.

141. Sharma N, Benechet AP, Lefrançois L, Khanna KM. CD8 T Cells Enter the Splenic T Cell Zones Independently of CCR7, but the Subsequent Expansion and Trafficking Patterns of Effector T Cells after Infection Are Dysregulated in the Absence of CCR7 Migratory Cues. *J Immunol.* 2015;195(11):5227-5236.

142. Wherry EJ, Teichgräber V, Becker TC, et al. Lineage relationship and protective immunity of memory CD8 T cell subsets. *Nat Immunol.* 2003;4(3):225-234.

143. Henao-Tamayo MI, Ordway DJ, Irwin SM, Shang S, Shanley C, Orme IM. Phenotypic definition of effector and memory T-lymphocyte subsets in mice chronically infected with Mycobacterium tuberculosis. *Clin Vaccine Immunol.* 2010;17(4):618-625.

144. Zhang X, Sun S, Hwang I, Tough DF, Sprent J. Potent and selective stimulation of memory-phenotype CD8+ T cells in vivo by IL-15. *Immunity.* 1998;8(5):591-599.

145. Schluns KS, Kieper WC, Jameson SC, Lefrançois L. Interleukin-7 mediates the homeostasis of naïve and memory CD8 T cells in vivo. *Nat Immunol.* 2000;1(5):426-432.

146. Clark WH. Tumour progression and the nature of cancer. *Br J Cancer.* 1991;64(4):631-644.

147. Sato E, Olson SH, Ahn J, et al. Intraepithelial CD8+ tumor-infiltrating lymphocytes and a high CD8+/regulatory T cell ratio are associated with favorable prognosis in ovarian cancer. *Proc Natl Acad Sci U S A.* 2005;102(51):18538-18543.

148. Gooden MJ, de Bock GH, Leffers N, Daemen T, Nijman HW. The prognostic influence of tumour-infiltrating lymphocytes in cancer: a systematic review with meta-analysis. *Br J Cancer.* 2011;105(1):93-103.

149. Farhood B, Najafi M, Mortezaee K. CD8. *J Cell Physiol.* 2019;234(6):8509-8521.

150. Topalian SL, Taube JM, Anders RA, Pardoll DM. Mechanism-driven biomarkers to guide immune checkpoint blockade in cancer therapy. *Nat Rev Cancer.* 2016;16(5):275-287.

151. Chang AL, Miska J, Wainwright DA, et al. CCL2 Produced by the Glioma Microenvironment Is Essential for the Recruitment of Regulatory T Cells and Myeloid-Derived Suppressor Cells. *Cancer Res.* 2016;76(19):5671-5682.

152. Borst J, Ahrends T, Bąbała N, Melief CJM, Kastenmüller W. CD4. *Nat Rev Immunol.* 2018;18(10):635-647.

153. Kim DH, Park HJ, Lim S, et al. Regulation of chitinase-3-like-1 in T cell elicits Th1 and cytotoxic responses to inhibit lung metastasis. *Nat Commun.* 2018;9(1):503.

154. Pardoll DM. The blockade of immune checkpoints in cancer immunotherapy. *Nat Rev Cancer.* 2012;12(4):252-264.

155. Sharma P, Hu-Lieskovan S, Wargo JA, Ribas A. Primary, Adaptive, and Acquired Resistance to Cancer Immunotherapy. *Cell.* 2017;168(4):707-723.

156. Khalil DN, Smith EL, Brentjens RJ, Wolchok JD. The future of cancer treatment: immunomodulation, CARs and combination immunotherapy. *Nat Rev Clin Oncol.* 2016;13(6):394.

157. Sadelain M, Brentjens R, Rivière I. The basic principles of chimeric antigen receptor design. *Cancer Discov.* 2013;3(4):388-398.

158. Kowolik CM, Topp MS, Gonzalez S, et al. CD28 costimulation provided through a CD19-specific chimeric antigen receptor enhances in vivo persistence and antitumor efficacy of adoptively transferred T cells. *Cancer Res.* 2006;66(22):10995-11004.

159. Brudno JN, Somerville RP, Shi V, et al. Allogeneic T Cells That Express an Anti-CD19 Chimeric Antigen Receptor Induce Remissions of B-Cell Malignancies That Progress After Allogeneic Hematopoietic Stem-Cell Transplantation Without Causing Graft-Versus-Host Disease. *J Clin Oncol.* 2016;34(10):1112-1121.

160. Rosenberg SA, Yang JC, White DE, Steinberg SM. Durability of complete responses in patients with metastatic cancer treated with high-dose interleukin-2: identification of the antigens mediating response. *Ann Surg.* 1998;228(3):307-319.

161. Smith FO, Downey SG, Klapper JA, et al. Treatment of metastatic melanoma using interleukin-2 alone or in conjunction with vaccines. *Clin Cancer Res.* 2008;14(17):5610-5618.

162. Cheever MA. Twelve immunotherapy drugs that could cure cancers. *Immunol Rev.* 2008;222:357-368.

163. Robinson TO, Schluns KS. The potential and promise of IL-15 in immuno-oncogenic therapies. *Immunol Lett.* 2017;190:159-168.

164. Smith GA, Uchida K, Weiss A, Taunton J. Essential biphasic role for JAK3 catalytic activity in IL-2 receptor signaling. *Nat Chem Biol.* 2016;12(5):373-379.

165. Ali AK, Nandagopal N, Lee SH. IL-15-PI3K-AKT-mTOR: A Critical Pathway in the Life Journey of Natural Killer Cells. *Front Immunol.* 2015;6:355.

166. Schluns KS, Klonowski KD, Lefrançois L. Transregulation of memory CD8 T-cell proliferation by IL-15Ralpha+ bone marrow-derived cells. *Blood.* 2004;103(3):988-994.

167. Berger C, Berger M, Hackman RC, et al. Safety and immunologic effects of IL-15 administration in nonhuman primates. *Blood.* 2009;114(12):2417-2426.

168. Anthony SM, Rivas SC, Colpitts SL, Howard ME, Stonier SW, Schluns KS. Inflammatory Signals Regulate IL-15 in Response to Lymphodepletion. *J Immunol.* 2016;196(11):4544-4552.

169. Stoklasek TA, Schluns KS, Lefrançois L. Combined IL-15/IL-15Ralpha immunotherapy maximizes IL-15 activity in vivo. *J Immunol.* 2006;177(9):6072-6080.

170. Waldmann TA. The biology of interleukin-2 and interleukin-15: implications for cancer therapy and vaccine design. *Nat Rev Immunol.* 2006;6(8):595-601.

171. Tang F, Zhao LT, Jiang Y, Ba dN, Cui LX, He W. Activity of recombinant human interleukin-15 against tumor recurrence and metastasis in mice. *Cell Mol Immunol.* 2008;5(3):189-196.

172. Klebanoff CA, Finkelstein SE, Surman DR, et al. IL-15 enhances the in vivo antitumor activity of tumor-reactive CD8+ T cells. *Proc Natl Acad Sci U S A.* 2004;101(7):1969-1974.

173. Kobayashi H, Dubois S, Sato N, et al. Role of trans-cellular IL-15 presentation in the activation of NK cell-mediated killing, which leads to enhanced tumor immunosurveillance. *Blood.* 2005;105(2):721-727.

174. Conlon KC, Lugli E, Welles HC, et al. Redistribution, hyperproliferation, activation of natural killer cells and CD8 T cells, and cytokine production during first-in-human clinical trial of recombinant human interleukin-15 in patients with cancer. *J Clin Oncol.* 2015;33(1):74-82.

175. Czajkowsky DM, Hu J, Shao Z, Pleass RJ. Fc-fusion proteins: new developments and future perspectives. *EMBO Mol Med.* 2012;4(10):1015-1028.

176. Rubinstein MP, Kovar M, Purton JF, et al. Converting IL-15 to a superagonist by binding to soluble IL-15R{alpha}. *Proc Natl Acad Sci U S A.* 2006;103(24):9166-9171.

177. Epardaud M, Elpek KG, Rubinstein MP, et al. Interleukin-15/interleukin-15R alpha complexes promote destruction of established tumors by reviving tumor-resident CD8+ T cells. *Cancer Res.* 2008;68(8):2972-2983.

178. Evans R, Fuller JA, Christianson G, Krupke DM, Troutt AB. IL-15 mediates anti-tumor effects after cyclophosphamide injection of tumor-bearing mice and enhances adoptive immunotherapy: the potential role of NK cell subpopulations. *Cell Immunol.* 1997;179(1):66-73.

179. Chapoval AI, Fuller JA, Kremlev SG, Kamdar SJ, Evans R. Combination chemotherapy and IL-15 administration induce permanent tumor regression in a mouse lung tumor model: NK and T cell-mediated effects antagonized by B cells. *J Immunol.* 1998;161(12):6977-6984.

180. Yu P, Steel JC, Zhang M, Morris JC, Waldmann TA. Simultaneous blockade of multiple immune system inhibitory checkpoints enhances antitumor activity mediated by interleukin-15 in a murine metastatic colon carcinoma model. *Clin Cancer Res.* 2010;16(24):6019-6028.

181. Yu P, Steel JC, Zhang M, et al. Simultaneous inhibition of two regulatory T-cell subsets enhanced Interleukin-15 efficacy in a prostate tumor model. *Proc Natl Acad Sci U S A.* 2012;109(16):6187-6192.

182. Dubois SP, Waldmann TA, Müller JR. Survival adjustment of mature dendritic cells by IL-15. *Proc Natl Acad Sci U S A.* 2005;102(24):8662-8667.

183. Zhang M, Yao Z, Dubois S, Ju W, Müller JR, Waldmann TA. Interleukin-15 combined with an anti-CD40 antibody provides enhanced therapeutic efficacy for murine models of colon cancer. *Proc Natl Acad Sci U S A.* 2009;106(18):7513-7518.

184. Cooley S, He F, Bachanova V, et al. First-in-human trial of rhIL-15 and haploidentical natural killer cell therapy for advanced acute myeloid leukemia. *Blood Adv.* 2019;3(13):1970-1980.

185. Pollock PM, Cohen-Solal K, Sood R, et al. Melanoma mouse model implicates metabotropic glutamate signaling in melanocytic neoplasia. *Nat Genet.* 2003;34(1):108-112.

186. Yajima I, Kumasaka MY, Thang ND, et al. RAS/RAF/MEK/ERK and PI3K/PTEN/AKT Signaling in Malignant Melanoma Progression and Therapy. *Dermatol Res Pract.* 2012;2012:354191.

187. Wen Y, Li J, Koo J, et al. Activation of the glutamate receptor GRM1 enhances angiogenic signaling to drive melanoma progression. *Cancer Res.* 2014;74(9):2499-2509.

188. Namkoong J, Shin SS, Lee HJ, et al. Metabotropic glutamate receptor 1 and glutamate signaling in human melanoma. *Cancer Res.* 2007;67(5):2298-2305.

189. Mehta MS, Dolfi SC, Bronfenbrener R, et al. Metabotropic glutamate receptor 1 expression and its polymorphic variants associate with breast cancer phenotypes. *PLoS One.* 2013;8(7):e69851.

190. Speyer CL, Smith JS, Banda M, DeVries JA, Mekani T, Gorski DH. Metabotropic glutamate receptor-1: a potential therapeutic target for the treatment of breast cancer. *Breast Cancer Res Treat.* 2012;132(2):565-573.

191. Sexton RE, Hachem AH, Assi AA, Bukhsh MA, Gorski DH, Speyer CL. Metabotropic glutamate receptor-1 regulates inflammation in triple negative breast cancer. *Sci Rep.* 2018;8(1):16008.

192. Koochekpour S. Glutamate, a metabolic biomarker of aggressiveness and a potential therapeutic target for prostate cancer. *Asian J Androl.* 2013;15(2):212-213.

193. Martino JJ, Wall BA, Mastrantoni E, et al. Metabotropic glutamate receptor 1 (Grm1) is an oncogene in epithelial cells. *Oncogene.* 2013;32(37):4366-4376.

194. Conti L, Ruiu R, Barutello G, et al. Microenvironment, oncoantigens, and antitumor vaccination: lessons learned from BALB-neuT mice. *Biomed Res Int.* 2014;2014:534969.

195. Hosseini H, Obradović MMS, Hoffmann M, et al. Early dissemination seeds metastasis in breast cancer. *Nature.* 2016;540(7634):552-558.

196. Hollmann M, Heinemann S. Cloned glutamate receptors. *Annu Rev Neurosci.* 1994;17:31-108.

197. Dong XX, Wang Y, Qin ZH. Molecular mechanisms of excitotoxicity and their relevance to pathogenesis of neurodegenerative diseases. *Acta Pharmacol Sin.* 2009;30(4):379-387.

198. Peng S, Zhang Y, Zhang J, Wang H, Ren B. Glutamate receptors and signal transduction in learning and memory. *Mol Biol Rep.* 2011;38(1):453-460.

199. Sontheimer H. A role for glutamate in growth and invasion of primary brain tumors. *J Neurochem.* 2008;105(2):287-295.

200. Platt SR. The role of glutamate in central nervous system health and disease--a review. *Vet J.* 2007;173(2):278-286.

201. Conn PJ, Pin JP. Pharmacology and functions of metabotropic glutamate receptors. *Annu Rev Pharmacol Toxicol.* 1997;37:205-237.

202. Traynelis SF, Wollmuth LP, McBain CJ, et al. Glutamate receptor ion channels: structure, regulation, and function. *Pharmacol Rev.* 2010;62(3):405-496.

203. Hinoi E, Takarada T, Ueshima T, Tsuchihashi Y, Yoneda Y. Glutamate signaling in peripheral tissues. *Eur J Biochem.* 2004;271(1):1-13.

204. Kalariti N, Pissimissis N, Koutsilieris M. The glutamatergic system outside the CNS and in cancer biology. *Expert Opin Investig Drugs.* 2005;14(12):1487-1496.

205. Skerry TM, Genever PG. Glutamate signalling in non-neuronal tissues. *Trends Pharmacol Sci.* 2001;22(4):174-181.

206. Ganor Y, Levite M. The neurotransmitter glutamate and human T cells: glutamate receptors and glutamate-induced direct and potent effects on normal human T cells, cancerous human leukemia and lymphoma T cells, and autoimmune human T cells. *J Neural Transm (Vienna).* 2014;121(8):983-1006.

207. Meldrum BS. Glutamate as a neurotransmitter in the brain: review of physiology and pathology. *J Nutr.* 2000;130(4S Suppl):1007S-1015S.

208. Eck HP, Frey H, Dröge W. Elevated plasma glutamate concentrations in HIV-1-infected patients may contribute to loss of macrophage and lymphocyte functions. *Int Immunol.* 1989;1(4):367-372.

209. Bai W, Zhu WL, Ning YL, et al. Dramatic increases in blood glutamate concentrations are closely related to traumatic brain injury-induced acute lung injury. *Sci Rep.* 2017;7(1):5380.

210. Shah R, Singh SJ, Eddy K, Filipp FV, Chen S. Concurrent Targeting of Glutaminolysis and Metabotropic Glutamate Receptor 1 (GRM1) Reduces Glutamate Bioavailability in GRM1. *Cancer Res.* 2019;79(8):1799-1809.

211. Malaisé M, Rovira J, Renner P, et al. KLRG1+ NK cells protect T-bet-deficient mice from pulmonary metastatic colorectal carcinoma. *J Immunol.* 2014;192(4):1954-1961.

212. Kroemer A, Xiao X, Degauque N, et al. The innate NK cells, allograft rejection, and a key role for IL-15. *J Immunol.* 2008;180(12):7818-7826.

213. Schiffner S. Molekulare Analyse von Modulatoren der Melanomentstehung und -progression anhand eines murinen Modellsystems2012.

214. Alvarez M, Simonetta F, Baker J, et al. Regulation of murine NK cell exhaustion through the activation of the DNA damage repair pathway. *JCI Insight.* 2019;5.

215. Long EO. Tumor cell recognition by natural killer cells. *Semin Cancer Biol.* 2002;12(1):57-61.

216. Alter G, Malenfant JM, Altfeld M. CD107a as a functional marker for the identification of natural killer cell activity. *J Immunol Methods.* 2004;294(1-2):15-22.

217. Elpek KG, Rubinstein MP, Bellemare-Pelletier A, Goldrath AW, Turley SJ. Mature natural killer cells with phenotypic and functional alterations accumulate upon sustained stimulation with IL-15/IL-15Ralpha complexes. *Proc Natl Acad Sci U S A.* 2010;107(50):21647-21652.

218. Felices M, Lenvik AJ, McElmurry R, et al. Continuous treatment with IL-15 exhausts human NK cells via a metabolic defect. *JCI Insight.* 2018;3(3).

219. Zheng Y, Fang YC, Li J. PD-L1 expression levels on tumor cells affect their immunosuppressive activity. *Oncol Lett.* 2019;18(5):5399-5407.

220. Mittal D, Gubin MM, Schreiber RD, Smyth MJ. New insights into cancer immunoediting and its three component phases--elimination, equilibrium and escape. *Curr Opin Immunol.* 2014;27:16-25.

221. Shrikant P, Mescher MF. Control of syngeneic tumor growth by activation of CD8+ T cells: efficacy is limited by migration away from the site and induction of nonresponsiveness. *J Immunol.* 1999;162(5):2858-2866.

222. Weng NP, Liu K, Catalfamo M, Li Y, Henkart PA. IL-15 is a growth factor and an activator of CD8 memory T cells. *Ann N Y Acad Sci.* 2002;975:46-56.

223. Liu K, Catalfamo M, Li Y, Henkart PA, Weng NP. IL-15 mimics T cell receptor crosslinking in the induction of cellular proliferation, gene expression, and cytotoxicity in CD8+ memory T cells. *Proc Natl Acad Sci U S A.* 2002;99(9):6192-6197.

7 Appendix

7.1 List of abbreviations

Abbreviation	Description
NCDs	Noncommunicable diseases
IARC	International Agency for Research on Cancer
UV	Ultra violett
Fig	figure
EMT	epithelial mesenchymal transition
DTCs	disseminated tumor cells
mABs	Monoclonal antibodies
ADCC	antibody-dependent cell cytotoxicity
NK cells	Natural killer cells
APCs	Antigen-presenting cells
MHC	Major histocompatibilty comlex
CTLs	Cytotoxic lymphocytes
EGFR	Epidermal growth factor receptor
CTLA-4	Cytotoxic T lymphocyte antigen 4
PD-1	Programmed death-1
LAG-3	Lymphocyte antigen gene 3
PD-L1	Programmed death ligand 1
CD	Cluster of differentiation
FDA	Food and Drug Administration
IFN	Interferon
γ	gamma
CAR	Chimeric antigen receptor
TAA	Tumor-associated antigens
CRISPR	Clustered Regularly Interspaced Short Palindromic Repeats
Cas9	Caspase 9
4th	Forth

IL	Interleukin
Tregs	Regulatory T cells
MDSCs	Myeloid derived suppressor cells
GM-CSF	Granulocyte-macrophage colony-stimulating factor
DCs	Dendritic cells
α	alpha
TGF	Tumor growth factor
β	beta
TNF	Tumor necrosis factor
DAMPs	Danger associated molecular patterns
TSA	tumor-specific antigens
VEGF	Vascular endothelial froth fatcor
IDO	Indoleamine 2,3-dioxygenase
%	percentage
TRAIL	tumor necrosis factor-related apoptosis-inducing ligand
IP-10	Interferon gamma-induced protein 10
KIRs	killer immunoglobulin-like receptors
Ly49	Membrane C-type lectin-like receptors
HLA	Histocompatibility antigen
ITIMs	immune receptor tyrosine-based inhibitory motifs
KLRG1	Killer cell lectin-like receptor subfamily G member 1
ITAMs	through immune-receptor tyrosine-based activating motifs
NCRs	Natural cytotoxicity receptors
neg	negative
pos	positive
iNK	Immature NK cells
mNKs	Mature NK cells
hi	high
lo	low
γc	Common gamma chain

TCR	T cell receptor
T_N	Naïve T cell
T_{SCM}	Stem cell memory T cell
T_{CM}	Central memory T cell
T_{EM}	Effector memory T cell
T_{eff}	Effector T cell
CCR7	C-C chemokine receptor 7
TILs	tumor infiltrating lymphocytes
MCA	methylcholanthrene
Ig	Immunoglobulin
Grm1	Metabotropic glutamate receptor 1
kb	kilobase
Dct	dopachrome tautomerase
IP3	Inositol triphosphate
DAG	diacylglycerol
wt	Wildtype
RAG	Recombination activating gene
-/-	Knockout (KO)
Glu	glutamate
CNS	Central nerve system
µM	micromolar
mGluR	Metabotropic glutamate receptor
iGluR	Ionotropic glutamate receptor
NMDAR	N-methyl-D-aspartate receptors
AMPA	2-amino-3-hydroxy-5-methyl-oxazole-4-propionic acid
KA	kainic ammonia acid
M	Molar
mM	millimolar
B6	C57BL/6J mice
CRC	Colorectal carcinoma

i.v.	Intravenous
µg	Microgram
ml	milliliter
o/n	Overnight
PBS	Phosphate buffered saline
E:T	Effector:target
RT	Room temperature
FCS	Fetal calf serum
i.p.	intraperitoneal
min	minutes
mg	milligram
d	day
µm	micrometer
HRP	Horseradish peroxidase
DNA	Deoxyribonucleic acid
RNA	Ribonucleic acid
WTA	Whole transcriptome amplification
PNAs	Peptide nucleic acids
cm	centimeter
CS	Curative surgery
MG	Mammary gland
Ca^{2+}	Calcium 2+
MLR	Mixed leukocyte reaction
PT	Primary tumor

7.2 List of figures